Submerged Reverse Osmosis Desalination

by

Joseph Ragan

A dissertation submitted to the Graduate Faculty of
Auburn University
in partial fulfillment of the
requirements for the Degree of
Doctor of Philosophy

Auburn, Alabama
August 2, 2014

Approved by

David Dyer, Chair, Professor of Mechanical Engineering
Dan Marghitu, Professor of Mechanical Engineering
P. Raju, Thomas Walter Professor of Mechanical Engineering
Peter Jones, Professor of Mechanical Engineering

Abstract

Over the past three decades, advances is reverse osmosis technology have led to dramatic increases in the number and capacities of reverse osmosis desalination plants. One key component in all efficient traditional reverse osmosis plants is an energy recovery turbine that recovers energy from the waste stream of the reverse osmosis process. The works documented herein describe and analyzes a system in which no recovery turbine is needed for efficient operation. The proposed system requires submerging a reverse osmosis element to a depth sufficient to provide the pressure required to overcome the osmotic pressure of the salt water. The fresh water that passes the reverse osmosis membrane is then pumped to the surface with a high pressure pump.

First and second law analysis is performed on the proposed system and compared to traditional systems. The energy analyses include parametric studies to determine energy optimized recovery rates. The effect of adding stages to traditional systems is analyzed and compared to the proposed system. An experimental apparatus is designed, built, and used to simulate submerged reverse osmosis desalination. The experimental work shows good quality fresh water (TDS< 300 ppm) from brackish water (TDS=10 ppt) at low recovery rates (3%-20%), and low net driving pressure (100 psi). The experimental work for artificial seawater resulted in

permeate with concentrations of 1000 ppm to 2000 ppm for net driving pressures up to 200 psi.

Variations for the design are also presented. The primary design includes submerged pretreatment and submerged reverse osmosis. The depth required to achieve good permeate quality is found to be 1100 ft to 1500 ft for typical seawater. A design alternative is presented to accommodate surface pretreatment and submerged desalination. A land based design alternative is also described in which the reverse osmosis membrane is submerged in a seawater or brackish water well.

Acknowledgements

I owe many for the support and opportunities that I've been afforded. I must first thank my wife, Addison, and three daughters, Clara, Myla, and Millie. My wife and children showed unwavering support and patience that allowed me to complete this work.

A special note of thanks is also extended to my committee chairman, Dr. David Dyer. He has been an important source of academic, professional, and personal guidance. Dr. Dyer has given me the opportunity to grow professionally, while patiently encouraging me to complete my degree requirements. Without his support, this work would not have been possible.

I also thank my parents, Steve and Donna Ragan, for raising me and for the sacrifices they made to provide for our family. They taught me the value of respect and hard work. My grandmother, Mildred Ragan, also impacted my life. She shared herself with me and instilled good core values.

Finally, I humbly thank God for the intellectual and physical gifts that make my life's work possible.

Table of Contents

Abstract ii

Acknowledgements iv

List of Figures ix

List of Tables xi

List of Symbols and Subscripts xiii

Greek Symbols xv

Subscripts xvi

1. Introduction 1

2. Literature Review 3

3. Description of Proposed System 8

3.1. Normal Operation 11

3.2. System Purge 12

3.3. Pre-Screen Backwash 13

3.4. Pre-Filter Backwash 13

3.5. Adding Cleaner 14

3.6. Soaking Cleaner 14

4. Advantages of the Proposed System 16

4.1. Description of a Traditional System 16

4.2. Advantages of the Proposed System 18

5. Energy Analysis of the Proposed System 23

5.1. Required Depth of the System 23

5.2. Approximate Required Depth of the System 24

5.3. Concentration factor 25

5.4. Actual Required Depth 27

5.5. High Pressure Pump Work 27

5.6. Low Pressure Pump Work 32

5.7. Total Pump Work Excluding Shore Line Head Loss 33

6. Energy Analysis of the Traditional System 37

7. Generalized Minimum Work Requirements 41

7.1. Gibbs Function and Second Law Computations 41

7.2. Minimum Work Computed with Osmotic Pressure 45

7.3. Work Comparison of Sub. and Conv. Multistage RO-- Ideal Equipment 61

7.4. Work Comparison of Sub. and Conv. Multistage RO-- Real Equipment 64

8. Experimental Apparatus 69

8.1. Artificial Seawater Mixing Assembly 71

8.2. Process Tank Subassembly 73

8.3. Nitrogen Supply Subassembly 77

8.4. Reverse Osmosis Subassembly 86

8.5. Reverse Osmosis Exploded View 88

9. Experimental Procedure and Results 90

9.1. Mixing Artificial Seawater 90

9.2. Transferring the Artificial Seawater 91

9.3. Desalination Startup 92

9.4. Desalination Data Capture 92

9.5. Desalination Shutdown and System Rinse 93

9.6. Results and Analysis 94

9.6.1. Salt Passage 96

9.6.2. Permeate Production Rates 102

10. Design Alternatives for Future Study 106

10.1. Submerged RO with Surface Pretreatment 106

10.2. Submerged RO with No Low Pressure Pump 109

10.3. Submerged RO in a Brackish or Seawater Well 111

11. Conclusions and Recommendations 113

References 117

Appendix A: MATLAB Code 119

Appendix B: Manufacturer Figures 132

List of Figures

Figure 1: Submerged Reverse Osmosis System 9

Figure 2: Simplified Typical Traditional RO Desalination 17

Figure 3: Simplified Proposed Submerged RO Desalination 20

Figure 4: Friction Losses 31

Figure 5: Work to Overcome Friction 31

Figure 6: Total Pump Power Neglecting Line Losses 35

Figure 7: Desalination Control Volume..... 42

Figure 8: Minimum RO Work via Gibbs..... 46

Figure 9: Single Stage RO Control Volume 47

Figure 10: Multiple Stage Reverse Osmosis..... 53

Figure 11: Minimum Work Comparisons 20 PPT..... 59

Figure 12: Minimum Work Comparisons 35 PPT..... 60

Figure 13: Multiple Stage RO with Ideal Recovery vs Submerged RO—35 ppt..... 63

Figure 14: Multiple Stage versus Submerged Non-Ideal Pumping-NDP=0..... 65

Figure 15: Multiple Stage versus Submerged Non-Ideal Pumping NDP =10 atm.... 68

Figure 16: Experimental Apparatus- Main Assembly System 70

Figure 17: Experimental Apparatus- Seawater Supply Assembly..... 72

Figure 18: Experimental Apparatus- Process Tank Assembly 74

Figure 19: Experimental Apparatus- Nitrogen Supply Assembly 78

Figure 20: Orifice Flow Rates..... 83

Figure 21: Experimental Apparatus- Reverse Osmosis System 87

Figure 22: Reverse Osmosis Membrane 89

Figure 23: Design Option-Surface Pretreatment..... 108

Figure 24: Design Option-Use Ocean Current..... 110

Figure 25: Design Option-Land Based Well 112

List of Tables

Table 1: Component Labels and Descriptions 10

Table 2: Component States for Different Operational Modes 15

Table 3: Proposed Versus Traditional 19

Table 4: Head Loss Parameters 29

Table 5: Pumping Parameters for Work Computations 36

Table 6: Optimum Concentration Factor 36

Table 7: Traditional System Assumed Constants 39

Table 8: Traditional System Computed Values 40

Table 9: Ionic Molar Concentration of Seawater 50

Table 10: Osmotic Pressure Calculator Results—25 °C 52

Table 11: Minimum Work Comparison 61

Table 12: Manufacturer Flow Data for Orifice 82

Table 13: Orifice Flow Rate Estimates at Experimental Pressures 84

Table 14: Reverse Osmosis Desalination Data from Experiments 95

Table 15: Results—Calculated Concentrations and Osmotic Pressures 98

Table 16: Membrane Salt Permeability—36 ppt Supply 99

Table 17: Membrane Salt Permeability—10 ppt Supply 99

Table 18: Salt Permeability Multiple Regression—36 ppt Supply 101

Table 19: Salt Permeability Multiple Regression—10 ppt Supply 101

Table 20: Water Permeability—36 ppt Supply..... 104

Table 21: Water Permeability—10 ppt Supply..... 105

List of Symbols and Subscripts

CF	concentration factor
D	depth
e	pipe roughness
E	energy
f	friction factor
F	membrane water permeability
g	acceleration due to gravity
$\hat{g}$	Gibbs function
h	enthalpy
h_L	head loss
$\dot{m}$	mass flow rate
m	mass
M_{ion}	ionic concentration

NDP	net driving pressure
P	pressure
ΔP_S	concentrate side pressure drop
ΔP_T	transmembrane pressure difference
$\dot{Q}$	heat rate per unit time
R	universal gas constant
Re	Reynolds number
RR	recovery rate
s	specific entropy
$\dot{S}_{gen}$	rate of entropy generation
T	temperature
v	velocity
V	volume
$\dot{V}$	volumetric flow rage
W	work
$\dot{W}$	work rate or power

x	salt mass concentration
z	height
Z	compressibility factor

Greek Symbols

μ	dynamic viscosity
η	pump or turbine efficiency
υ	specific volume
ρ	density
Π	osmotic pressure
$\overline{\Pi}$	average osmotic pressure
Φ	osmotic coefficient

Subscripts

0	reference state
C	concentrate
HP	high pressure pump
LP	low pressure pump
max	maximum
min	minimum
P	permeate
R	recovery
S	supply
v	per unit volume basis

1. Introduction

Worldwide, population growth has led to increased consumption and pollution of the world's very limited fresh water supplies. Arid regions of the planet have long struggled with inadequate fresh water supplies, but densely populated areas even in humid regions are dealing with water shortages. With over 96% of the earth's surface covered in salt water, there is an obvious need to develop cost effective methods of desalination. Today, almost all desalination plants can be categorized as using one of two mechanisms to achieve fresh water production: evaporation or filtration.

This work proposes and investigates a desalination process based on reverse osmosis (a filtration method) located deep in the ocean. While installing and operating a submerged system presents some technical challenges not included in traditional land based systems, the proposed system does offer several key advantages that make consideration of the system worthwhile. The design of the proposed system eliminates the need for an energy recovery device, reduces energy consumption requirements, relaxes the performance requirements for the components, and utilizes water supplied that requires much less pre-filtering when compared to surface water sources.

This dissertation describes the system and its various modes of operation and maintenance. The system is compared to traditional systems, and the advantages of

the proposed system are highlighted. In order to quantify energy requirements, thermodynamic analysis is presented for both the proposed system and the traditional system. An experimental apparatus is designed and built to verify the concept and investigate unpublished RO membrane characteristics.

2. Literature Review

2.1. Desalination Options and Literature Surveys

(Buros, 2000) presents a nice overview of desalination technologies including Multiple Stage Flash (MSF), Multiple Effect Distillation (MED), Mechanical Evaporation, and Reverse Osmosis. The review includes process diagrams, current industry practice and trends, and some economic data.

(Greenlee, 2009) compiled an impressive literature survey of works that concentrates on desalination by reverse osmosis. This survey includes a vast amount of information ranging from reverse osmosis history and background to specific information about membrane technology and pretreatment requirements. The primary purpose of the work is to present the differences in seawater and brackish reverse osmosis, but it also serves an excellent resource for gaining perspective on the role of reverse osmosis as compared to the other major desalination methods.

(Whyte, 2013) submitted a patent application for deep water submerged desalination. Whyte recognized some energy saving potential for submerging the unit to avoid pumping the supply/concentrate stream to very high pressure changes. Whyte's design does have problems and limitations that are not addressed in the patent application. The most obvious design problem is the fact a single pump is

included to provide the permeate flow and the supply/concentrate flow. These flows must be separate and require different volumetric rates and different pressure rises. Therefore, two pumps are required to operate the system in a practical manner.

Whyte's design does not include details for executing cleaning cycles and backwash operations without surfacing the unit. The patent also suggests operating the reverse osmosis at pressures comparable to that of conventional land based reverse osmosis plant. Whyte does not present the benefit of operating the submerged system at lower recovery rates.

The submerged reverse osmosis design presented in this dissertation gives detailed requirements for two submerged pumps, includes plumbing details for typical "in-place" maintenance cycles, and presents optimized operation at low recovery rates.

(Kim, 2009) proposed energy consumption improvements for the reverse osmosis plant in Fujairah, South Korea. Two years of actual operational data were used to develop control schemes to optimize the feedwater pressure as a function of controlled feedwater temperature. The proposed control scheme reduces the required supply pressure by approximately 10 bar while maintaining the required permeate quality.

2.2. Energy and Economics

(Wade N. , 2001) presents an economical and operational comparison of modern multiple effect distillation, multiple stage flash, and reverse osmosis plants.

According to his work, the costs of desalination are dropping rapidly (as much as 50% in the years leading up to the study). He reported that costs of $\$0.7/m^3$ are possible with modern reverse osmosis and evaporative plants. The comparison also includes itemized capital and operational costs for each of the primary desalination technologies. This study was a follow-up to work completed eight years earlier (Wade N. M., 1993) .

(Borsani, 2005) also presents cost estimating data for the three major desalination technologies. Borsani indicates that competition and design approach changes have led to decreased installation costs for large desalination plants. Borsani predicts that evaporative methods will continue to dominate markets where thermal energy is relatively inexpensive and water supplies are low in quality (such as the Middle East). However, reverse osmosis will continue to gain market share in other locations.

(Mistry, 2013) performed a thermodynamic analysis of generalized heat (e.g. evaporative) and work (e.g. reverse osmosis) desalination methods. Mistry applied the first and second laws of thermodynamics to determine the absolute minimum amounts of energy required to achieve separation using the two generalized approaches. Mistry used Gibbs function data for saltwater for the computations.

(Burch, 1992) identified energy savings possibilities using the submerged osmosis desalination concept. Based on osmotic pressure data available in the literature, Burch estimated the permeate pumping power requirements. Burch

considered various salinity and temperature profiles in his parametric studies with the aim of optimizing operating depth for a given temperature and salinity profile.

(Maghrabi, 2005) performed an experiment to determine the effect of increasing feedwater temperature for a reverse osmosis desalination membrane. The reverse osmosis system did not include an energy recovery device. Increasing the feedwater temperature from 30°C to 40°C reduced reversed osmosis power requirements by 18%

(Vince, 2008) created a multi-objective RO optimization model for desalination plants. The model presented accommodates both direct economic costs and environmental impacts and specifications. Vince also reported the characterization values for two Dow membranes: SW30-HR380 and BW30LE-440.

2.3. Seawater Properties

(Puyate, 2008) measured ocean characteristics of Atlantic Ocean water at depths ranging from the surface to more than 1500 meters deep. The measured properties include several parameters needed for desalination design and modeling including: temperature, turbidity, and salinity. From the surface to a depth of 500 meters, Puyate reported that the temperature dropped from 28 C to 7 C, and the salinity dropped from approximately 35.5 ppt to approximately 34.5.

(Sharqawya, Lienhard, & Zubair, 2010) reviewed correlations for the thermophysical correlations of seawater. Properties including enthalpy, entropy,

osmotic coefficient, density, and boiling point elevation were covered. Calculators using the specific correlations are maintained at http://web.mit.edu/seawater/.

(Bromley, 1974) measured and correlated data for properties of seawater. Values presented include boiling point elevation, osmotic coefficient, and osmotic pressure.

3. Description of Proposed System

This chapter gives a brief description of the primary modes of operation of the proposed reverse osmosis (RO) desalination plant. A diagraming showing the major components of the system is shown in Figure 1. The modes of operation covered in this chapter include: normal operation, system purge, pre-screen backwash, pre-filter backwash, cleaning solution addition, and cleaning solution soak. In this text, the components are referenced using labels as defined in Table 1 and Figure 1. A short description of each component is given in Table 1. This section is limited to a brief description of operation. More operational details such as operating pressures, flow rates, and concentration levels are given in subsequent chapters.

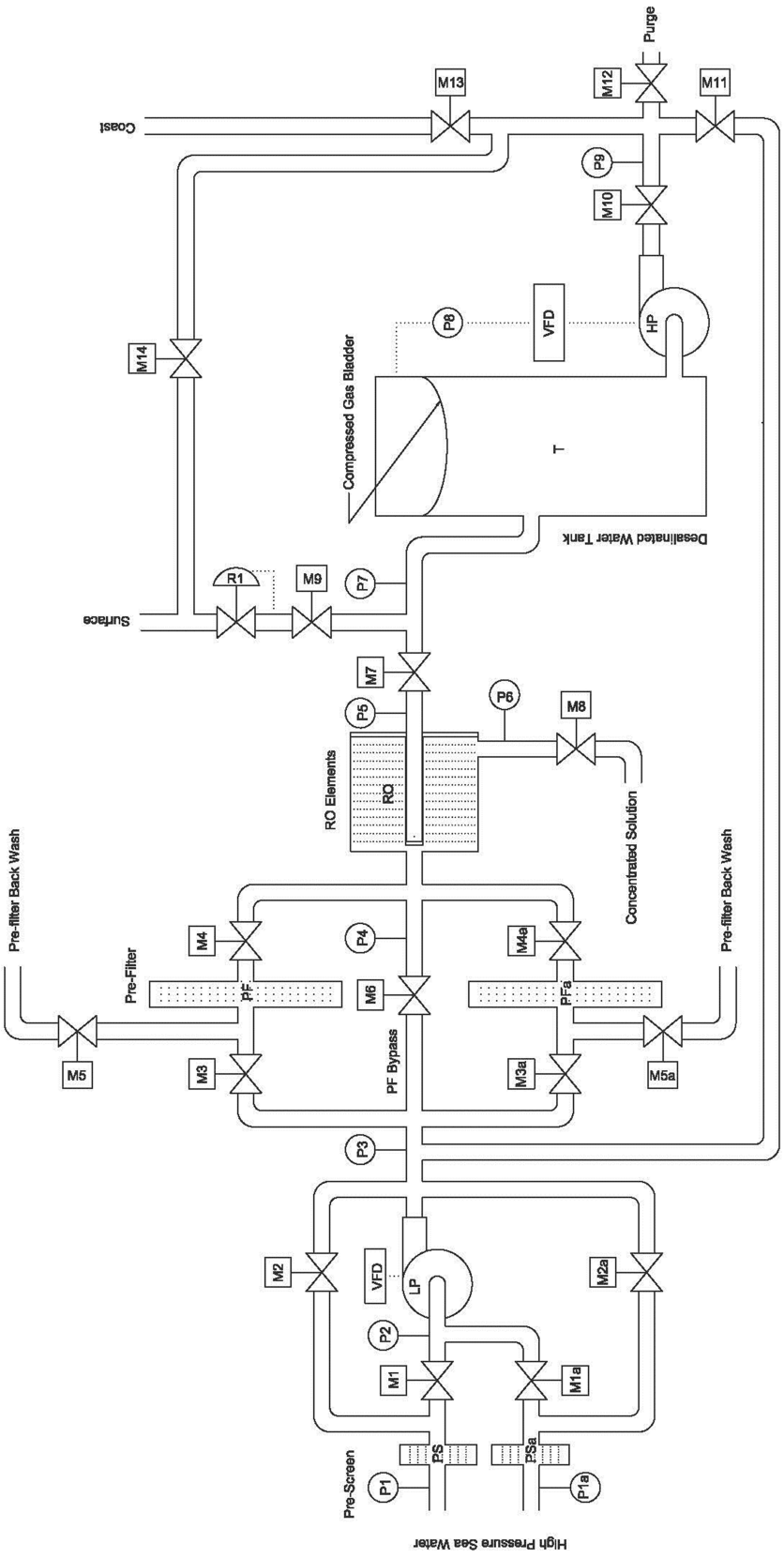

Figure 1: Submerged Reverse Osmosis System

Table 1: Component Labels and Descriptions

Component Label	Component Description
P1	Pressure of the seawater supply to the Pre-Screen mesh
P2	Suction pressure for seawater supply pump
P3	Discharge pressure for the seawater supply pump
P4	Supply pressure for the RO elements
P5	Permeate discharge pressure for the RO elements
P6	Concentrate discharge pressure for the RO elements
P7	Desalinated water tank pressure
P8	Tank gas bladder pressure
P9	Desalinated water supply pump discharge pressure
M1, M1a*	Seawater supply valve
M2, M2a*	Pre-screen backwash valve
M3, M3a**	Pre-filter supply valve
M4, M4a**	Pre-filter discharge valve
M5, M5a**	Pre-filter backwash valve
M6	Pre-filter bypass valve
M7	Permeate discharge valve
M8	Concentrate discharge valve
M9	Cleaning solution supply valve
M10	High pressure desalinated water pump discharge valve
M11	Recirculation valve for cleaning and backwash
M12	System purge valve for start-up
M13	Desalinated water supply valve
M14	Fresh water supply to the surface platform
R1	Cleaning solution pressure regulator
LP	Low pressure salt water pump
HP	High pressure desalinated water pump
VFD	Variable frequency drive
Pre-Screen	Pre-screen mesh for large debris
Pre-Filter	Precautionary filter to prevent RO fouling
Reverse Osmosis Elements	Manufactured RO elements such as DOW Filmtec
Desalinated Water Tank	Storage tank for desalinated water. Also used for cleaning solution in cleaning mode
Coast	Supply line to the coast

*PSa, M1a, and M2a serve for alternate seawater supply in case the primary is fouled

**M3a, M4a, and M5a serve for alternate pre-filtration in case the primary PF is fouled

3.1. Normal Operation

The system is designed to operate submerged deep in the ocean. The seawater intake is at P1 and flows through a pre-screen mesh that blocks any large debris. The seawater then flows through the motorized valve M1 and is pumped to a pressure high enough to overcome the differential pressure of the pre-filter and RO elements on the salt water supply side of the membranes. At the required depth the typical turbidity is expected to be approximately 0.05 NTU (Krock, 2010). This turbidity is very low and well within the range specified by RO manufacturers. A typical allowable turbidity is 0.5 NTU (Krock, 2010). Therefore, the pre-filters are precautionary elements used to protect against unexpected anomalies and potential disturbances in the water composition.

Since the unit is located deep in the ocean, filter changes would require a great deal of effort. For this reason, the system is designed with a back-up pre-screen intake, and a back-up pre-filter. The system could be expanded to include multiple backups for both the pre-screen and the pre-filter. In the event of pre-screen or pre-filter fouling, a backwashing and cleaning cycle would be executed. If backwashing and cleaning do not restore the elements to an acceptable state, the backup elements would be utilized to provide clean seawater to the RO elements.

As shown in Figure 1, the backup intake consists of the "Pre-screen alternate" (PSA), "Motorized Valve 1 Alternate" (M1A), and "Motorized Valve 2 Alternate" (M2A). The backup pre-filter unit consists of the "Pre-filter Alternate" (PFA), "Motorized Valve 3 Alternate" (M3A), and "Motorized Valve 4 Alternate" (M4A).

Once the water exits the pre-filter unit, it flows through valve M4 and is supplied to the RO elements. As the water flows through the RO elements, the high transmembrane pressure drives clean water across the osmotic membrane where it is collected in the permeate tube. As the seawater flows through elements, the salt is blocked from crossing the osmotic membrane. This increases the salt concentration of the water on the outside of the membrane. The fresh water collected in the permeate tube flows through valve M7 and into a holding tank. The concentrated saltwater flow exits the RO unit through valve M8 to the sea at the RO unit depth. Note that during normal operation valve M9 will be closed.

The high pressure fresh water supply pump (HP) pumps the desalinated water from the tank. The water flows through valves M10 and M13 to the shore. During normal operation valves M11, M12, and M14 will be closed.

3.2. System Purge

During startup, after an outage, after maintenance, or after cleaning, it will be necessary to purge any contaminants from the system before restoring water production to the shore. The proposed design includes motorizes valves to accomplish this task. In order to purge the system all components except valves M12 and M13 will be in the normal operation setting. Valve M13 will be closed, and valve M12 will be open. This will discharge the water produce by the RO elements to the open ocean. Once the system is thoroughly purged, water production to the shore will be restored by opening valve M13 and closing valve M12.

3.3. Pre-Screen Backwash

If the pre-screen mesh that supplies the intake pumps becomes blocked, pump HP can be utilized to backwash the element with desalinated water. If necessary, clean water could be supplied to the submerged desalinated water tank from the surface through the pressure reducing valve R1 and the motorized valve M9. The surface water supply for this operation would be needed if the desalinated water tank volume is insufficient to provide the amount of backwash needed to clear the pre-screen mesh.

In order to perform pre-screen backwash, valve M7 should be closed and pump LP should be off. Pump HP will be used to flow water through valves M10 and M11. Valves M12, M13, and M14 must be closed. Valves M3a, M6, and M3 will be closed to force the water through the open valve M2. Valve M1 must be closed. This setup will cause reverse flow of clean water through the pre-screen mesh.

3.4. Pre-Filter Backwash

Pump HP can also be used to back wash the pre-filter elements with desalinated water. Pump HP will be supplied in the same manner as described for the Pre-screen backwash. Pump LP will be off and valves M1, M1a, M2, M2a, M3 and M3a will be closed. Valves M6, M4, and M5 will be open. This setup will cause water to be pumped by pump HP from the desalinated water tank through valves M10, M11, M6, M4, and M5 to the open ocean. This will result in reverse flow of clean water through the pre-filter element.

3.5. Adding Cleaner

The system includes a supply line from the surface local to the reverse osmosis unit. This supply line can be used to provide clean water to the submerged desalinated water tank for backwash or other uses. In the event of RO membrane fouling it is common practice to use a cleaning solution to separate the foulants from the membrane. For this design the cleaning solution will flow from the supply at the surface through the regulator R1 and valve M9. Valves M7 and M14 will be closed. The low pressure pump LP will be off and the high pressure pump HP will pump the solution from the submerged tank through valve M10. Valves M13 and M12 will be closed forcing the cleaning solution through valve M11 and the recirculation line. Valves M1 and M2 will be closed and valves M3, M4 and M8 will be open. The cleaning solution will pass through the pre-filter, into the RO elements, and be discharged to the ocean through valve M8. Once an adequate amount of cleaner has been added to fill the RO elements the pump will shut down and all valves will be closed.

3.6. Soaking Cleaner

As mentioned above, once the cleaner has been added to the system, the elements will soak for a period of time. During this time, all valves will be shut and the pumps will be off. After the elements have soaked for the required amount of time, the system must be purged before coming back online. It should be noted that the expected cleaning frequency is extremely low.

Table 2: Component States for Different Operational Modes

Label	Normal Opera-tion	Add Cleaning Solution	Soak Clean Solution	Purge RO	Purge Clean Supply	Pre-filter Back wash	Pre-Screen Back wash
P1	P_S	P_S	P_S	P_S	P_S	P_S	P_S
P2	P_S	NA	NA	NA	NA	NA	NA
P3	$P_{F,S}$	$P_{F,S}$	P_S	$P_{F,S}$	P_S	$P_{F,S}$	$P_{F,S}$
P4	$P_{F,S}$	$P_{F,S}$	P_S	$P_{F,S}$	P_S	$P_{F,S}$	NA
P5	1 atm	NA	NA	1 atm	NA	NA	NA
P6	P_S	P_S	P_S	P_S	P_S	P_S	NA
P7	1 atm	1 atm	1 atm	1 atm	1 atm	1 atm	1 atm
P8	1 atm	1 atm	1 atm	1 atm	1 atm	1 atm	1 atm
P9	$P_S + P_L$	$P_{F,S}$	P_S	P_S	P_S	$P_{F,S}$	$P_{F,S}$
M1	O	C	C	O	C	C	C
M2	C	C	C	C	C	C	O
M3	O	O	C	O	C	C	C
M4	O	O	C	O	C	O	C
M5	C	C	C	C	C	O	C
M6	C	C	C	C	C	O	C
M7	O	C	C	O	C	C	C
M8	O	O	C	O	C	C	C
M9	C	O	C	C	O	O	O
M10	O	O	C	O	O	O	O
M11	C	O	C	C	C	O	O
M12	C	C	C	O	O	C	C
M13	O	C	C	C	C	C	C
M14	C	C	C	C	C	C	C
R1	C	O	C	C	O	O	O
LP	on	off	off	on	off	off	off
HP	on	on	off	on	on	on	on
PS	N	N	N	N	N	N	BW
PF	N	CS	CS	CS->N	N	BW	N
RO	N	CS	CS	CS->N	CS	CW	CW
T	DW	CS	CS	CS->CW	CS	CW	CW
SC	CW	CW	CW	CW	CW	CW	CW

O=open CW=clean water DW=desalinated water
C=closed CS=cleaning solution
N=normal BW=backwash

4. Advantages of the Proposed System

4.1. Description of a Traditional System

A simplified schematic for a modern typical process for RO desalination system is shown in Figure 2. In this system, the seawater supply pressure, PS, is atmospheric pressure. The supply pump then pumps the supply stream to a high pressure. Similar to the proposed system, the pressure P3 is the sum of the osmotic pressure of the concentrate, the supply to concentrate differential, and the net driving pressure (NDP), $\left(\Pi + \Delta P_S + NDP\right)$. After undergoing the pressure increase provided by the supply pump (HP), the seawater passes through the pre-filter and then into the reverse osmosis unit. As it flows through the reverse osmosis unit, some pure water crosses the membrane and is collected in the collection tube which is maintained near atmospheric pressure. The seawater passing through the RO unit is therefore being concentrated to a higher salt content during the process.

When the salt water flow discharges from the RO unit, the pressure has only been reduced by the supply to concentrate differential (typically less than 5 psi). This means that pressure of the concentrate stream, P6, is very high and the flow has relatively high thermodynamic availability. The state of the concentrate stream at the RO discharges results in the requirement to include an energy recovery device in

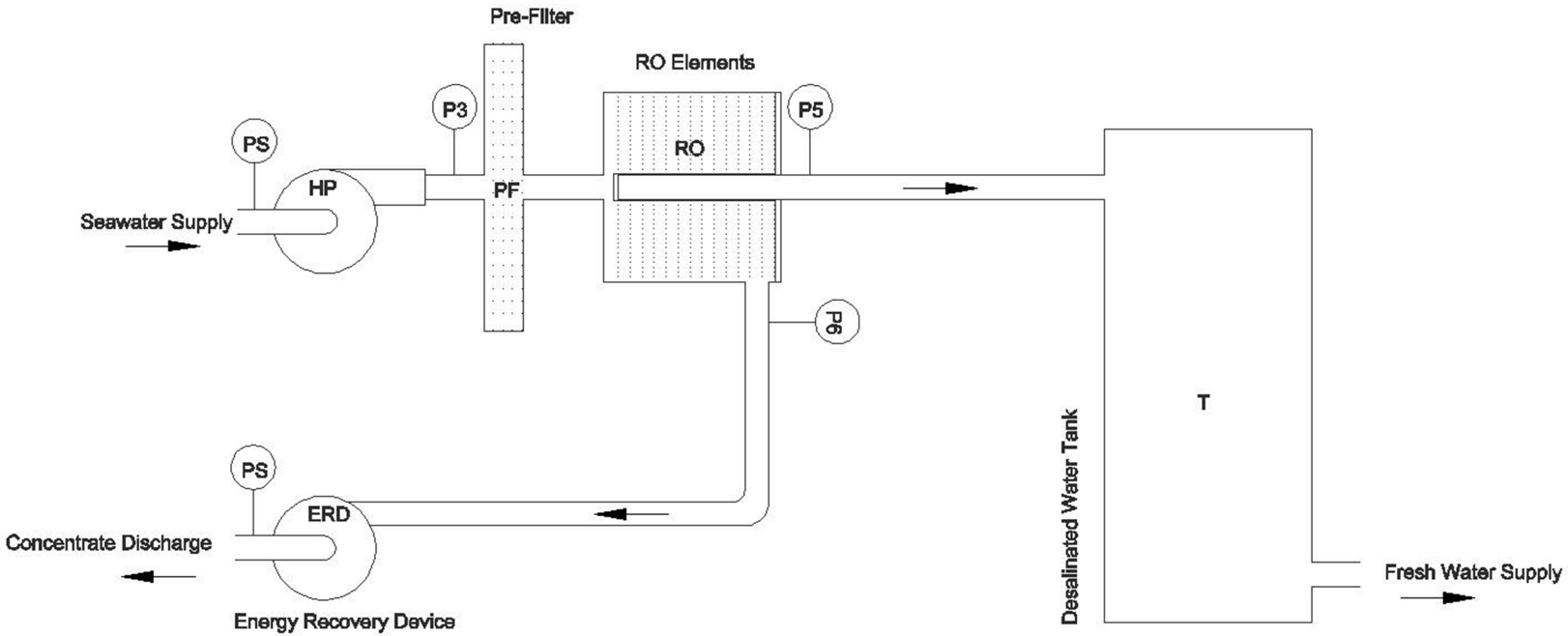

Figure 2: Simplified Typical Traditional RO Desalination

order to operate the system in an efficient cost effective manner. For modern processes, the concentrate passes through an energy recovery device. The effectiveness of the energy recovery device varies with cost, but some devices recover up to 97% of the available energy in the concentrate stream. To achieve high efficiency, the recovery turbine must operate at slow speeds which require a physically large unit and higher capital costs.

For modern systems the supply pump must be sized large enough to flow the entire supply stream and robust enough to provide a very large pressure lift (around 60 atm). The energy recovery device must also be built to operate at very high pressure differentials. The energy recovery device must be size large enough to handle the concentrate stream. The pump and energy recovery device for this are expensive due to the operational requirements. The cost of the recovery turbine is expected to be at least 50% of the cost of the high pressure pump (for recovery rates around 50%). Energy requirements and typical recovery rates for these systems are covered in chapters 6 and 7 of this text.

4.2. Advantages of the Proposed System

A simplified schematic of the proposed system is shown in Figure 3. There are several advantages to the proposed submerged RO system. The primary advantage is the pressure resulting from the depth of submersion. The proposed system is located at a depth sufficient to provide the pressure needed to overcome the osmotic pressure of the salt water and provide good flow of pure water into the permeate collector. A

variable frequency drive (VFD) is used to control the speed of the high pressure pump (HP). The speed of the pump is varied so that the permeate local to the RO unit will be maintained at 1 atm by the high pressure pump (HP). While the low pressure pump (LP) will have to move the entire supply stream (high volume), it will operate under a low differential pressure. This is in contrast to the "high-differential", "high-flow" supply pump required by the traditional system. Since this supply pump (LP) is only providing enough pressure rise to push the supply through the pre-filter and RO units (around 5 psi), the concentrate stream is discharged with very little thermodynamic availability. This setup removes the need for an energy recovery device such as the one required for the traditional system.

In the proposed system, the high pressure pump (HP) only pumps desalinated water. So while the pump must be engineered robustly for the high lift requirements, the size requirement is decreased when compared to the supply pump required by the traditional system. This is an advantage for the proposed system. Table 3 compares the required components of the two systems.

Table 3: Proposed Versus Traditional

Component	Proposed System	Traditional System
Low Pressure Pump (LP)	Low Pressure High Volume	Not needed
High Pressure Pump (HP)	High Pressure Minimized Volume	High Pressure High volume
Energy Recovery Device (ERD)	Not needed	High Pressure High volume

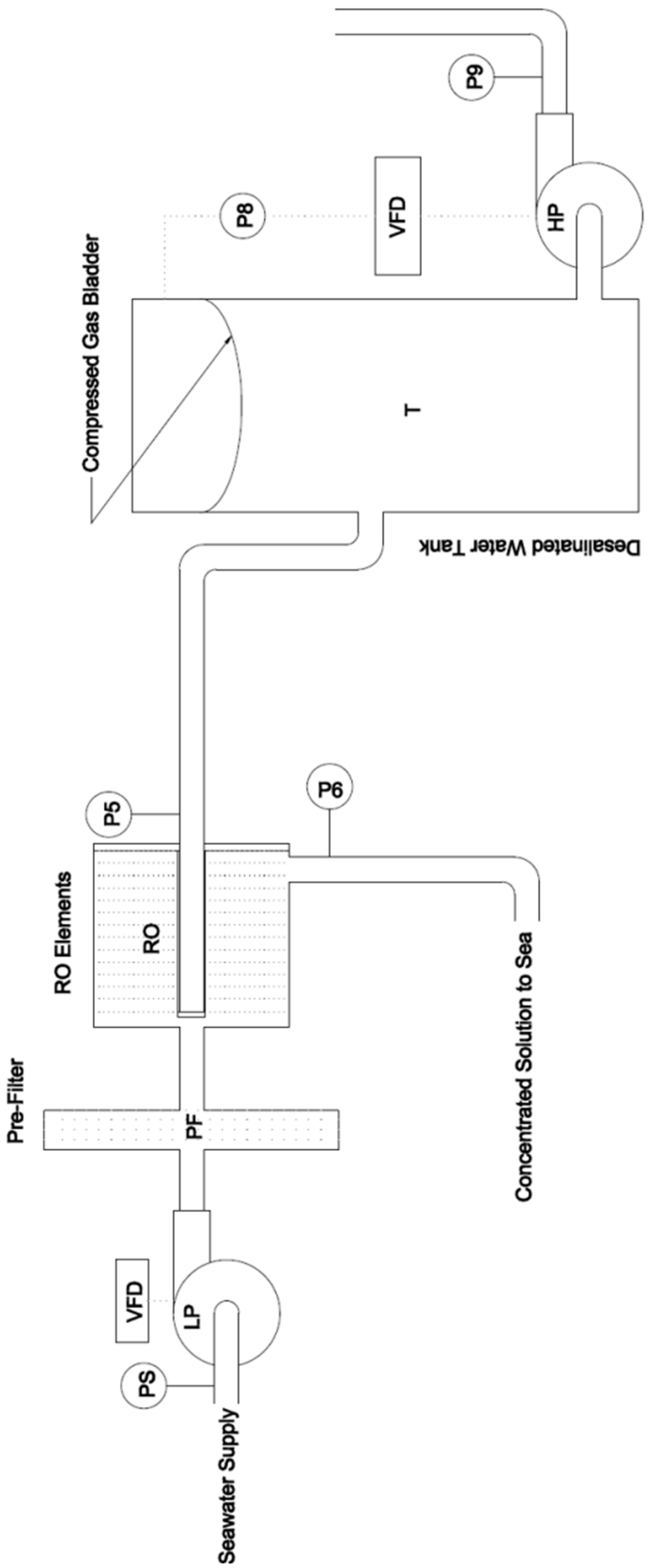

Figure 3: Simplified Proposed Submerged RO Desalination

Potential secondary benefits to the proposed design could result strategically locating the apparatus in waters with favorable properties. Generally, the salinity and temperature profiles of the ocean vary with depth. Salinity in the ocean decreases with depth for the first 500 meters. The osmotic pressure requirements decrease with decreasing salinity. The salinity at the operational depth of the proposed system is expected to be about 1% less than the salinity at the surface (Puyate, 2008).

In ocean water, temperature generally decreases with depth for the first few hundred meters. This decrease in temperature also decreases the osmotic pressure. While the lowered osmotic pressure is advantageous a second effect of lowering the temperature must be considered (Puyate, 2008). Lowering the water temperature increases the viscosity of the water. For example, the viscosity of water is 0.653 mPa·s at 40 °C and 1.002 mPa·s at 20 °C (White, 1991). To achieve the same production rate, water with higher viscosity requires a higher net driving pressure than water with lower viscosity. In the absence of energy recovery, decreasing feedwater temperature generally decreases the efficiency of RO systems that do not have energy recovery. For example (Maghrabi, 2005) found that increasing the temperature from 30°C to 40°C increased the RO efficiency by 18% assuming no energy recovery from the waste stream.

However for the proposed design the only additional power requirement due to the increased viscosity would be in the low pressure rise pump. Additionally, this increase in pumping power can easily be offset with filter design to keep the pressure drop from the supply to concentrate supply low. So for the proposed design, the

impacts of lowering the supply temperature for a given reverse osmosis unit include: reduced osmotic pressure of the feedwater, increased net driving pressure, decreased salt passage, and decreased permeate rates. These factors will influence package design, recovery rate optimization, and operational depth, but will not have a dramatic impact on the overall efficiency of the proposed system.

5. Energy Analysis of the Proposed System

During RO desalination, as the salt water passes through the unit, some fresh water crosses the membrane resulting in a more highly concentrated salt water stream. The osmotic pressure is directly proportional to the concentration level of the salt. This results in an optimization problem to determine the optimum salt concentration of the reject stream. Pump power is directly proportional to the required pressure and flow rate. Increasing the flow rate provided by the low pressure pump (LP) has the effect of decreasing the maximum salt concentration (which decreases the pressure and power requirements of the high pressure pump (HP)). Of course the increased flow rate provided by the low pressure pump increases its power requirement. This setup yields an optimization problem to minimize the total pumping power.

5.1. Required Depth of the System

The total pressure required at the inlet (P_S) for the RO system is the sum of the maximum osmotic pressure (Π), the net driving pressure (NDP), and the permeate discharge pressure. The net driving pressure is the difference in the actual

transmembrane pressure difference (ΔP_T) and the osmotic pressure of the concentrate stream. The rate of permeate production is proportional to the net driving pressure.

5.2. Approximate Required Depth of the System

To begin understanding the geometric requirements of the proposed submerged desalination system, an approximate minimum depth requirement is calculated. This approximation is based on a recovery rate that approaches zero (the supply stream is not concentrated as it flows through the RO unit). The actual required depth will increase when the most economical recovery rate is used.

The osmotic pressure of typical ocean water is 26 atm (Greenlee, 2009). In order to produce permeate, the pressure difference across the RO membrane must be greater than the osmotic pressure. This "extra" pressure is known as the net driving pressure (NDP). Typical net driving pressure is around 7 atm. For these conditions, the system requires a submersion depth (D) that will yield 33 atm (gauge) assuming the permeate discharge is maintained at atmospheric pressure. Given the density of supplied seawater (ρ_S) to be approximately 1025 kg/m^3 and the acceleration due to gravity (g) to be 9.81 m/s^2, the depth may be computed by equation (1). For typical values the required depth would be approximately 330 m (1100 ft).

$$D = \frac{P_S}{\rho_S \cdot g} \tag{1}$$

5.3. Concentration factor

The mass fraction of salt in ocean water is denoted as x_S. The concentration factor (CF) is the ratio of the mass fraction of salt in the concentrate stream to the mass fraction of the salt in the supply stream. The mass fraction of the salt in the permeate stream is considered to be zero for this analysis. So the concentration factor is given in equation (2)

$$CF = \frac{x_C}{x_S} \tag{2}$$

Performing a mass balance on the salt in the streams yields a relationship between the mass flow rate of the permeate and the concentration factor. This is expressed in equations (3) and (4) with $\dot{m}_P$ the mass flow rate of the permeate and $\dot{m}_C$ the mass flow rate of the concentrate.

$$\left(\dot{m}_P + \dot{m}_C\right) x_S = \dot{m}_C \cdot x_C \tag{3}$$

$$CF = \frac{\left(\dot{m}_P + \dot{m}_C\right)}{\dot{m}_C} = \frac{\dot{m}_P}{\dot{m}_C} + 1 \tag{4}$$

Since the maximum osmotic pressure during the process is proportional to the concentration factor the maximum osmotic pressure may be computed by equation (5) with Π the osmotic pressure.

$$\Pi_{\max} = CF \cdot \Pi_S \tag{5}$$

Another fraction used to quantify the percentage of water that is "recovered" into fresh water is called the recovery rate (RR). The recovery rate is defined in equation (6).

$$RR = \frac{\dot{m}_P}{\dot{m}_S} \tag{6}$$

In order to relate the recovery rate to the concentration factor, equation (4) is written substituting $\dot{m}_S$ for $\left(\dot{m}_P + \dot{m}_C\right)$ and $\left(\dot{m}_S - \dot{m}_P\right)$ for $\dot{m}_C$. The resulting expression is given in equation (7).

$$CF = \frac{\dot{m}_S}{\dot{m}_S - \dot{m}_P} \tag{7}$$

Equation (7) is manipulated into the form given in equation (8).

$$\frac{1}{CF} = \frac{\dot{m}_S - \dot{m}_P}{\dot{m}_S} = 1 - \frac{\dot{m}_P}{\dot{m}_S} \tag{8}$$

Using the definition of the recovery rate given in equation (6), the appropriate substitution is made into equation (8). The expression relating CF and RR is given in equation (9).

$$\frac{1}{CF} = 1 - RR \tag{9}$$

Equation (9) is then rearranged to solve for CF and RR. The results are given in equations (10) and (11).

$$RR = \left(1 - \frac{1}{CF}\right) \tag{10}$$

$$CF = \frac{1}{1 - RR} \tag{11}$$

5.4. Actual Required Depth

The supply pressure, P_S, is computed in terms of the concentration factor according to equation (12).

$$P_S = \Pi_{\max} + NDP = CF \cdot \Pi_S + NDP \tag{12}$$

The required depth, D, is computed by using equations (1) and (12) resulting in equation (13).

$$D = \frac{CF \cdot \Pi_S + NDP}{\rho_S \cdot g} \tag{13}$$

5.5. High Pressure Pump Work

For a given depth and distance to shore, the pressure and power requirements for the high pressure pump may be calculated. The required pressure P_9 is the sum of the head due to the elevation change and head loss, h_L, due to the transmission to shore. This is expressed in equation (14).

- $$P_9 = \rho_P \cdot g \cdot D + h_L \tag{14}$$

The pump power required deliver the fresh water from the permeate tank to the shore neglecting head losses, $\dot{W}_{HP1}$, is given by equation (15).

$$\dot{W}_{HP1} = \dot{V}_P \cdot \rho_P \cdot g \cdot D \tag{15}$$

Equation (16) gives the lift component of the high pressure pump on a per unit volume of permeate delivered basis.

$$w_{HP1,V} = \rho_P \cdot g \cdot D \tag{16}$$

Combining equations (13) and (16) gives the high pressure pump equation in terms of the concentration factor. The resulting equation is given as equation (17).

$$w_{HP1,V} = \frac{\rho_P}{\rho_S} \cdot \left(CF \cdot \Pi_S + NDP \right) \tag{17}$$

The head loss may be estimated using a friction factor determined by typical piping standards and characteristics. A typical optimized design velocity is 1 m/s (McGhee, Water Supply and Sewerage, 6). For this analysis, a medium sized RO desalination plant that will produce 50,000 $\frac{\mathrm{m}^3}{\mathrm{day}}$ is considered (Greenlee, 2009).

The friction factor, f, may be estimated in terms of pipe roughness, e, pipe diameter D_{pipe}, and the Reynolds number $\left(\mathrm{Re}\right)$ from the Colebrook correlation for turbulent flows which is given in equation (18). MATLAB code that performs iterations to compute the friction factor is given as Program 1 in Appendix A.

$$\frac{1}{f^{0.5}} = -2 \cdot \log\left(\frac{\frac{e}{D_{pipe}}}{3.7} + \frac{2.51}{\mathrm{Re} \cdot f^{0.5}} \right) \tag{18}$$

The Reynolds number (Re) depends on density (ρ), the dynamic viscosity (μ), and the velocity (v). The Reynolds number formula is given by equation (19).

$$\mathrm{Re} = \frac{\rho \cdot v \cdot D_{pipe}}{\mu} \tag{19}$$

The values of roughness, water density, and dynamic viscosity used for head loss calculations of fresh water delivered to shore are given in Table 4 (White, 1991).

Table 4: Head Loss Parameters

Parameter	Value Used
Roughness	0.046 mm
Density	1000 kg/m^3
Dynamic Viscosity	1.3 x 10^{-3} Pa·s
Temperature	30°C
Volumetric Flow Rate	50,000 m^3/day

Once the friction factor is determined, the pressure loss per unit length of pipe due to friction may be computed by equation (20).

$$\frac{\Delta P_L}{L_{Pipe}} = f \cdot \frac{\rho}{D_{Pipe}} \frac{v^2}{2} \tag{20}$$

In order to investigate the potential impact of pipe size on pumping power requirements, the pressure losses (per kilometer of pipe) are computed for pipe diameters varying from 0.4 m to 1 m. The pressure loss data are given in Figure 4. The work per unit length of pipe per unit volume pumped, W_L, required to overcome the line pressure loss, ΔP_L, is given in equation (21) in terms of the line pressure loss per unit length of pipe $\left(\frac{\Delta P_L}{L_{Pipe}} \right)$ and high pressure pump efficiency (η_{HP}). The work required to overcome friction to deliver a cubic meter of water a distance of 1 kilometer is given in Figure 5 for pipe diameters varying from 0.4 m to 1 m. The pipe diameter range is set based on the assumption that the optimal design velocity (including capital) is around 1 m/s. The code for these plots is given in as program 4.

$$\frac{W_L}{L_{Pipe} \cdot V_{Pumped}} = \frac{\Delta P_L}{\eta_{HP} \cdot L_{Pipe}} \tag{21}$$

These calculations show that for a plant size of 50,000 m^3/day, a 1 meter diameter pipe results in a flow velocity of 0.74 m/s, a head loss rate of 3.78 kPa/km, and a work rate of 1.21 x 10^{-3} kWh/m^3/km. Bathymetry data show ocean depths reach 1000 m within 50 km of shore in many places on all continents (NOAA , 2014). In select coastal regions occur much closer to shore. Based on a distance to shore of 50 km and a pipe diameter of 1 m, the horizontal pumping power requirement is 0.06 kWh/m^3. This work is less than 5% of the total work required to deliver fresh water to the surface (see chapter 5.7).

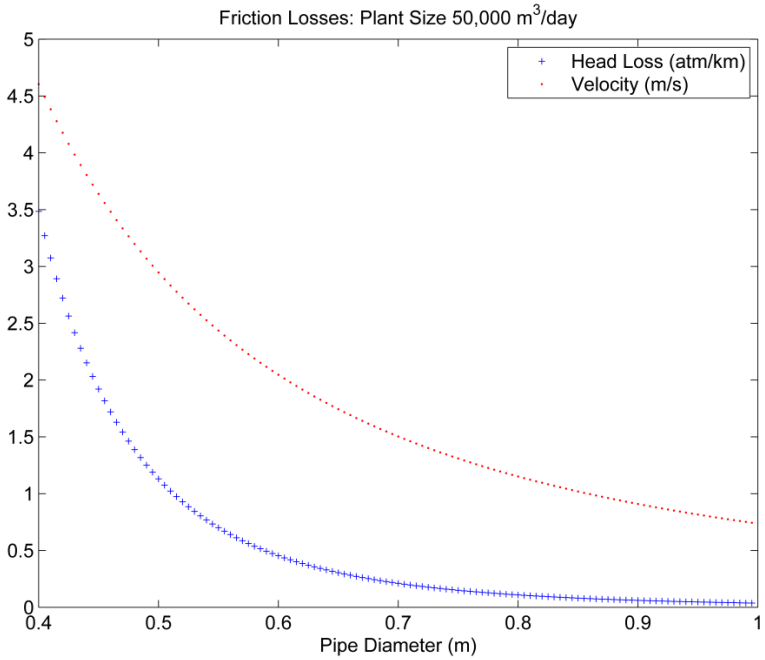

Figure 4: Friction Losses

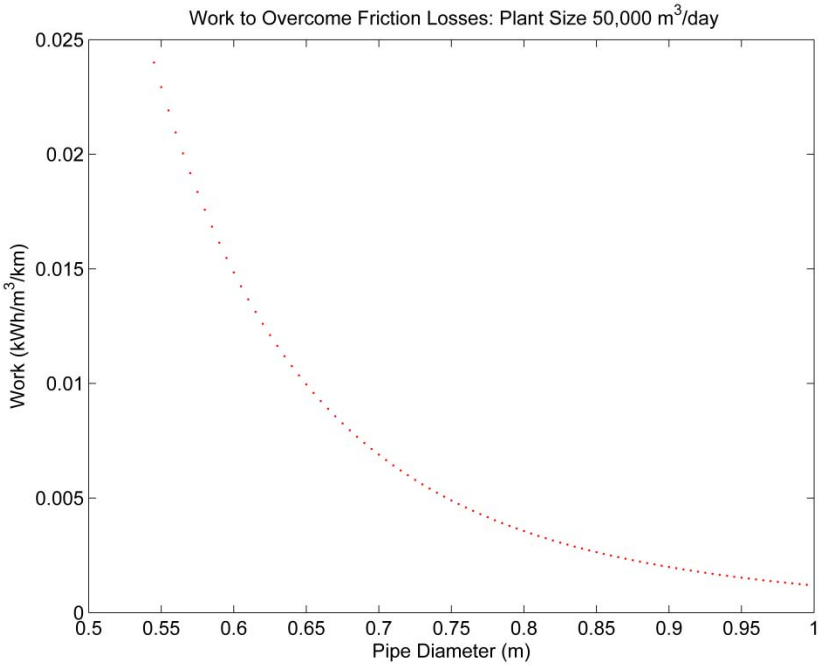

Figure 5: Work to Overcome Friction

5.6. Low Pressure Pump Work

The pump power required by the low pressure pump $\left(\dot{W}_{LP}\right)$ may be computed by equation (22).

$$\dot{W}_{LP} = \frac{\dot{V}_S \cdot \left(P_S - P_C\right)}{\eta_{LP}} \tag{22}$$

The low pressure pump rate equation is divided by the mass flow rate of permeate produced to yield equation (23). The density of the supply is denoted by ρ_S.

$$w_{LP} = \frac{\dot{m}_S \cdot \left(\Delta P_S\right)}{\rho_S \cdot \eta_{LP} \cdot \dot{m}_P} \tag{23}$$

The low pressure pump rate equation is divided by the mass flow rate of permeate produced and the specific volume is formulated as one over the density to yield equation (23), where w_{LP} is the low pressure pumper work per unit mass.

$$w_{LP} = \frac{\dot{m}_S \cdot \left(\Delta P_S\right)}{\rho_S \cdot \eta_{LP} \cdot \dot{m}_P} \tag{24}$$

Utilizing conservation of mass the work equation is modified to the form given in equation (25).

$$w_{LP} = \frac{1}{\rho_S \cdot \eta_{LP}} \cdot \left(\frac{\dot{m}_C}{\dot{m}_P} + 1 \right) \cdot \left(\Delta P_S \right) \tag{25}$$

The formulation given in equation (25) is then used with equation (8) to give a formula for low pressure work in terms of the concentration factor as defined in equation (26).

$$w_{LP} = \frac{1}{\rho_S \cdot \eta_{LP}} \cdot \left(\frac{CF}{CF - 1} \right) \cdot \left(\Delta P_S \right) \tag{26}$$

Equation (26) gives the work per unit mass of fresh water produced. In order to compute the work per unit volume produced, $w_{LP,V}$, the expression must be multiplied by the density of the water being produced. This product is reflected in equation (27).

$$w_{LP,V} = \frac{\rho_P}{\eta_{LP} \cdot \rho_S} \cdot \left(\frac{CF}{CF - 1} \right) \cdot \left(\Delta P_S \right) \tag{27}$$

5.7. Total Pump Work Excluding Shore Line Head Loss

In order to determine the concentration factor that minimizes pumping power, the total pumping work (per unit volume of permeate) is computed with equation (28). MATLAB programs to produce the results are given in Appendix A as Programs 4, 5, 6, and 7.

For Figure 6, four curves are produced for differential pressures ranging from 0.1 psi to 10 psi. A typical value for this differential is 5 psi or less, but the figure

shows the impact of a variation of this parameter due to fouling or change in design. These data may be used to estimate the savings potential of reducing the differential pressure by increasing the available flow area in the system. Figure 6 also shows that required work is more sensitive to changes in CF for values of CF that are less than the optimum value. Water property data used for the analysis are given in Table 5 5 (Bromley, 1974), (White, 1991).

Table 6 lists the optimum CF values for differential pressures of 1, 5 and 10 psi. These data show that, when operating at the optimum CF value, a change in differential pressure of 5 psi results in an energy requirement change of approximately 0.1 kWh/m^3. Further analysis will be performed for the typical differential pressure value of 5 psi. This differential pressure corresponds to an optimum CF value of 1.12 and a required work of 1.31 kWh/m^3.

$$w_{LP,V} + w_{HP1,V} = \frac{\rho_P}{\eta_{LP} \cdot \rho_S} \cdot \left(\frac{CF}{CF - 1} \right) \cdot \left(\Delta P_S \right) + \frac{\rho_P}{\eta_{HP} \cdot \rho_S} \cdot \left(CF \cdot \Pi_S + NDP \right) \qquad (28)$$

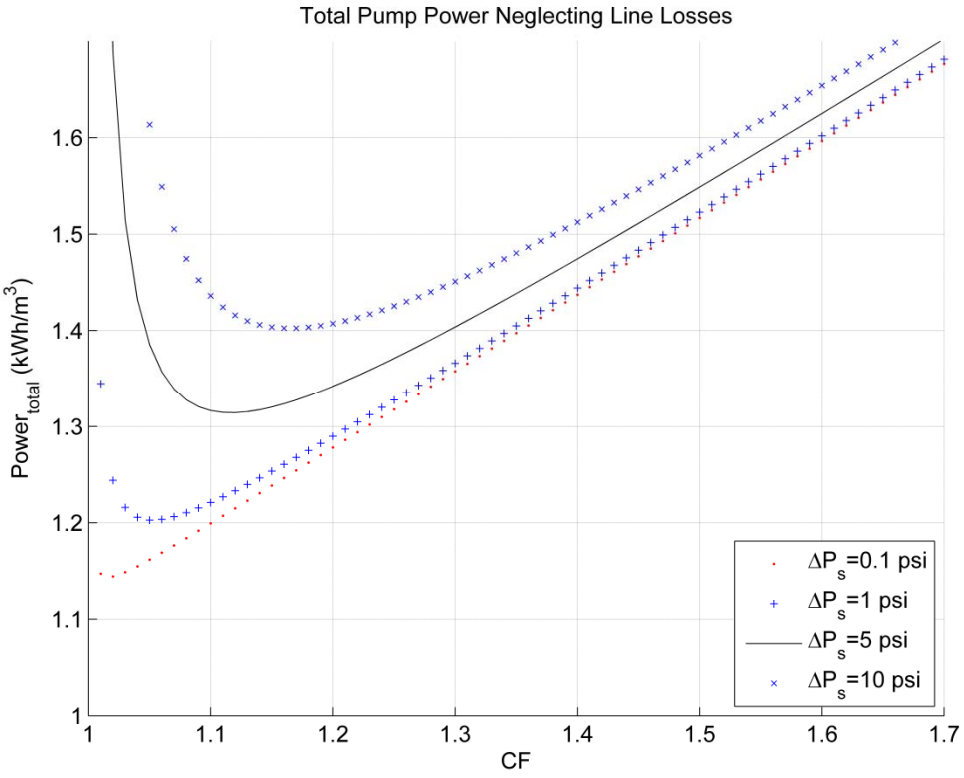

Figure 6: Total Pump Power Neglecting Line Losses

Table 5: Pumping Parameters for Work Computations

Parameter	Value Used
ρ_P	$1000 \frac{\text{kg}}{\text{m}^3}$
ρ_S	$1025 \frac{\text{kg}}{\text{m}^3}$
ΔP_S	1 psi, 5 psi , and 10 psi
NDP	7 atm
Π_S	26 atm
η_{LP}	0.86
η_{HP}	0.86

Data from (Bromley, 1974), (White, 1991)

Table 6: Optimum Concentration Factor

ΔP_S (psi)	CF_{best}	W_{min} (kWh/m^3)
0.1	1.02	1.14
1	1.05	1.20
5	1.12	1.31
10	1.17	1.40

6. Energy Analysis of the Traditional System

A simplified schematic for a traditional RO desalination plant is given in Figure 2. Traditional RO desalination plants operate near a coast and utilize surface seawater or brine water from a well. Plants utilizing surface seawater intake the seawater and pretreat the water. The supply is then pumped to a pressure around 7 atm above the osmotic pressure of the concentrate stream. Energy from the concentrate stream is then transferred by an energy recovery system to the supply stream. The efficiency of modern energy recovery devices is very high and approaches 95% (Greenlee, 2009). Due to capital costs and pumping power required to overcome the pressure differential (supply to concentrate), modern systems are typically designed to operate at a recovery rate of around 50% (Greenlee, 2009). The following analysis is performed to determine the minimum pumping power required to operate a traditional system at this typical recovery rate.

The pressure rise requirement of the pump, ΔP_{HP}, is given equation (29) .

$$\Delta P_{HP} = \Pi_{\max} + NDP + \Delta P_S = CF \cdot \Pi_S + NDP + \Delta P_S \tag{29}$$

For a system using an energy recovery device that has an efficiency of η_R and a pump that has efficiency η_{HP}, the required pumping power is given in equation (30).

$$\dot{W}_{HP} = \frac{\dot{V}_S \cdot \Delta P_{HP}}{\eta_{HP}} - \eta_R \cdot \dot{V}_C \cdot \left(\Delta P_{HP} - \Delta P_S \right) \tag{30}$$

The work requirement per unit volume of permeate produced is found by dividing equation (30) by the volumetric flow rate of permeate produced as shown in equation (31).

$$\frac{\dot{W}_{HP}}{\dot{V}_P} = \frac{\dot{V}_S}{\eta_{HP} \cdot \dot{V}_P} \cdot \Delta P_{HP} - \eta_R \cdot \frac{\dot{V}_C}{\dot{V}_P} = \frac{\dot{V}_S}{\dot{V}_P} \cdot \Delta P_{HP} - \eta_R \cdot \frac{\dot{V}_S - \dot{V}_P}{\dot{V}_P} \cdot \left(\Delta P_{HP} - \Delta P_S \right) \tag{31}$$

Using the definition of the recovery rate (RR), substitutions are made to simplify the expression given above. The work per unit volume for the traditional system is then given in its final form in equation (32).

$$w_{\mathrm{HP},v} = \frac{\dot{W}_{TS}}{\dot{V}_P} = \frac{1}{\eta_{HP} \cdot RR} \cdot \Delta P_{HP} - \eta_R \cdot \left(\frac{1}{RR} - 1 \right) \cdot \left(\Delta P_{HP} - \Delta P_S \right) \tag{32}$$

Assumed values used for computing the work requirement are given in Table 7. MATLAB code used to compute the work and concentration factor for this case is given in Appendix A as Program 1.

Table 7: Traditional System Assumed Constants

Parameter	Value Used
ρ_P	$1000\frac{\text{kg}}{\text{m}^3}$
ρ_S	$1025\frac{\text{kg}}{\text{m}^3}$
ΔP_S	5 psi (34.5 kPa)
RR	50%
Π_S	26 atm
ΔP_T	7 atm
η_{HP}	0.86
η_R	0.97

Data from (Bromley, 1974), (Greenlee, 2009)

Table 8 gives the computed data from Program 1. The data show that for a recovery rate of 50% that the concentration factor is 2.05. For the assumptions given in Table 8, the pumping work required is 2.3 kWh/m^3. This computation assumes that the energy recovered from the concentrate stream is used to offset the power requirement of the pump. The work number given for the required work is the net requirement after credit is given for energy recovery.

Table 8: Traditional System Computed Values

Parameter	Value Computed
CF	2.05
$w_{TS,v}$	$2.3\ \frac{\text{kWh}}{\text{m}^3}$

7. Generalized Minimum Work Requirements

The previous chapter contains an energy analysis of a specific submerged reverse osmosis system. In order to compute data for absolute minimum work requirements of filter separation, two approaches are presented in this chapter. Method one utilizes the second law of thermodynamics and the Gibb's function; this method has been published by (Mistry, 2013). Mistry's results are repeated, and a second method using osmotic pressure and the first law of thermodynamics to compute the minimum work is presented.

The effect on efficiency of adding stages to a traditional reverse system is also presented. The thermodynamic model of the multistage system using osmotic pressure to compute work requirements is modified to include the effects of non-ideal pumping and energy recovery.

7.1. Gibbs Function and Second Law Computations

In order to develop a measure of the minimum work that must be provided to desalinate water, the first and second law is applied. Figure 7 illustrates a control volume for an arbitrary desalination plant. It includes 1 inlet stream which is the salt water supply and two outlet streams. One outlet stream is pure water and the other is a concentrated salt water stream. It is located in an area where the environment

temperature and pressure are T_0 and P_0 respectively. Keeping the apparatus and environmental conditions arbitrary, a heat term, $\dot{Q}_0$, is shown flowing into the boundary. The work that must be supplied to the apparatus is given as $\dot{W}_{\min}$.

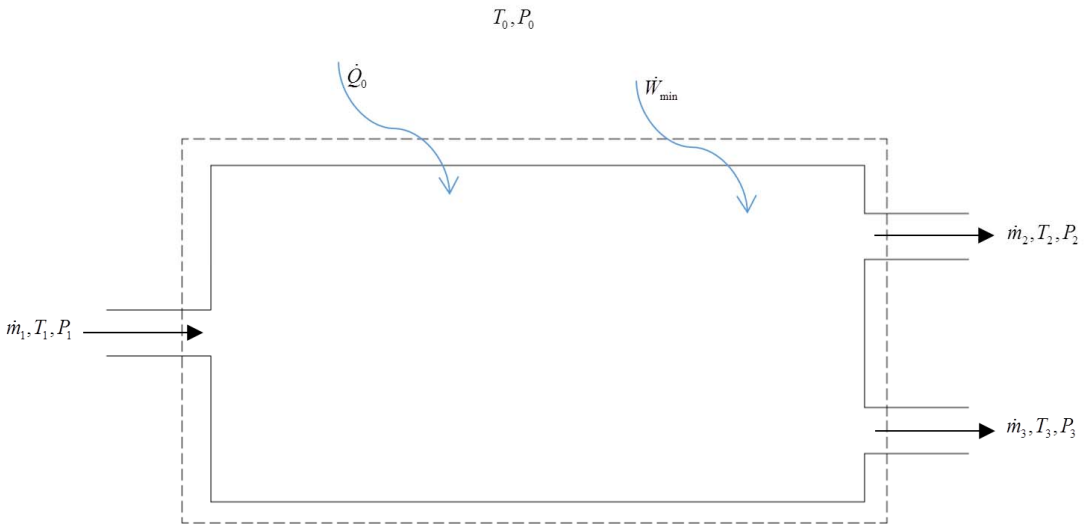

Figure 7: Desalination Control Volume

The first law, for the apparatus shown in Figure 7, is then given by equation (33).

$$\dot{Q}_0 + \dot{W}_{\min} + \dot{m}_1\left(h_1 + \frac{v_1^2}{2} + g \cdot z_1\right) - \dot{m}_2\left(h_2 + \frac{v_2^2}{2} + g \cdot z_2\right) - \dot{m}_3\left(h_3 + \frac{v_3^2}{2} + g \cdot z_3\right) = \left(\frac{dE}{dt}\right)_{\text{system}} \tag{33}$$

Assuming steady state, negligible kinetic energy, and negligible potential energy in the flows, the first law simplifies to equation (34).

$$\dot{Q}_0 + \dot{W}_{\min} + \dot{m}_1 \cdot h_1 - \dot{m}_2 \cdot h_2 - \dot{m}_3 \cdot h_3 = 0 \tag{34}$$

To apply the second law, an entropy balance, for the apparatus shown in Figure 7, is given in equation (35).

$$\frac{\dot{Q}_0}{T_0} + \dot{m}_1 \cdot s_1 - \dot{m}_2 \cdot s_2 - \dot{m}_3 \cdot s_3 + \dot{S}_{gen} = \left(\frac{dS}{dt}\right)_{\text{system}} \tag{35}$$

In order to minimize the work required, all processes within the device are assumed to be reversible. Therefore the entropy generation within the device, $\dot{S}_{gen}$, is zero. Assuming steady state conditions and solving equation (35) for the heat term yields equation (36).

$$\dot{Q}_0 = T_0\left(-\dot{m}_1 \cdot s_1 + \dot{m}_2 \cdot s_2 + \dot{m}_3 \cdot s_3\right) \tag{36}$$

Substituting equation (36) into equation (34) and solving for $\dot{W}_{\min}$ yields equation (37).

$$\dot{W}_{\min} = -\dot{m}_1\left(h_1 - s_1 T_0\right) + \dot{m}_2\left(h_2 - s_2 T_0\right) + \dot{m}_3\left(h_3 - s_3 T_0\right) \tag{37}$$

Assuming the inlet and exit streams are in thermal equilibrium with the surroundings equation (37) simplifies to equation (38).

$$\dot{W}_{\min} = -\dot{m}_1\left(h_1 - s_1 T_1\right) + \dot{m}_2\left(h_2 - s_2 T_2\right) + \dot{m}_3\left(h_3 - s_3 T_3\right) \tag{38}$$

The definition of the Gibbs function, $\hat{g}$, is given in equation (39).

$$\hat{g} \equiv h - Ts \tag{39}$$

Substituting equation (39) into equation (38) yields equation (40).

$$\dot{W}_{\min} = -\dot{m}_1 \cdot \hat{g}_1 + \dot{m}_2 \cdot \hat{g}_2 + \dot{m}_3 \cdot \hat{g}_3 \tag{40}$$

In Figure 7 stream 1 is the supply stream, stream 2 is the pure water or permeate stream, and stream 3 is the concentrate or waste stream. The recovery rate is then given in equation (41).

$$RR = \frac{\dot{m}_2}{\dot{m}_1} \tag{41}$$

Applying conservation of mass yields equation (42).

$$\left(\frac{dm}{dt}\right)_{sys} = \dot{m}_1 - \dot{m}_2 - \dot{m}_3 \tag{42}$$

Applying the steady state condition to equation (42) and solving for the mass flow rate of the waste stream yields equation (43).

$$\dot{m}_3 = \dot{m}_1 - \dot{m}_2 \tag{43}$$

Solving equation (41) for the supply mass flow rate and substituting into equation (43) gives equation (44).

$$\dot{m}_3 = \frac{\dot{m}_2}{RR} - \dot{m}_2 = \dot{m}_2\left(\frac{1}{RR} - 1\right) \tag{44}$$

Now equation (40) is rewritten in terms of the recovery rate and the mass flow rate of the permeate. This expression is given in equation (45).

$$\dot{W}_{\min} = -\frac{\dot{m}_2}{RR} \cdot \hat{g}_1 + \dot{m}_2 \cdot \hat{g}_2 + \dot{m}_2 \left(\frac{1}{RR} - 1 \right) \cdot \hat{g}_3 \tag{45}$$

The power equation given in (45) is divided by the mass flow rate of the permeate. The work per unit mass of pure water produced, w_{gibbs}, is given in equation (46).

$$w_{gibbs} = \frac{\dot{W}_{\min}}{\dot{m}_2} = -\frac{\hat{g}_1}{RR} + \hat{g}_2 + \left(\frac{1}{RR} - 1 \right) \cdot \hat{g}_3 \tag{46}$$

Using equation (46) and thermodynamic property calculators (MATLAB) available at http://web.mit.edu/seawater/, the Mistry's minimum work plots are verified in Figure 8. The MATLAB code is presented in Appendix A as Program 8.

7.2. Minimum Work Computed with Osmotic Pressure

For separation by reverse osmosis driven by pumping power, the power required assuming reversible ideal pumping and reversible ideal energy recovery is calculated. In Figure 9, salt water enters at 1 and is pumped into a single stage RO unit. Permeate is produced and discharged at 3. The waste stream flows through the ideal recovery device. The first and second laws are applied to the pump and recovery turbine to give equations 15 and 16 for the isentropic work rates. The pressure at states 1, 3, and 5 is equivalent to P_0. The pump must boost the pressure of the supply stream sufficiently to drive the reverse osmosis process throughout the RO unit. This means that the pressure at 2 must exceed the pressure at 3 by at least the osmotic pressure of the discharge stream (at 4). The minimum power required by

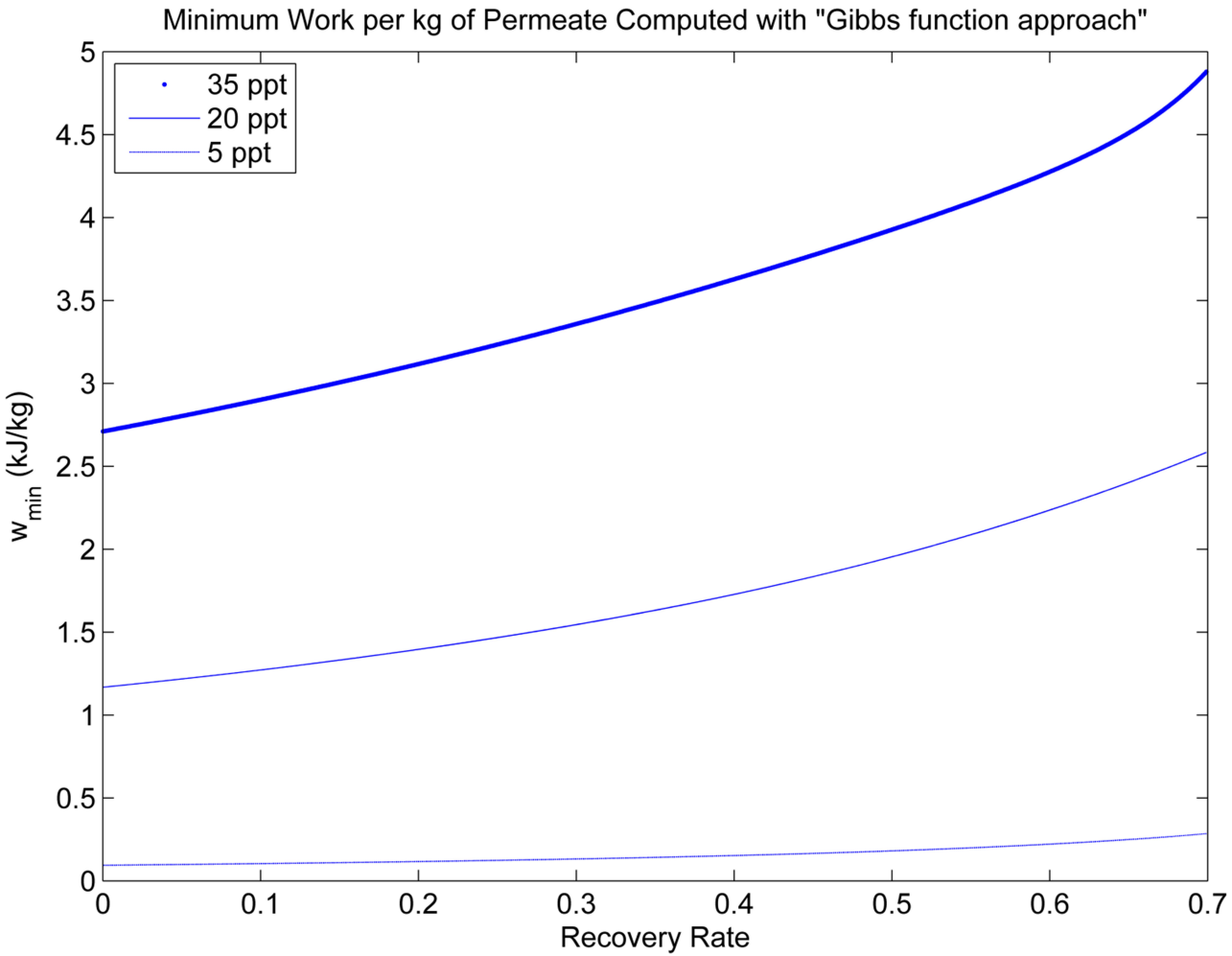

Figure 8: Minimum RO Work via Gibbs

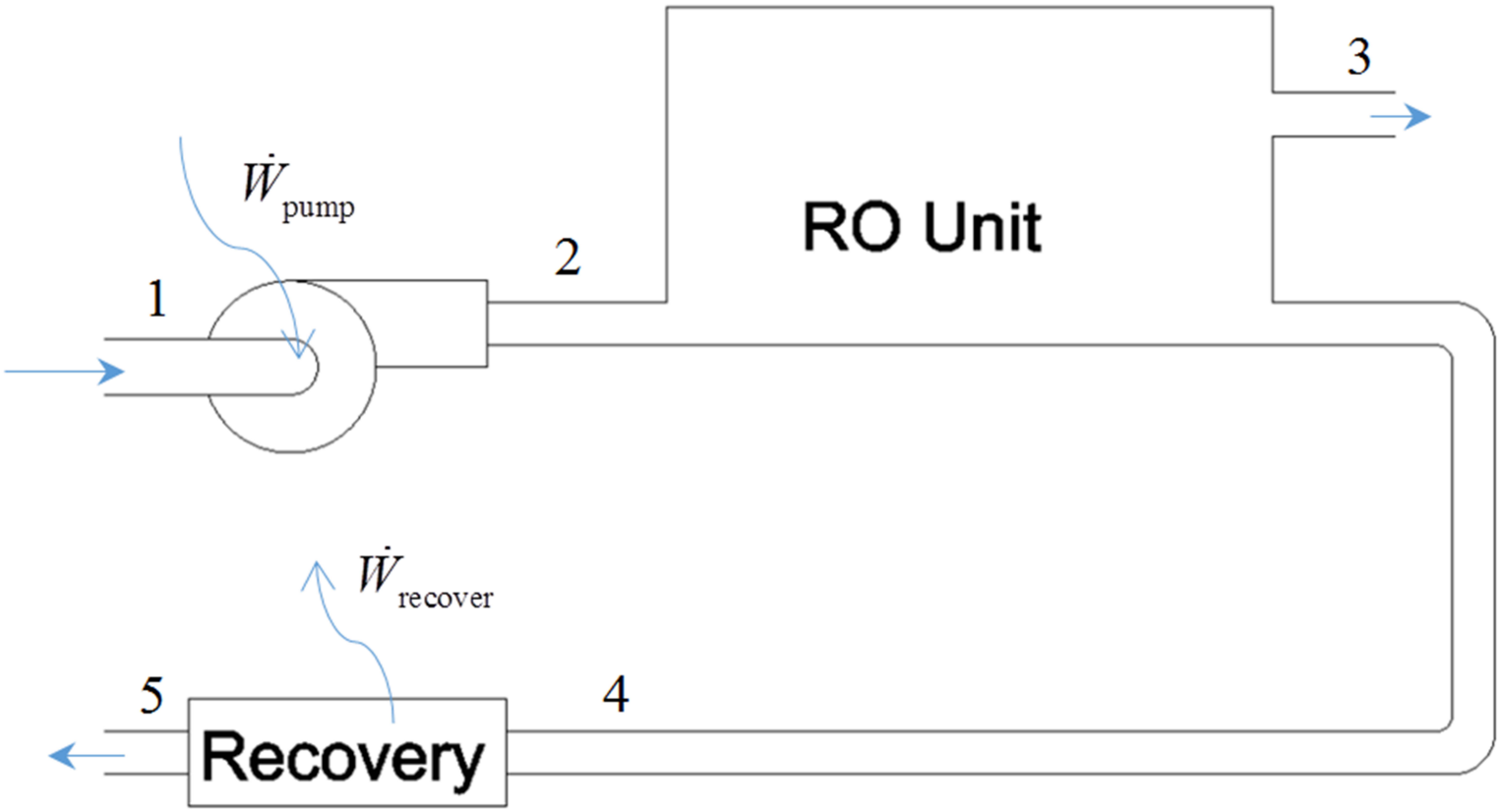

Figure 9: Single Stage RO Control Volume

the pump, $\dot{W}_{\mathrm{HP,min}}$, and maximum power recovered by the recovery device, $\dot{W}_{\mathrm{R,max}}$, are given in equations (47) and (48) respectively where υ is the specific volume of the water.

$$\dot{W}_{\mathrm{HP,min}} = \upsilon \cdot \dot{m}_1 \cdot \left(\Pi_4\right) \tag{47}$$

$$\dot{W}_{\mathrm{R,max}} = \upsilon \cdot \dot{m}_5 \cdot \left(\Pi_4\right) \tag{48}$$

The net power required, $\dot{W}_{\mathrm{net,min}}$, is calculated by taking the difference of the pump power and recovery power in equation (49).

$$\dot{W}_{\mathrm{net,min}} = \upsilon \cdot \left(\Pi_4\right)\left(\dot{m}_1 - \dot{m}_5\right) \tag{49}$$

Applying conservation of mass equation (49) is rewritten as equation (50).

$$\frac{\dot{W}_{\mathrm{net,min}}}{\dot{m}_3} = \upsilon \cdot \left(\Pi_4\right) \tag{50}$$

A mass balance is performed on the salt ions entering and leaving the RO unit, equation (51) gives the concentration of the waste stream, x_3, as a function of the recovery rate and the inlet concentration.

$$x_3 = \frac{1}{1 - \frac{1}{RR}} x_1 \tag{51}$$

Therefore, in order to compute the minimum work required to perform reverse osmosis, a method to estimate the osmotic pressure as a function of salt concentration is sought. One method to estimate the osmotic pressure is to use van't Hoff's Law which is given by equation (52).

$$\prod = R \cdot T \cdot M_{\text{ion}} \tag{52}$$

Van't Hoff's Law states that the osmotic pressure is proportional to the molar concentration of ions in the water, M_{ion}, the universal gas constant, R, and the temperature, T. Data are available to apply a correction factor (the osmotic coefficient, Φ) to van't Hoff's Law. This correction is formulated in equation (53).

$$\prod_{\text{corrected}} = \Phi \cdot R \cdot T \cdot M_{\text{ion}} \tag{53}$$

Data for the ionic concentration of standard seawater (35 ppt) are available on the CDIAC website (http://cdiac.ornl.gov/). These data are presented in Table 9.

Table 9: Ionic Molar Concentration of Seawater

Ion	Concentration (mol/L)
Cl^-	0.546
Na^+	0.469
Mg^{2+}	0.0528
SO_4^{2-}	0.0282
Ca^{2+}	0.0103
K^+	0.0102
CO_2	0.00001
HCO_3	0.00177
CO_3	0.00026
Br^-	0.000844
$B(OH)_3$	0.00032
$B(OH)_4^-$	0.0001
Sr^{2+}	0.000091
F^-	0.000068
Total	**1.119963**

The osmotic coefficient, Φ, is a function of temperature and concentration. Data and calculators for the osmotic coefficient are available. The MATLAB calculator maintained at http://web.mit.edu/seawater/ is used in this work.

Since data are available for seawater at 35 ppt, the molarity of seawater at any concentration is estimated by multiplying the standard molarity, $M_{\text{ion},35}$, by ratio of the actual concentration, PPT, and standard concentration, 35 ppt. This formula is presented as equation (54).

$$M_{\text{ion}} = M_{\text{ion},35} \frac{\text{PPT}}{35} \tag{54}$$

Substituting equation (54) into equation (53) yields equation (55). These formulations are implemented in Program 9 and presented in Appendix A.

$$\prod_{\text{corrected}} = \Phi \cdot R \cdot T \cdot M_{\text{ion},35} \cdot \frac{\text{PPT}}{35} \tag{55}$$

The osmotic pressures calculated with equation **(55)** are compared to results produced by Bromley at 25 °C for concentrations varying from 10 ppt to 120 ppt in Table 10. These data show the osmotic pressure calculator used in this work produces pressure estimates that are consistently lower than those presented by Bromley. The data in the table show good agreement between two estimates of osmotic pressure up to concentrations of 40 ppt (within 3.1%). At higher concentrations, the predicted values are less consistent and have a difference of up to 11.8%. It is not clear which osmotic pressure data are more accurate. However, in the range of brackish water (10 ppt) to open seawater (35 ppt) the two data sets are

closely aligned. In performing analysis to compare two desalination methods it is important to use the same osmotic pressure data for both analyses. Any error introduced by the osmotic pressure data will then push the solution of both analyses (e.g. total energy required) in same direction and minimize the error in the difference or comparison of the two desalination methods.

Table 10: Osmotic Pressure Calculator Results—25 °C

Concentration (ppt)	$P_{Bromley}$ (atm)	$P_{calculated}$ (atm)	Difference
10	7.1	7.05	0.7%
12	14.27	14.12	1.1%
34.5	25.11	24.47	2.5%
40	29.38	28.46	3.1%
60	45.86	43.32	5.5%
80	64.06	59.01	7.9%
100	84.3	75.85	10.0%
120	106.8	94.15	11.8%

In order to compute the absolute minimum work requirement for desalination by RO, multiple stage RO is considered. Figure 10 illustrates an n-stage reverse osmosis setup with energy recovery. It is drawn with intercooling between stages to

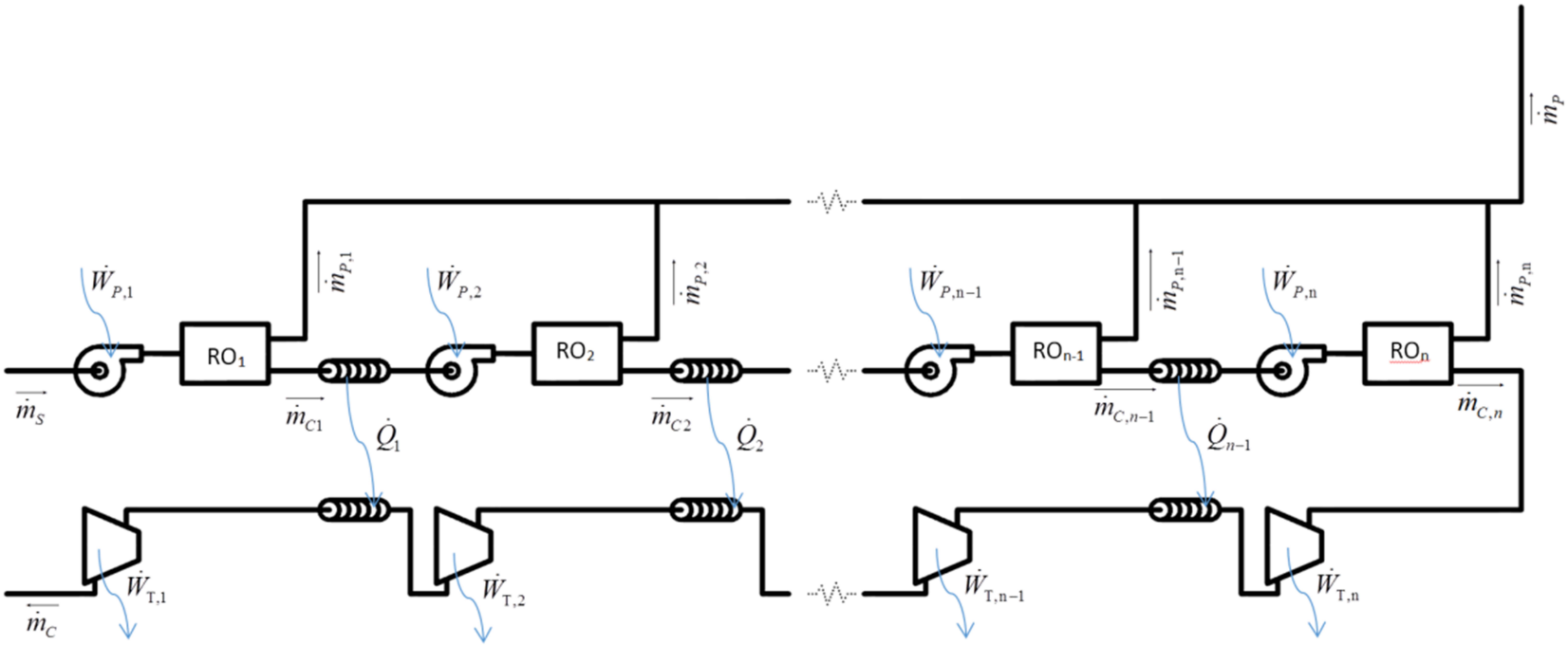

Figure 10: Multiple Stage Reverse Osmosis

accommodate isothermal pumping and isothermal energy recovery in the turbines. The reversible pump and turbine work may be computed with equation (56).

$$w = \int v dP \tag{56}$$

The water is assumed to be incompressible, so the pump power for the nth pump, $\dot{W}_n$, becomes equation (57).

$$\dot{W}_n = \dot{m}_{c,n-1} \cdot v_{c,n-1} \cdot \left(\Pi_{c,n} - \Pi_{c,n-1} \right) \tag{57}$$

Taking the pressure at the inlets and exits of the total system to be P_0, the total pumping power, $\dot{W}_{HP,total}$, may be computed by equation (58).

$$\dot{W}_{HP,total} = \dot{m}_s \cdot v_s \cdot \left(\Pi_2 \right) + \sum_{n=2}^{n} \left(\dot{m}_{c,n-1} \cdot v_{c,n-1} \cdot \left(\Pi_{c,n} - \Pi_{c,n-1} \right) \right) \tag{58}$$

Letting the salinity of the permeate be zero, a mass balance is performed on the total dissolved solids entering and exiting the first n stages of the system. This balance is given in equation (59).

$$\dot{m}_s \cdot x_s = \dot{m}_{c,n} \cdot x_{c,n} \tag{59}$$

Solving the mass balance for the mass flow rate of concentrate gives equation (60).

$$\dot{m}_{c,n} = \dot{m}_s \cdot \frac{x_s}{x_{c,n}} \tag{60}$$

Now the flow rate for the nth pump may be computed with equation (60), and the total pump power may be computed with equation (61).

$$\dot{W}_{HP,total} = \dot{m}_s \cdot v_s \cdot \left(\Pi_2\right) + \sum_{n=2}^{n} \left(\dot{m}_s \cdot \frac{x_s}{x_{c,n-1}} \cdot v_{c,n-1} \cdot \left(\Pi_{c,n} - \Pi_{c,n-1}\right) \right) \tag{61}$$

The recovery rate is defined in equation (62).

$$RR = \frac{\dot{m}_P}{\dot{m}_s} \tag{62}$$

Using the definition of the recovery rate presented equation (61) the work per unit mass of permeate delivered, $w_{HP,total}$, is given in equation (63).

$$w_{HP,total} = \frac{\dot{W}_{HP,total}}{\dot{m}_P} = \frac{v_s}{RR} \cdot \left(\Pi_2\right) + \sum_{n=2}^{n} \left(\left(\frac{1}{RR} \right) \cdot \frac{x_s}{x_{c,n-1}} \cdot v_{c,n-1} \cdot \left(\Pi_{c,n} - \Pi_{c,n-1}\right) \right) \tag{63}$$

Using equation (56) the formula for energy recovered from the waste stream may be developed. Since the concentration of the waste stream is constant through the entire recovery section and the expansion is isothermal, the specific volume is considered to be constant. The total power recovered by the turbine, $\dot{W}_R$, is given in equation (64).

$$\dot{W}_R = \dot{m}_c \cdot v_c \cdot \left(\Pi_c\right) \tag{64}$$

Conservation of mass is applied to the multiple stage RO in equation (65)

$$\dot{m}_s = \dot{m}_P + \dot{m}_c \tag{65}$$

Equation (65) is combined with the definition of the recovery rate to yield the mass flow rate of the concentrated stream in terms of mass flow rate of the permeate. This expression is given in equation (66).

$$\dot{m}_c = \dot{m}_s - \dot{m}_p = \dot{m}_p \left(\frac{1}{RR} - 1 \right) \tag{66}$$

Combining equations (64) and (66) yields the work per unit mass of permeate produced. This expression is given in equation (67).

$$w_R = \frac{\dot{W}_R}{\dot{m}_p} = \left(\frac{1}{RR} - 1 \right) \cdot v_c \cdot \left(\Pi_c \right) \tag{67}$$

The net work required to deliver permeate is then formulated in equation (68)

$$\begin{aligned} w_{\min} &= w_{HP,total} - w_R \\ &= \frac{v_s}{RR} \cdot \left(\Pi_2 \right) + \sum_{n=2}^{n} \left(\left(\frac{1}{RR} \right) \cdot \frac{x_s}{x_{c,n-1}} \cdot v_{c,n-1} \cdot \left(\Pi_{c,n} - \Pi_{c,n-1} \right) \right) - \left(\frac{1}{RR} - 1 \right) \cdot v_c \cdot \left(\Pi_c \right) \end{aligned} \tag{68}$$

Equation (68) is used with 1000 stages (practically infinite stages) of reverse osmosis to find the minimum work required. The results are given in Figure 11 for a supply concentration of 20 ppt and Figure 12 for a supply concentration of 35 ppt. Equation (68) requires estimates for the osmotic pressure at various salt concentration levels. The computations are performed using equation (55). The curve corresponded to this approach is labeled w_{pdv} . Equation (68) is also used with osmotic pressures reported by Bromley found in Table 10. Linear interpolation is applied to the Bromley data to estimate the osmotic pressure between given data

values. The results of the work computations using the Bromley values for osmotic pressure are plotted in Figure 11 and Figure 12. The curves are labeled $w_{pdv,Bromley}$. The code used to produce these plots is presented as Program 10 in Appendix A.

The work estimates computed from the Gibbs function as formulated in equation (46) are also plotted in Figure 11 and Figure 12. These plots show some inconsistency between the estimated work values. For example, the minimum work values for the different formulations are given in Table 11. These values correspond to a recovery rate approaching zero and deviate from each other by as much as 20%.

The discrepancies in the work estimates may be explained by error analysis of the property estimates. For example, the Gibbs function provided has an error limit of plus or minus 0.5%. The impact of this error is magnified at low recovery rates. To illustrate this concept maximum and minimum values for a given computed value of the Gibbs function are given in equation (69).

$$\begin{aligned} \hat{g}_{\mathrm{i,max}} &= \hat{g}_{\mathrm{i}} \cdot (1.005) \\ \hat{g}_{\mathrm{i,min}} &= \hat{g}_{\mathrm{i}} \cdot (0.995) \end{aligned} \tag{69}$$

Error bands are then created by computing the work using the maximum error assumption for the Gibbs function as formulated in equations (70) and (71). These functions are also plotted in Figure 11 and Figure 12. The figures show that the work calculations are extremely sensitive to error for low recovery rates. The code used to perform these calculations is presented as Program 10 in Appendix A.

$$w_{gibbs,\max} = -\frac{\hat{g}_{1,\max}}{RR} + \hat{g}_{2,\min} + \left(\frac{1}{RR} - 1\right) \cdot \hat{g}_{3,\min} \tag{70}$$

$$w_{gibbs,\min} = -\frac{\hat{g}_{1,\min}}{RR} + \hat{g}_{2,\max} + \left(\frac{1}{RR} - 1\right) \cdot \hat{g}_{3,\max} \tag{71}$$

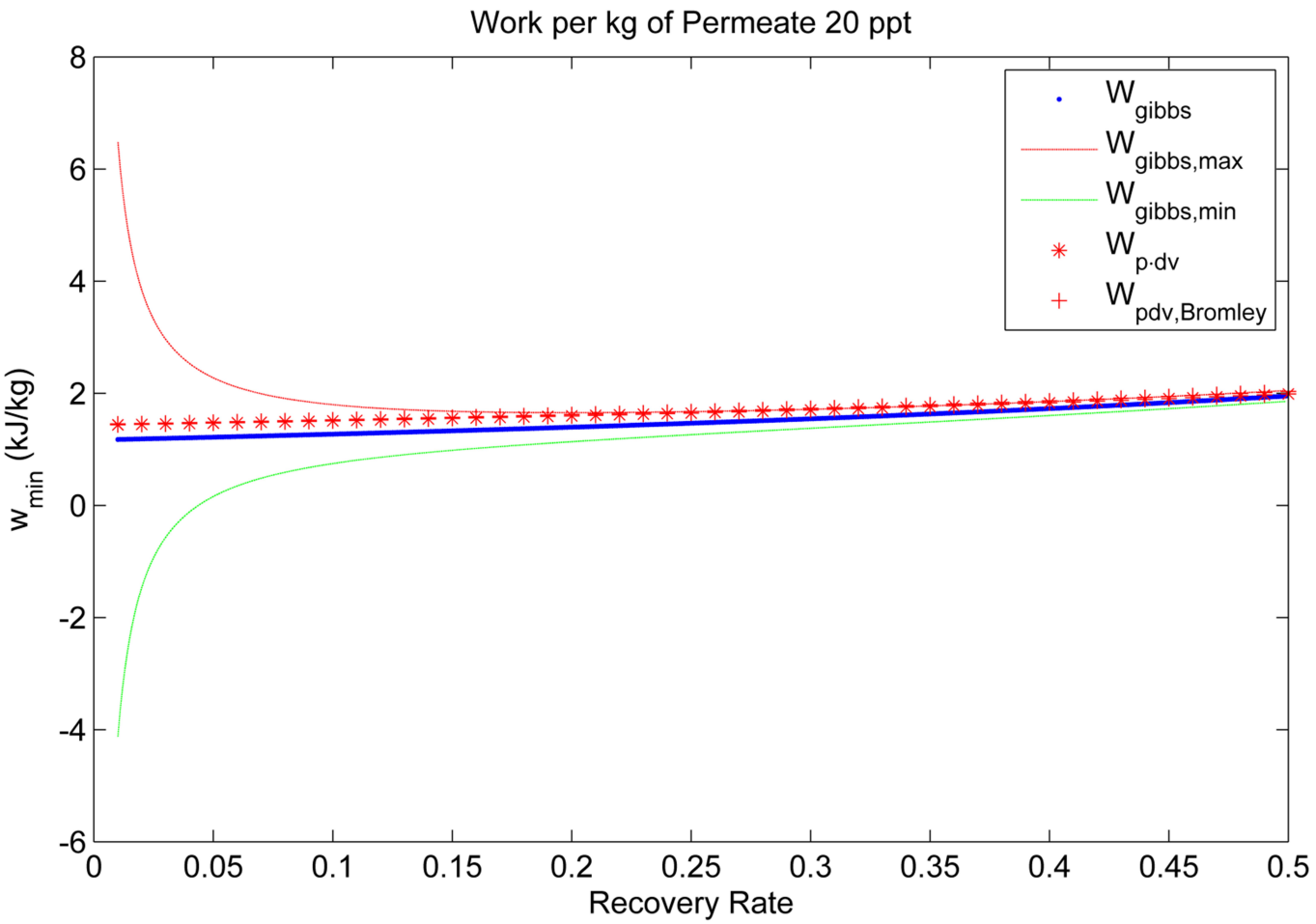

Figure 11: Minimum Work Comparisons 20

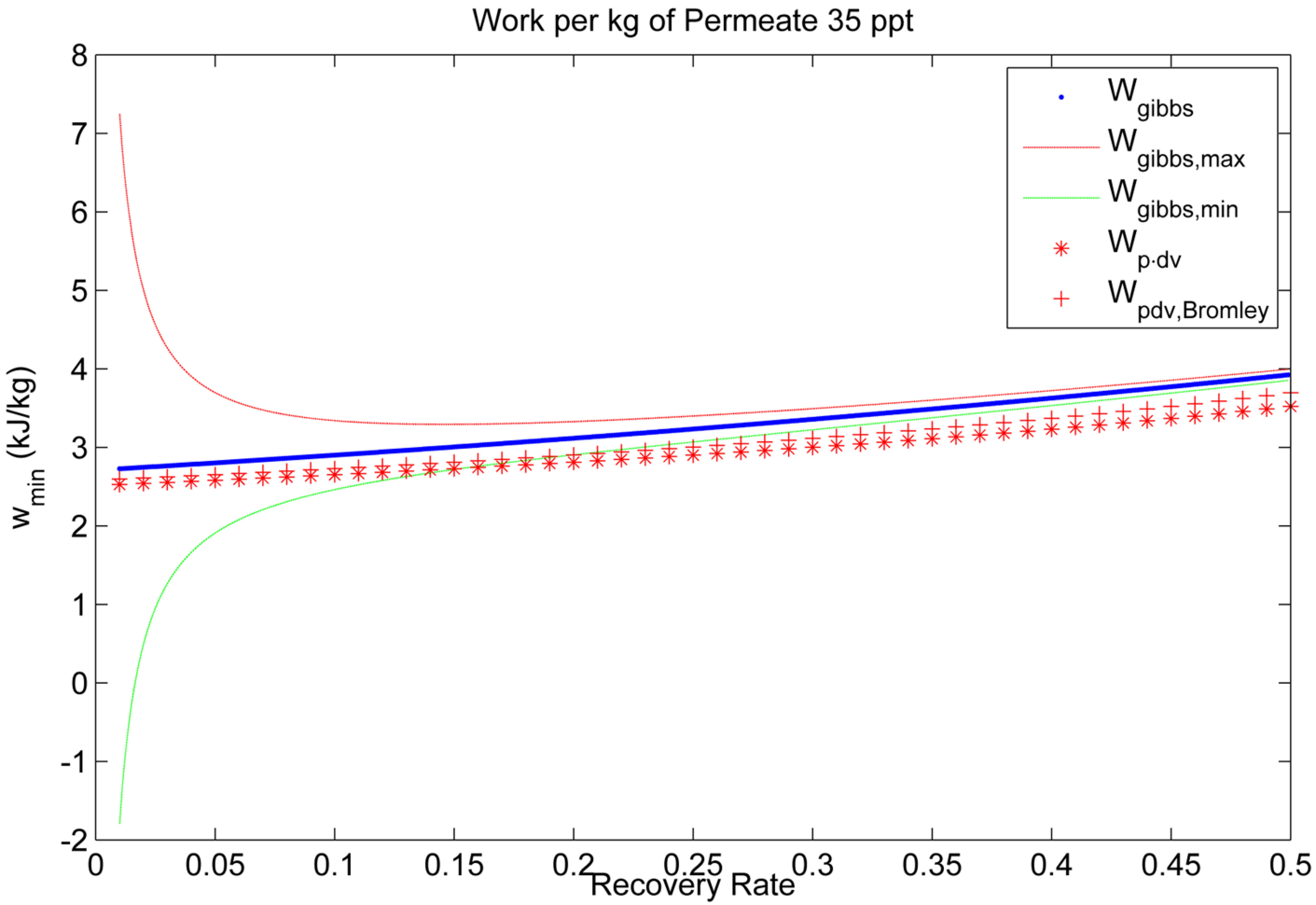

Figure 12: Minimum Work Comparisons 35

Table 11: Minimum Work Comparison

Concentration	Recovery Rate	W_{Gibbs}	W_{vdP}
(ppt)	(kg/kg)	kJ/kg	kJ/kg
20	0.01	1.18	1.44
35	0.01	2.73	2.53

7.3. Work Comparison of Submerged and Conventional Multistage RO--Idealized Equipment

With the proposed submerged reverse osmosis desalination system, if the flow losses due to friction in supply to concentrate stream are neglected, the only power required is for the pump that delivers the permeate to the surface. For the ideal case, it is also assumed that the reverse osmosis membrane is perfect and no net driving pressure is needed for good permeate production. Therefore, the work require per unit of permeate delivered, $w_{submerged,ideal}$, is given in equation (72).

$$w_{submerged,ideal} = \frac{\dot{W}_{HP}}{\dot{m}_p} = v_P \cdot \left(\Pi_c\right) \tag{72}$$

Since frictional losses are neglected in equation (72), the least total work will coincide with recovery rate that approaches zero and a pressure requirement that

approaches the osmotic pressure of the supply. So equation (72) is rewritten as equation (73).

$$w_{submerged,ideal} = \frac{\dot{W}_{HP}}{\dot{m}_p} = v_P \cdot \left(\Pi_S\right) \tag{73}$$

Equations (68) and (73) are used to compare the required work per unit permeate for a traditional reverse osmosis setup with varying stages to the requirement for the proposed system. The results are shown in Figure 13. As illustrated, the ideal submerged system achieves the same minimum power as a traditional idealized one stage system. However, the traditional system requires energy recovery. The plots in Figure 13 are produced with Program 11 in Appendix A by setting the pump and recovery turbine efficiencies to 1.

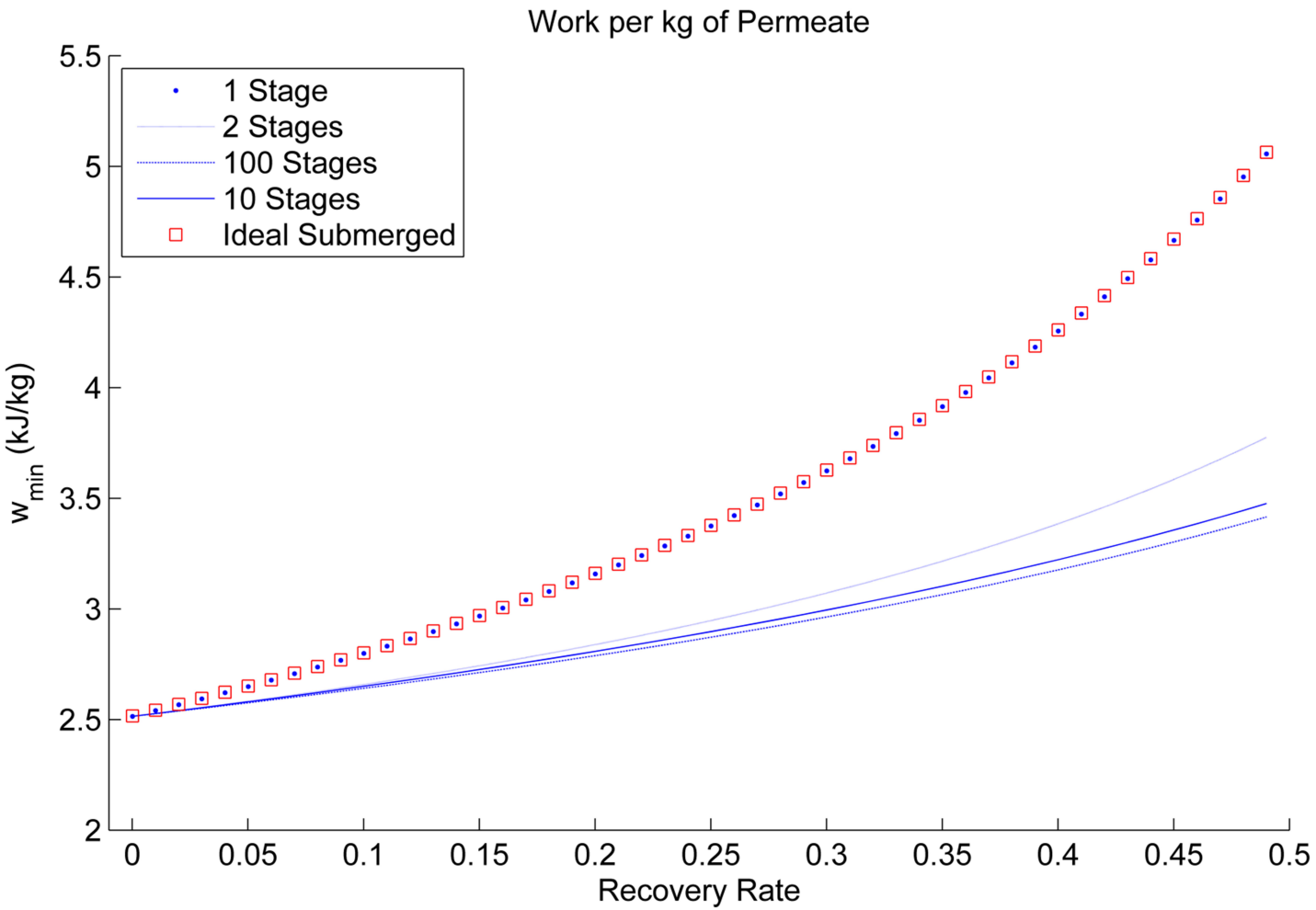

Figure 13: Multiple Stage RO with Ideal Recovery vs Submerged RO—35 ppt

7.4. Work Comparison of Submerged and Conventional Multistage RO--Real Equipment

For non-ideal pumping and energy recovery, the optimum recovery rate will not approach zero. Assuming frictionless flow, the non-ideal work for the n-stage reverse osmosis system, $w_{stage,real}$, may be computed by modifying equation (68). The resulting formulation is given in equation (74).

$$\begin{aligned} w_{stage,real} &= \frac{w_{HP,\min}}{\eta_{HP}} - w_{\mathrm{R,max}} \cdot \eta_R \\ &= \left(\frac{1}{\eta_{HP}}\right)\left[\frac{v_s}{RR}\cdot\left(\Pi_2\right) + \sum_{n=2}^{n}\left(\left(\frac{1}{RR}\right)\cdot\frac{x_s}{x_{c,n-1}}\cdot v_{c,n-1}\cdot\left(\Pi_{c,n}-\Pi_{c,n-1}\right)\right)\right] \\ &\quad -\left(\eta_R\right)\cdot\left(\frac{1}{RR}-1\right)\cdot v_c\cdot\left(\Pi_c\right) \end{aligned} \tag{74}$$

For the submerged reverse osmosis system, when frictional losses are neglected, only one pump is required. The required pump must deliver enough work to the permeate to move it to the surface. Applying pump efficiency to equation (72) yields equation (75) which gives appropriate non-ideal work, $w_{submerged,\mathrm{real}}$. Equations (74) and (75) are implemented in Program 11 which is presented in Appendix A.

$$w_{submerged,\mathrm{real}} = \frac{v_P\cdot\left(\Pi_c\right)}{\eta_{HP}} \tag{75}$$

The results are plotted in Figure 14. This shows that the minimum work for the traditional multistage system is around 5 kJ/kg and occurs with a recovery rate of approximately 40%. The proposed submerged system has a minimum work requirement of approximately 3 kJ/kg. According to this model, the optimum

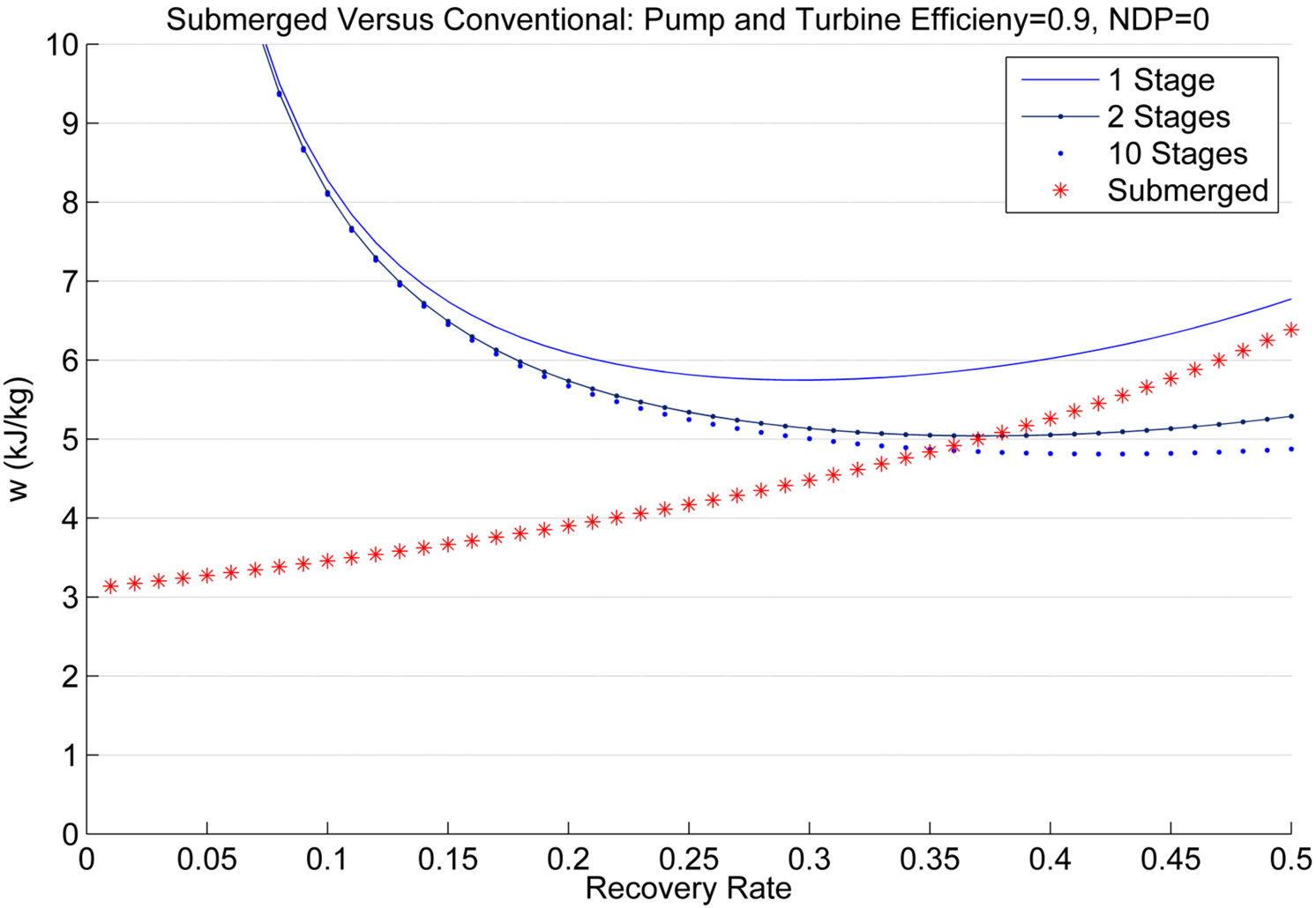

Figure 14: Multiple Stage versus Submerged Non-Ideal Pumping-NDP=0

recovery rate for the proposed system is infinitesimally small. This is true when the pressure drop from the feed to concentrated discharge is neglected. This approximation is also accurate if underwater currents are available to remove the need for the low pressure feedwater pump (see chapter 10.2).

For real reverse osmosis membranes, there is salt leakage across the membrane. As a percentage of permeate production, these leak rates are higher at low permeate production rates. So in order to achieve high quality permeate (low TDS) the pressure must be much higher than the osmotic pressure. Equation (76) gives the work for multistage reverse osmosis with non-ideal pumping, non-ideal recovery, non-ideal RO, and frictionless flow. The additional pressure requirement term is NDP or net driving pressure.

$$w_{stage,real} = \left(\frac{1}{\eta_{HP}}\right)\left[\frac{v_s}{RR}\cdot\left(\Pi_2 + NDP\right) + \sum_{n=2}^{n}\left(\left(\frac{1}{RR}\right)\cdot\frac{x_s}{x_{c,n-1}}\cdot v_{c,n-1}\cdot\left(\Pi_{c,n} - \Pi_{c,n-1}\right)\right)\right] - \left(\eta_R\right)\cdot\left(\frac{1}{RR} - 1\right)\cdot v_c\cdot\left(\Pi_c + NDP\right) \tag{76}$$

For the non-ideal membrane, the proposed submerged unit must be lowered to a depth sufficient to provide the additional net driving pressure. This means that the permeate must be pumped from a greater depth. The work for this system is given in equation (77).

$$w_{submerged,real} = \frac{v_P\cdot\left(\Pi_c + NDP\right)}{\eta_{HP}} \tag{77}$$

Equations (76) and (77) are used to compare the work requirements of the different systems. These calculations are performed with Program 11 which is

presented in Appendix A. Taking the NDP requirement to be 10 atm, the work rates are plotted for a range of recovery rates in Figure 15. For this example, the minimum work for the submerged system corresponds to a low recovery rate and is approximately 4.5 kJ/kg. The minimum work requirement for the traditional 2 stage system is about 6.5 kJ/kg. Therefore the minimum work requirement for a "real" submerged system is about 30% less than the requirement for a "real" 2 stage conventional system.

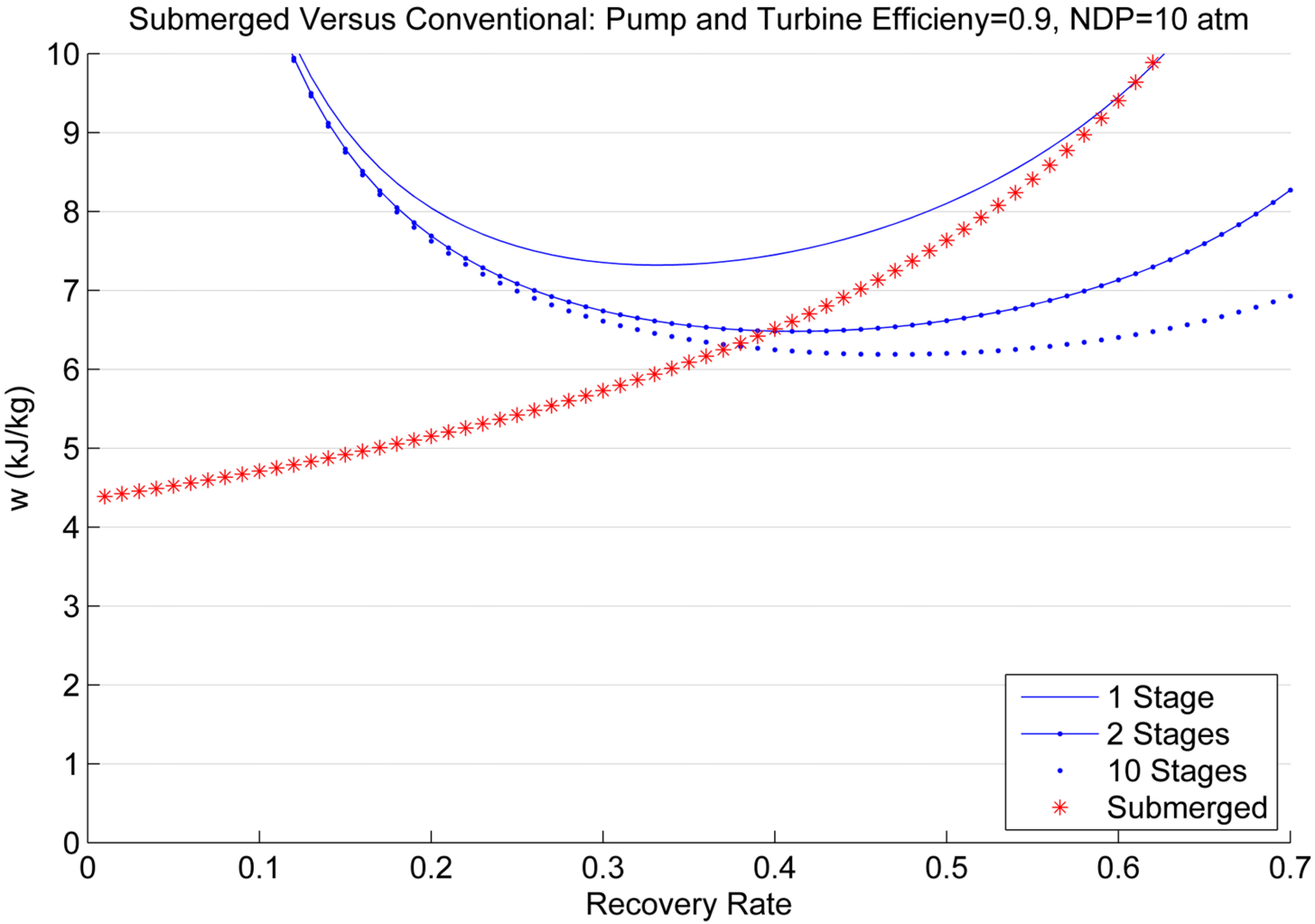

Figure 15: Multiple Stage versus Submerged Non-Ideal Pumping NDP =10

8. Experimental Apparatus

The desalination plant proposed in this study utilizes very low recovery rates which result in relatively low supply pressure requirements to overcome the osmotic pressure and deliver permeate through the membrane. For example, the FILMTEC seawater reverse osmosis membranes are designed to operate at 800 psig (Appendix B, Figure B-5). The proposed desalination process is designed to operate around 500 psig. In order to verify desalination at low recovery rates and at lower supply pressures, an experimental apparatus is designed and used to desalinated artificial seawater in batch processes.

As shown in Figure 16, the experimental apparatus consists of four subassemblies. These subassemblies include: Process Tank (item 1), Reverse Osmosis with Tubing (item 2), Nitrogen Supply (item 3), and Seawater Mixing & Transfer (item 4). Figure 16 also includes containers at the discharge of the reverse osmosis assembly used for collecting water from the concentrate stream and permeate stream separately. The containers are shown resting on scales used to quantify the amount of water collected in each container.

ITEM NO.	Part#	TITLE/DESCRIPTION	QTY.
1	A-005	PROCESS TANK ASSEMBLY	1
2	A-006	REVERSE OSMOSIS ASSEMBLY WITH TUBING	1
3	A-007	NITROGEN SUPPLY ASSEMBLY	1
4	A-008	SEA WATER MIXING AND SUPPLY ASSEMBLY	1
5	P-037	DRUM 55 GAL FOOD GRADE PLASTIC	1
6	P-042	BUCKET PLASTIC 5 GAL	1
7	P-043	SCALE 110 LB MASS	1
8	P-044	SCALE 1000 LB MASS	1

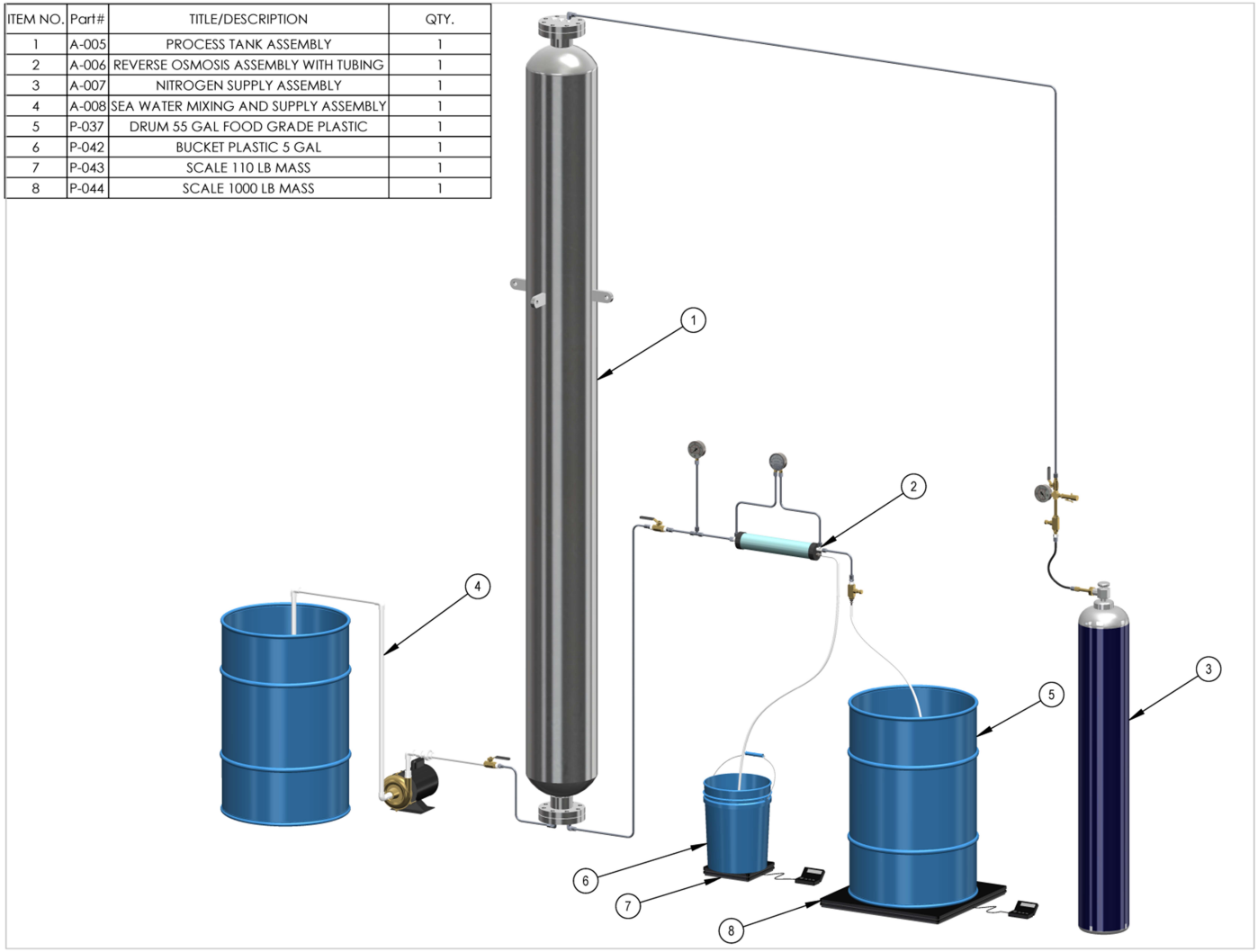

Figure 16: Experimental Apparatus- Main Assembly System

8.1. Artificial Seawater Mixing Assembly

The experimental apparatus is designed to operate in batches. An atmospheric pressure tank is provided for mixing and storage. The seawater mixing assembly is shown in Figure 16 as item 4. As shown in Figure 17, this assembly includes a fifty five gallon mixing container for preparing artificial seawater. In order to prevent corrosion, a plastic drum is used to mix and store the seawater. The pump shown in Figure 17 is present to transfer seawater to the process tank. To minimize corrosion, the pump and transfer lines are plumbed with polyvinyl chloride (PVC) pipe and fittings.

When transferring water from the mixing tank to the process tank, this pump must only be capable of overcoming the twelve feet of head created by static pressure of a full process tank vented to atmosphere. Therefore, the capacity requirements for this pump are minimal. The pump chosen is a centrifugal pump driven by a 120 volt, 1/3 hp motor designed to operate at 3450 rpm.

The pump discharge line includes a PVC union. This union accommodates quick disconnection and reconnection of PVC lines. This subassembly terminates with a ½ inch NPT threaded PVC nipple to provide easy connection to the inlet valve of the process tank subassembly.

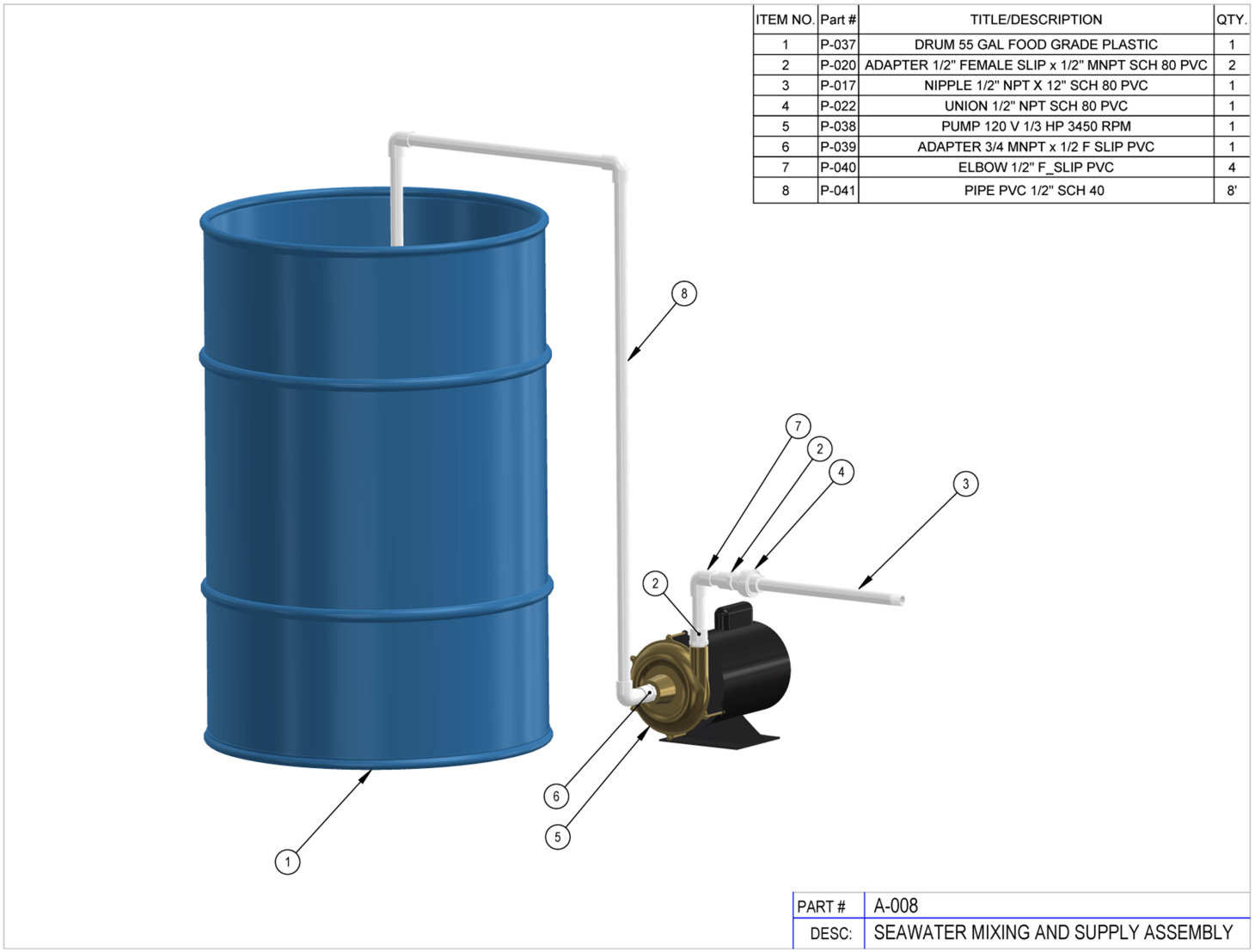

Figure 17: Experimental Apparatus- Seawater Supply Assembly

8.2. Process Tank Subassembly

The process tank subassembly is shown in Figure 16 as item 1. This subassembly is shown in greater detail in Figure 18. The main component of this assembly is a stainless steel pressure vessel. The construction details of the pressure vessel are given in Figure B- 1 and Figure B- 2 (located in Appendix B). As shown in the construction details, the pressure vessel is constructed of 12 inch diameter schedule 40S pipe. The outer diameter of the pipe is 12.75 inches, and the wall thickness is 3/8 inch. The inner diameter of the pipe is 12 inches. The main body of the tank is 11 feet long, so the approximate capacity of the tank is 64 gallons. The overall height of the tank is 12 feet.

The tank top and bottom of the tank terminate with flange connections. Blind flanges are modified and attached to the tank at each end to provide National Pipe Thread (NPT) connection ports. For each flange, three 1 ¼" holes are drilled. Each of these holes is outfitted with a ½" NPT coupling which is welded in place. After the flanges are installed to the ends of the tank, the tank is completely sealed except for the three female NPT taps in the top flange and the three female NPT taps in the bottom flange.

As shown in Figure B- 2, the tank has a maximum allowable working pressure (MAWP) of 600 psig.

As show in Figure 18, schedule 80 PVC fittings isolate the stainless steel tank assembly from the aluminum tubing used to transport the artificial seawater and

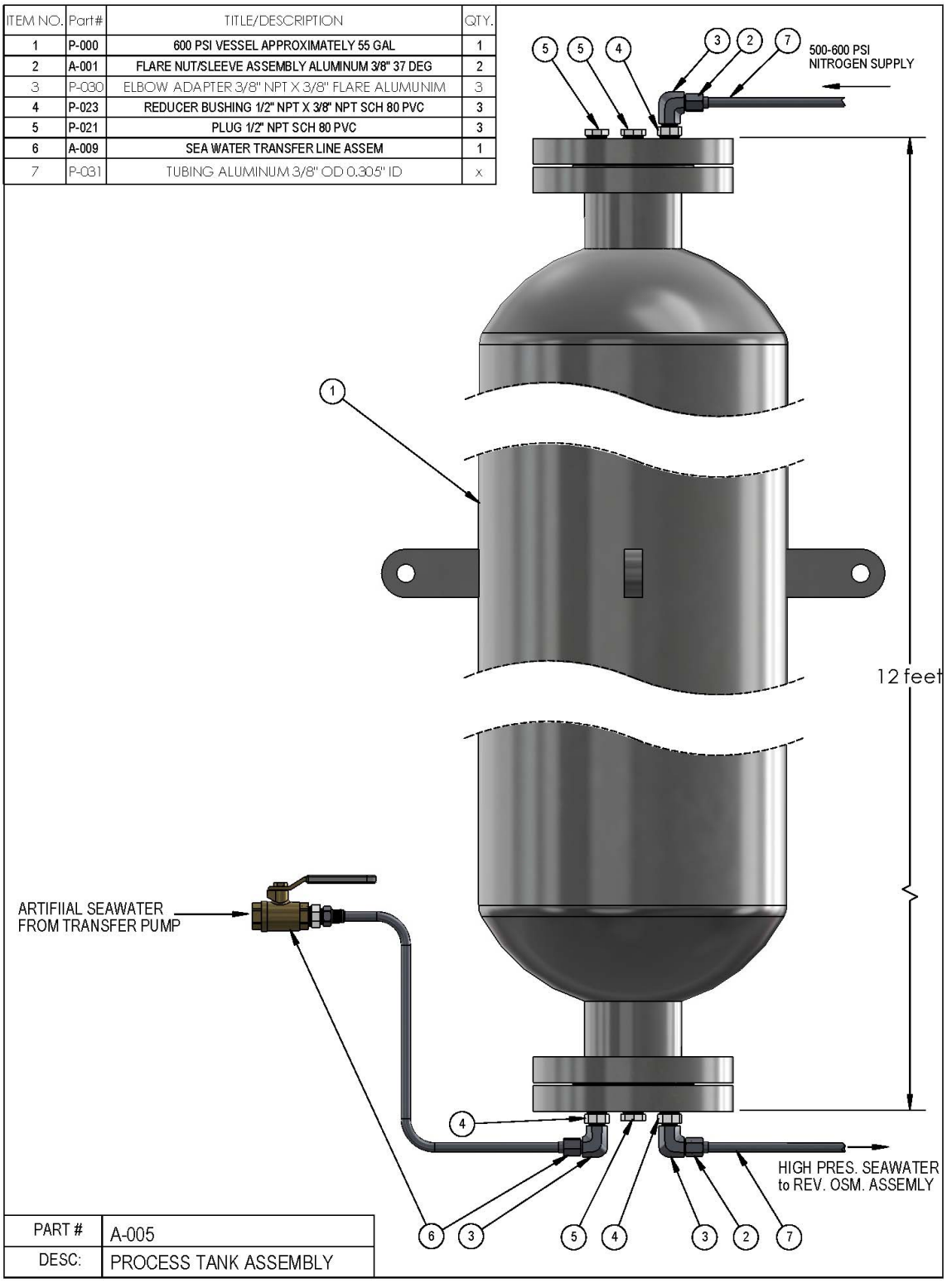

Figure 18: Experimental Apparatus- Process Tank Assembly

compressed nitrogen. By separating these dissimilar metals, the effects of galvanic corrosion are minimized. The schedule 80 PVC fittings meet ASTM D1784 and have a working pressure of 920 psig at 73°F.

The bottom flange is installed with one of the test ports plugged with a ½" schedule 80 PVC plug. The other two test ports in the bottom flange are reduced with a ½" male NPT by 3/8" female NPT schedule 80 PVC bushing. Aluminum adapters elbows are installed into each of these bushings. The adapter elbows are 3/8" NPT on one end and 37° male flare on the other end. The male flare is sized for 3/8" tubing and is threaded with a 9/16-18 male thread.

As shown in Figure 18, the left elbow in the bottom flange is connected to tubing used to transport artificial seawater from the mixing tank to the process tank. The aluminum tubing has an outer diameter of 3/8" and as wall thickness of 0.035". The working pressure of this tubing is 1,000 psig. All aluminum tubing in the entire experimental apparatus comes from a common fifty foot coil. Each end to the seawater supply line shown in Figure 18 is outfitted with a flare nut and a flare sleeve. The tubing is cut and flared on both ends to provide a high pressure seal and form the high pressure seawater transfer line. This line terminates with a ½" female NPT brass ball valve. A ½" male NPT by 3/8" female NPT schedule 80 CPVC reducing bushing is used to isolate the brass ball valve from the aluminum piping. This isolation minimizes galvanic corrosion. An aluminum adapter (3/8 male NPT x 3/8" male flare) is used to connect the aluminum tubing to the CPVC bushing.

As shown in Figure 18, the right elbow in the bottom flange is used to supply artificial seawater from the process tank to the reverse osmosis assembly. Flared aluminum tubing is used to transport the seawater.

Also detailed Figure 18 , two of the supply ports in the top flange are plugged with schedule 80 PVC plugs. The third port in the top flange is used to supply the process tank with compressed nitrogen. The nitrogen is supplied through 3/8" aluminum tubing. A schedule 80 PVC reducing bushing (1/2" male NPT x 3/8" female NPT) is used to isolate the aluminum tubing from the stainless steel flange. An elbow adapter (3/8" male NPT x 3/8 male flare) is used to connect the aluminum tubing to the PVC busing in the supply port.

The tank is constructed with four support lugs located 90° and about eight feet from the bottom of the tank (4 feet from the top of the tank). To support the tank, 4 pieces of dimensional lumber (4" x 6" x 10 feet long) are drilled and connected to the support lugs with ¾" bolt and nut assemblies. The lumber is secured to the bottom of the tank with strapping. The holes in the lumber are located so that the lumber supports the tank with bottom clearance of approximately 4 inches. The lumber and process tank are fastened to a wall for lateral stability.

8.3. Nitrogen Supply Subassembly

The process tank subassembly is shown in Figure 16 as item 3. This subassembly is shown in greater detail in Figure 19. As shown in Figure 19, the nitrogen is supplied from a 2000 psig nitrogen tank (rented from an industrial gas supplier). The tank capacity is 3000 cubic inches. During the experiment, nitrogen is supplied from this tank to the process tank to maintain the process pressure at the desired pressure. As water discharges from the process tank, compressed nitrogen is throttled and flows into the process tank. The process tank volume is approximately 64 gallons.

In order to calculate the number of batches one full nitrogen tank will supply, an equation of state must be chosen. The validity of the ideal gas equation is checked by determining the compressibility factor of nitrogen at the given state. The critical temperature, T_{critical}, for nitrogen is 126.2 K, and the critical pressure, P_{critical}, is 3,390 kPa (Sonntag, 2003). In this case, the temperature of the nitrogen is 296 K (73°F), and the pressure is 13,900 kPa (2015 psia). The reduced pressure, P_{Reduced}, and reduced temperature, P_{Reduced}, are then calculated using equations (78) and (79).

$$P_{\text{reduced}} = \frac{P}{P_{\text{critical}}} \tag{78}$$

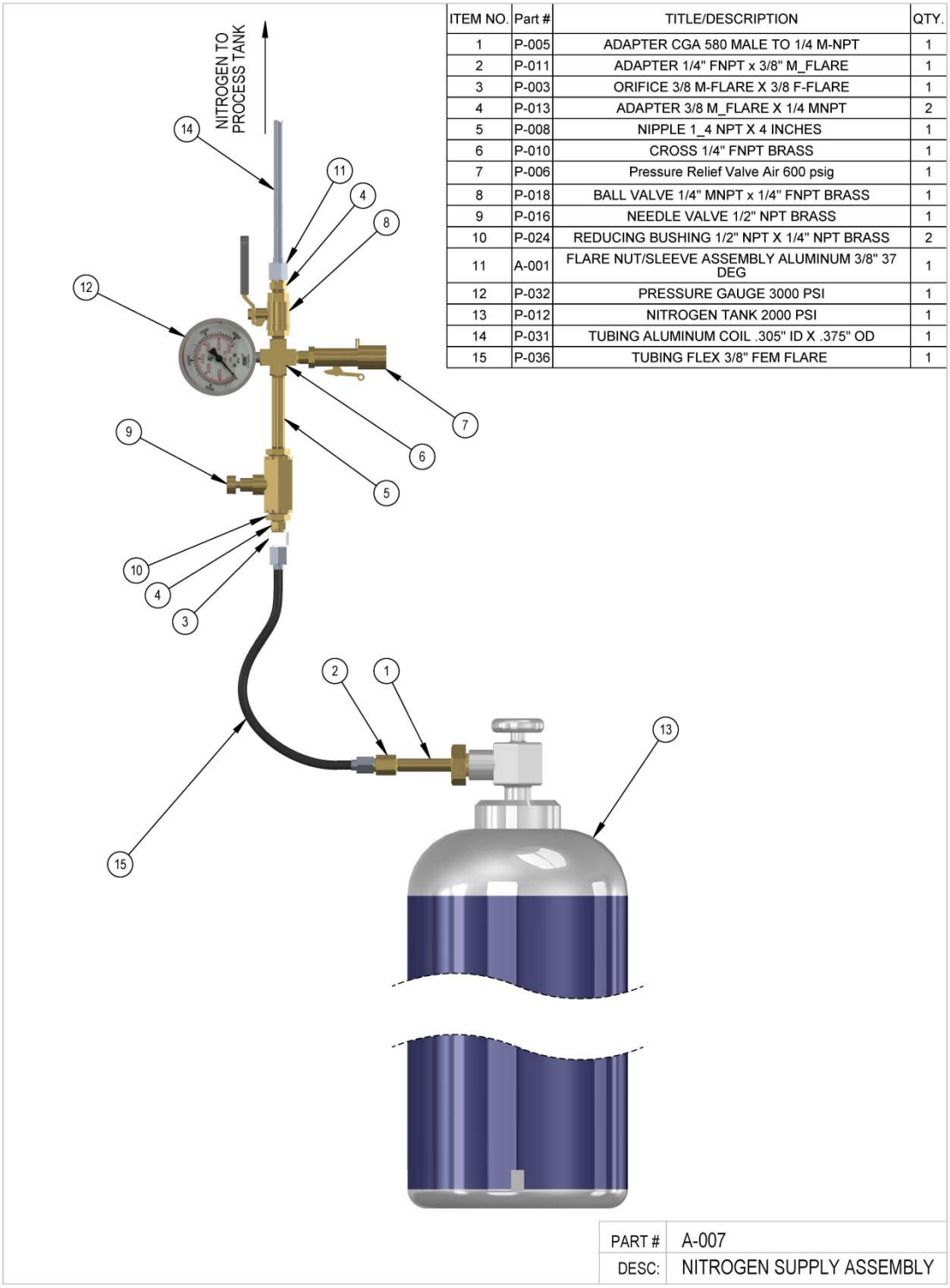

ITEM NO.	Part #	TITLE/DESCRIPTION	QTY.
1	P-005	ADAPTER CGA 580 MALE TO 1/4 M-NPT	1
2	P-011	ADAPTER 1/4" FNPT x 3/8" M_FLARE	1
3	P-003	ORIFICE 3/8 M-FLARE X 3/8 F-FLARE	1
4	P-013	ADAPTER 3/8 M_FLARE X 1/4 MNPT	2
5	P-008	NIPPLE 1_4 NPT X 4 INCHES	1
6	P-010	CROSS 1/4" FNPT BRASS	1
7	P-006	Pressure Relief Valve Air 600 psig	1
8	P-018	BALL VALVE 1/4" MNPT x 1/4" FNPT BRASS	1
9	P-016	NEEDLE VALVE 1/2" NPT BRASS	1
10	P-024	REDUCING BUSHING 1/2" NPT X 1/4" NPT BRASS	2
11	A-001	FLARE NUT/SLEEVE ASSEMBLY ALUMINUM 3/8" 37 DEG	1
12	P-032	PRESSURE GAUGE 3000 PSI	1
13	P-012	NITROGEN TANK 2000 PSI	1
14	P-031	TUBING ALUMINUM COIL .305" ID X .375" OD	1
15	P-036	TUBING FLEX 3/8" FEM FLARE	1

PART #	A-007
DESC:	NITROGEN SUPPLY ASSEMBLY

Figure 19: Experimental Apparatus- Nitrogen Supply Assembly

$$T_{\text{reduced}} = \frac{T}{T_{\text{critical}}} \tag{79}$$

These computations yield a reduced pressure of 4.1 and a reduced temperature of 2.35. Using the generalized compressibility factor table, the compressibility factor is estimated to be approximately 0.96 (Sonntag, 2003). Therefore, the ideal gas equation may be used to estimate the expanded volume capacity of the nitrogen, and the compressibility factor may be used to correct the ideal gas equation results.

The ideal gas equation and the compressibility factor, Z , are given in equation (80) and (81) respectively.

$$Pv = RT \tag{80}$$

$$Z = \frac{Pv}{RT} \tag{81}$$

To determine the process capacity of the nitrogen tank, state 1 is taken to be 2015 psia and 73°F (533 R). The process is considered to be isothermal (slow drain allowing heat to maintain near constant tank temperature). The pressure at state 2 is considered to be the required process pressure of 515 psia. The ideal gas equation of state 1 is given by equation (82).

$$P_1 v_1 = RT_1 \tag{82}$$

Applying the ideal gas equation to state 2 and using the isothermal nature of the process yields equation (83).

$$P_2 v_2 = RT_2 = RT_1 \tag{83}$$

Solving for the specific volume as state 2 yields equation (84).

$$v_2 = RT_2 = \frac{P_1 v_1}{P_2} \tag{84}$$

Using the compressibility factor defined in equation (81) the ideal gas equation estimate is improved to give the corrected specific volume, $v_{2,\text{corrected}}$, in equation (85)

$$v_{2,\text{corrected}} = Z \cdot RT_2 = Z \cdot \frac{P_1 v_1}{P_2} \tag{85}$$

Since the mass of the nitrogen is fixed from state 1 to state 2, multiplying both sides of equation (85) by the mass of the nitrogen yields a relationship for the total volume occupied by the nitrogen at state 2, $V_{2,\text{corrected}}$. The expression is given in equation (86).

$$V_{2,\text{corrected}} = Z \cdot \frac{P_1 V_1}{P_2} \tag{86}$$

Using equation (86) it is determined that a full nitrogen tank will displace approximately 50 gallons of water at 515 psia. For larger runs or higher process

pressures, a wye adapter at the nitrogen tank is used, so that two tanks may supply the process in parallel. For example, a single nitrogen tank would only displace approximately 40 gallons of water for a process run at 615 psia.

The nitrogen tank is outfitted with a CGA-580 connection. Item 1 in Figure 19, is a brass adapter (male CGA-580 x male ¼" NPT). This adapter is followed a separate adapter (1/4" female NPT x 3/8" male 37° flare) to transition to flared connections. A high pressure flexible hose with female flared fittings on both ends is used to transition to the fixed plumbing assembly that supplies the process tank.

Given that the nitrogen supply is 2000 psig and the process tank has a MAWP of 600 psig, safeguards are installed to prevent tank overpressure. Item 3 in Figure 19 is a flow limiting orifice. The orifice chosen for this application has a diameter of 0.113 inches and is supplied by Okeefe (http://www.okcc.com/) . In order to compute the maximum flow capacity for the orifice, the data given in Table 12 are provided by the hardware supplier. The pressures given in the table are orifice inlet pressures, and the flow is reported in standard cubic feet per hour.

Table 12: Manufacturer Flow Data for Orifice

Pressure (psig)	flow (scfh)
1	91.4
5	195
10	250
15	303
20	354
25	405
30	458
40	566
50	672
60	780
70	892
80	1000
90	1106
100	1225

The data from Table 12 are plotted in Figure 20. As illustrated in this graphic, choked flow is achieved at low pressure. The plot also shows that after choked flow is reached, the mass flow rate through the orifice increases linearly with inlet pressure. This phenomenon is explained by the fact that the density of the air increases linearly with pressure. A linear regression is applied to the data. The resulting formula is used to estimate maximum flow rates for the orifice at higher pressures.

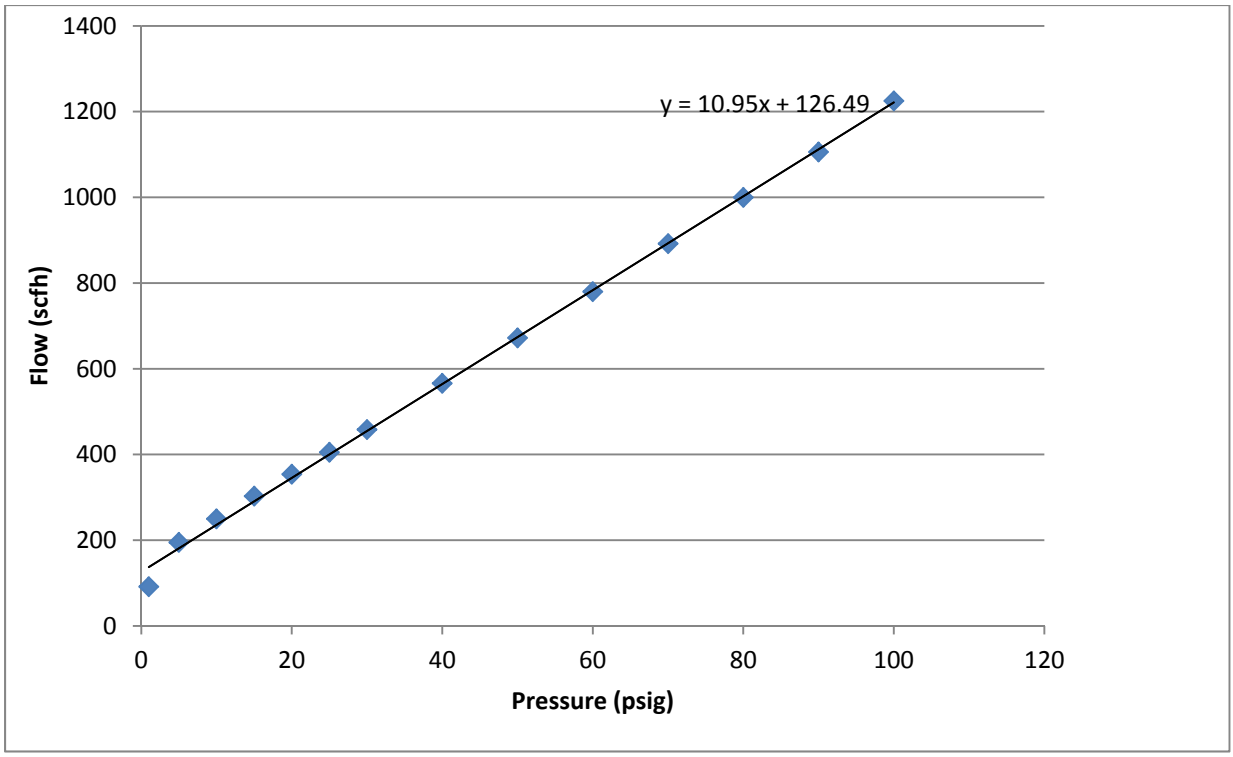

Figure 20: Orifice Flow Rates

The linear regression results in equation (87). In this expression, substituting a pressure in units of psig will result in a volumetric flow rate measured in standard cubic feet per hour.

$$\dot{V}_{\max} = 10.95 \cdot P + 126.49 \tag{87}$$

Equation (87) is used to estimate the maximum flow rates of the orifice as several pressures important for verifying that the orifice sizing is correct. Table 13 lists the calculated flow rates. For convenience, the volumetric flow rates are given in standard cubic feet per minute, standard gallons per minute and standard cubic feet per hour.

Table 13: Orifice Flow Rate Estimates at Experimental Pressures

Pressure	$\dot{V}_{max}$	$\dot{V}_{max}$	$\dot{V}_{max}$
psi	scfm	sgpm	scfh
100	20	152	1,221
515	96	719	5,766
615	114	855	6,861
2000	367	2,746	22,026

In order to insure safety, a pressure relief valve is installed near the nitrogen supply as shown in Figure 19. To meet safety requirements, this valve must have enough capacity to guarantee that the tank pressure does not exceed the maximum allowable pressure. The installed pressure relief valve is ASME certified to open at 600 psig. The manufacturer supplied capacity is given in Figure B- 3. As shown in this figure, the capacity of the relief valve at 600 psi is 400 scfm. In Table 13, it is shown that the orifice will limit flow to 367 scfm when the supply tank is at its maximum pressure of 2000 psi.

The maximum flow rate through the orifice is also given at 515 psi in Table 13. This flow rate is used to verify that the size of the orifice is large enough to flow the required amount of nitrogen to achieve the needed water flow rates in the reverse osmosis supply line. The maximum flow rate at this pressure is given as 719 standard gallons per minute. In order to adjust this flow rate to a volumetric flow rate at 500 psi, the ideal gas equation is used. The rate form of the ideal gas equation is given in equation (88).

$$P\dot{V} = \dot{m}RT \tag{88}$$

For an isothermal process with a constant mass flow rate, the ideal gas equation is used to yield equation (89).

$$P_1\dot{V}_1 = P_2\dot{V}_2 \tag{89}$$

Equation (89) is rearranged to solve for the volumetric flow rate at state 2 as given in equation (90).

$$\dot{V}_2 = \frac{P_1}{P_2}\dot{V}_1 \tag{90}$$

In order to convert units of standard gallons per minute to gallons per minute at another pressure P_1 is taken to be standard pressure (14.69 psi). The conversion formula is given by equation (91).

$$\dot{V}_2 = \frac{14.69 \text{ psi}}{P_2}\dot{V}_{\text{sgpm}} \tag{91}$$

Using equation (91) it is calculated that 719 sgpm yields a mass flow rate equivalent to flowing 21 gpm at 500 psi. The volumetric flow rates required by the reverse osmosis element are less than 10 gpm. Therefore, the size of the orifice is sufficient.

8.4. Reverse Osmosis Subassembly

In Figure 21 the high pressure artificial seawater is supplied to the reverse osmosis unit through a 3/8 inch brass ball valve. The reverse osmosis data sheet is given in as Figures B-5 and B-6 in appendix B. To minimize galvanic corrosion a schedule 80 cpvc bushing is used between the brass valve and connected 3/8 aluminum tubing. A calibrated 3000 psi bourdon tube pressure gauge is attached to the supply line. The reverse osmosis unit (item 1) includes ¼ inch npt x 3/8 inch flare x 3/8 inch flare aluminum fittings at the supply and concentrate discharge ports. These tee fittings are also connected to tubing leading to an Ashcroft 0-27 in. wc. piston type differential pressure gauge. The optimum differential gauge range for experiments in this work is zero to 30 inches of water column.

The concentrate stream exits the reverse osmosis assembly through a brass needle valve (item 9). Again, the1/2" brass needle valve assembly includes CPV bushings to minimize galvanic corrosion. The needle valve is used to throttle the discharge flow to control the pressure drop and recovery rate. Flexible PVC tubing is connected to the discharge of the needle valve to route the concentrate to a container for mass measurements. Flexible tubing is also connected to the permeate discharge to allow for measurements of fresh water production.

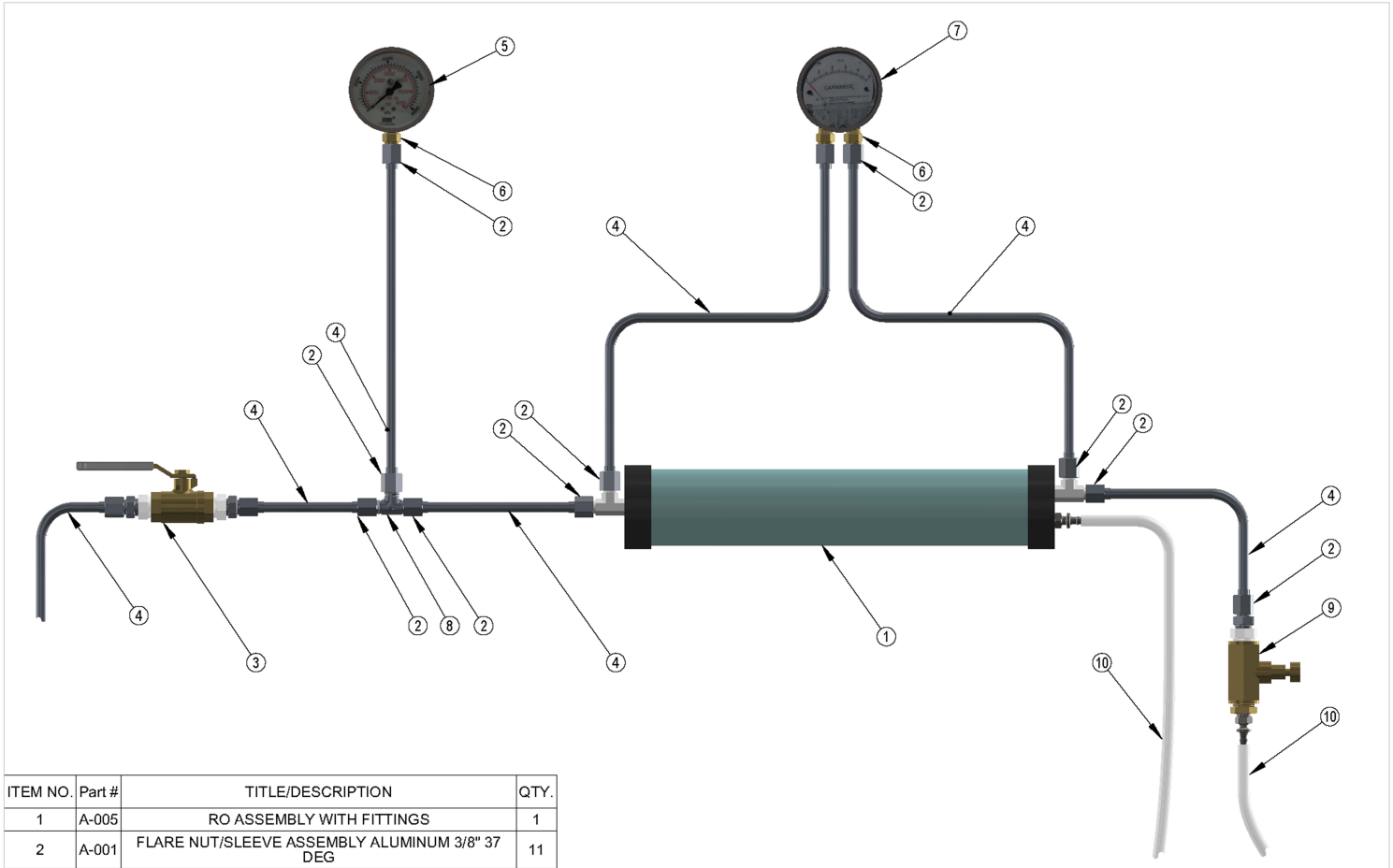

ITEM NO.	Part #	TITLE/DESCRIPTION	QTY.
1	A-005	RO ASSEMBLY WITH FITTINGS	1
2	A-001	FLARE NUT/SLEEVE ASSEMBLY ALUMINUM 3/8" 37 DEG	11
3	A-002	SUBASSEMBLY RO SUPPLY VALVE	1
4	P-031	TUBING 3/8" ALUMINUM	1
5	P-032	PRESSURE GAUGE 3000 PSI	1
6	P-013	ADAPTER 3/8 M_FLARE X 1/4 MNPT	3
7	P-033	DIF PRESSURE GAUGE 5 PSI	1
8	P-028	TEE 37 DEGREE FLARE ALUMINUM	1
9	A-003	SUBASSEMBLY CONCENTRATE DISCHARGE VAVLE	1
10	P-034	TUBING PVC FLEXIBLE 1/4" ID 7/16" OD	1

PART #	A-006
DESC:	REVERSE OSMOSIS ASSEMBLY WITH TUBING

Figure 21: Experimental Apparatus- Reverse Osmosis System

8.5. Reverse Osmosis Exploded View

To aid in the understanding of flow paths through the reverse osmosis pressure vessel and membrane, an exploded view is shown in Figure 22. As illustrated, high pressure seawater passes into the pressure vessel through the single inlet port. This flow continues through the pressure vessel flowing adjacent to a spiral wound membrane. The seawater flow undergoes very little pressure drop between the inlet and the off center concentrate discharge at the other end of the pressure vessel.

As shown, the spiral wound membrane is really a "sandwich" or envelope that is closed on three edges. Ideally, only fresh water crosses the membrane. Once across the membrane, the permeate (fresh water) flows inside the membrane "sandwich" in a spiral path toward the core of the unit. At the core of the unit, the "sandwich" is open allowing the fresh water to flow axially to the end of the pressure vessel. At the end of the pressure vessel, the fresh water discharges through the hole shown in the center of the end cap.

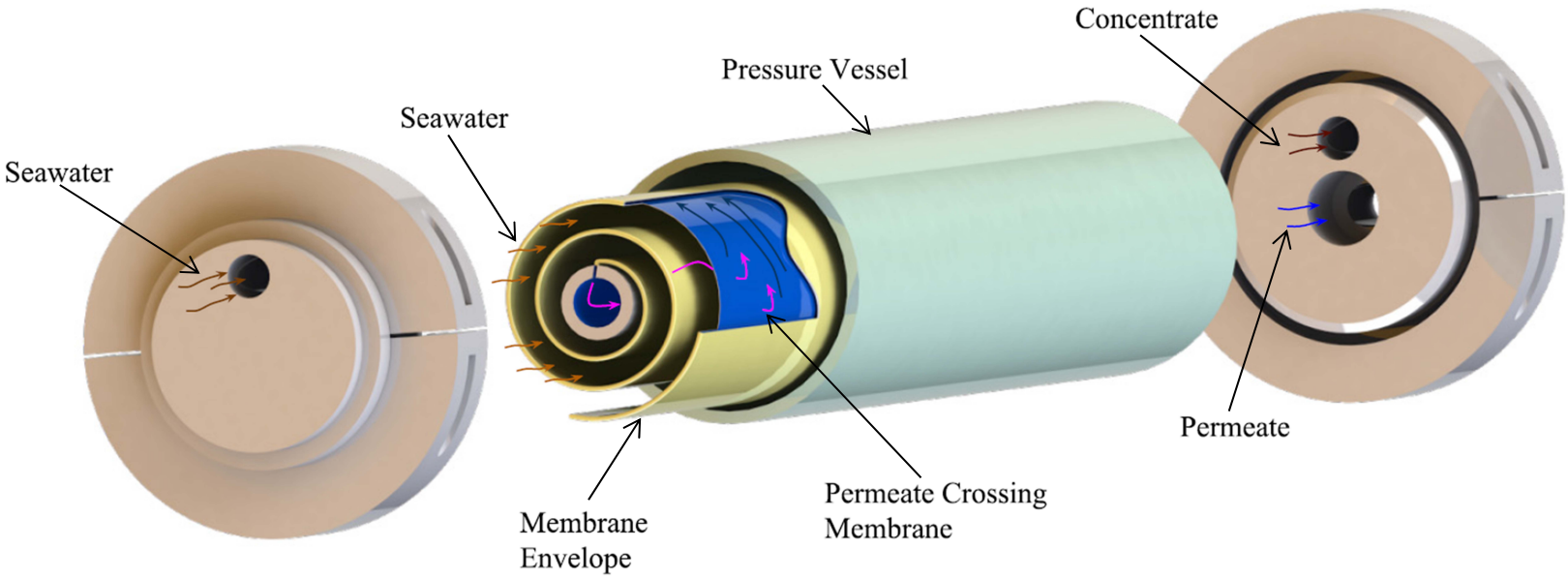

Figure 22: Reverse Osmosis Membrane

9. Experimental Procedure and Results

Experimental results and procedures are discussed. Throughout this chapter, Figure 16 is referenced to clarify the text. For any item number callout, this figure should be referenced.

9.1. Mixing Artificial Seawater

The completed experimental apparatus is illustrated in Figure 16. The artificial seawater is prepared according to ASTM D1148-98. Before mixing the stock water is purified by reverse osmosis to yield a purity of less than 10 parts per million total dissolved solids. The dry salt mix is purchased from Lake Products Company and the specification sheet is given in Appendix B. The mass of the barrel shown in item 4 of Figure 16 is measured. Approximately 50 gallons of pure water is added to the barrel. The mass is again measured and the mass of the water is calculated.

According to the instructions provided by Lake Products Company, 36 ppt seawater is created by combining 5.5 ounces of salt mix with enough pure water to yield 1 gallon of artificial seawater. The standard density of seawater is 8.55

lbm/gallon. This ratio is expressed in equation (92) where m_{salt} is the mass of the dry salt, and m_{water} is the mass of the pure water.

$$\frac{\frac{5.5}{16}\text{lbm}_{salt}}{8.55\ \text{lbm}_{seawater}} = \frac{m_{salt}}{m_{water} + m_{salt}} \tag{92}$$

Solving equation (92) for m_{salt} gives equation (93) which is used to compute the amount of salt to add to the pure water.

$$m_{salt} = 0.0419 \cdot m_{water} \tag{93}$$

9.2. Transferring the Artificial Seawater

The high pressure tank, initially at 0 psig, is vented to atmosphere by removing the flexible nitrogen supply line. The low pressure centrifugal transfer pump in item 4 is used to transfer the prepared artificial seawater into the high pressure tank. Since the tank is vented, pressure does not build in the top of the tank. This is important, because the low pressure pump will "stall" and loose its prime if the head pressure gets too high during the seawater transfer. Once the transfer is complete, the pump is turned off and the manual ball valve between the transfer pump and high pressure tank is closed.

9.3. Desalination Startup

The ball valve between the transfer pump and high pressure tank is checked to verify that it is closed. This is important because the components on the pump side of this valve are not rated for high pressure operation. The flexible nitrogen supply line is connected to the high pressure supply line that transports nitrogen to the top of the high pressure tank. The needle valve in assembly 3 is opened slightly to raise the salt water tank pressure to around 50 psig.

The supply valve for the reverse osmosis assembly (item 2) is opened slowly. Care is taken to allow water to start flowing through the reverse osmosis pressure vessel purging any non-condensable gases from the system. The needle valve on the concentrate discharge is used to control the flow rate and pressure drop across the reverse osmosis unit. The unit is rated for a maximum pressure drop of 15 psid, requiring care to limit the pressure drop.

9.4. Desalination Data Capture

Once the non-condensable gases are purged and water is flowing smoothly, the nitrogen supply needle valve is modulated to slowly raise the seawater tank to the desired pressure for the experiment (400 psig to 580 psig). The seawater tank is pressure rated for 600 psig, so care is taken to prevent tank overpressure.

After the desired seawater tank pressure is achieved, the reverse osmosis concentrate discharge needle valve is modulated to achieve the desired pressure drop and corresponding flow rate through the reverse osmosis pressure vessel. Once the supply pressure and pressure drop are stable, a timer is started and the permeate and concentrate streams are routed to containers for measurement. On specific time or production intervals, the time, permeate mass, concentrate mass, and permeate quality (ppm) are recorded.

9.5. Desalination Shutdown and System Rinse

When only a few gallons of artificial seawater remain in the high pressure tank, the experiment is discontinued. The nitrogen supply valve and reverse osmosis supply valve are closed. The flexible nitrogen supply line is removed. The small section of tubing downstream of the reverse osmosis supply valve is removed. A section of tubing (leading to a clean container) is connected to the discharge of the reverse osmosis supply valve. The reverse osmosis supply valve is opened slightly, and the remaining seawater and compressed nitrogen is purged from the tank.

Once the tank is empty, the transfer pump is used to add clean water to the tank for rinsing. This purging process helps limit corrosion due to salt water. The reverse osmosis supply tubing is reconnected. Shop air (150 psig) is connected to the top of the high pressure tank. The valves are opened and fresh water flows through the reverse osmosis assembly purging any remaining salt. After approximately 5

minutes of fresh water rinse, all valves are closed. The reverse osmosis membrane is stored wet per the manufacturer's instructions.

9.6. Results and Analysis

Data collected during experiments are given in Table 14. The data show the performance of the membrane for artificial seawater (36 ppt) and artificial brackish water (10 ppt). Experiments for the artificial seawater supply include supply pressures that vary from 500 psig to 580 psig. For each supply pressure, the recovery rate is varied by controlling the pressure drop on the concentrate side of the membrane. The concentrate side pressure drop is varied from 10 in. wc. to 25 in. wc. These data show that the purity of the permeate increases with increasing supply pressure and increases with concentrate side pressure drops. Using the 36 ppt supply, the maximum permeate achieved has a total dissolve solids (TDS) concentration of 1200 ppm. TDS levels above 1000 ppm cause taste and smell, so this purity is not quite good enough for most drinking supplies (Greenlee, 2009). For the given membrane, higher supply pressure is needed to generate purer water. However, the experimental apparatus used in this work is only rated for 600 psig. The maximum design pressure was set based on preliminary RO performance estimates with the objective of minimizing apparatus costs.

Experimental results for the brackish water show that good water purity (TDS< 500 ppm) is achieved with supply pressures ranging from 200 psig to 500 psig. Again, these data show that the permeate purity improves with increasing

supply pressure, and increasing supply flow rates. By increasing the supply pressure, the net driving pressure is increased which drives the pure water through the membrane at a higher rate. Increasing the concentrate side flow rate has the effect of decreasing the waste stream concentration level which decreases the average osmotic pressure that must be overcome. Both of these factors increase the net driving pressure.

Table 14: Reverse Osmosis Desalination Data from Experiments

run #	x_s	time	P_s	ΔP_s	m_p	m_c	x_p
	(ppm)	(s)	(psig)	(in. wc.)	(lbm)	(lbm)	(ppm)
1	36000	54	560	10	0.34	5.17	1300
2	36000	204	560	10	1.21	20.14	1300
3	36000	162	570	15	1.04	20.12	1220
4	36000	160	560	15	1.00	20.11	1220
5	36000	295	560	5	1.52	20.08	1475
6	36000	138	560	20	0.86	20.31	1200
7	36000	74	530	25	0.38	12.09	1310
8	36000	170	580	15	1.10	20.09	1260
9	36000	184	580	25	1.05	30.20	1230
10	36000	213	580	10	1.30	20.00	1320
11	36000	156	560	25	1.02	25.62	1250
12	36000	149	500	10	0.58	14.3	1820
13	36000	183	500	15	0.78	22.38	1720
14	36000	148	500	25	0.70	23.85	1540
15	10000	115	500	10	2.11	10.47	159
16	10000	113	500	20	2.15	15.31	136
17	10000	115	400	10	1.64	10.60	166
18	10000	116	400	20	1.67	15.94	145
19	10000	117	300	10	1.12	10.94	197
20	10000	97	300	20	0.95	13.48	180
21	10000	120	200	10	0.61	11.71	298
22	10000	211	200	20	1.07	30.14	282

9.6.1. Salt Passage

The mass flow rate of salt across the membrane, $\dot{m}_{salt}$, is governed by diffusion and is proportional to the concentration difference across the membrane. The diffusion equation is given in equation (94) with , A the active area of the membrane, B the salt passage coefficient of the membrane, x_p the concentration of salt in on the permeate side of the membrane, and $\bar{x}_c$ the average salt concentration on the feed water side of the membrane (DOW, 2006). Experimental measurements are used to compute the salt concentrations and salt passage rates. Equation (94) is then used to determine the salt passage coefficient for the membrane. The concentration data are given in Table 15.

$$\dot{m}_{salt} = B \cdot A \cdot \left(\bar{x}_c - x_p \right) \tag{94}$$

The membrane permeability is a function of supply concentration (DOW, 2006). Experimental results and computed values for membrane salt permeability are given in Table 16 for a supply concentration of 36 ppt and Table 17 for a supply concentration of 10 ppt. Equation (94) is used to compute the salt permeability coefficient for each experimental result. As given in Table 16 and Table 17, the average membrane salt permeability is computed to be 1.29 lbm/(hr m^2) for the 36 ppt supply and 1.19 lbm/(hr m^2) for the 10 ppt supply. So the average salt permeability coefficient is around 16 x 10^{-5} kg/m^2/s.

Table 16 and Table 17 also give the deviation from the average for the permeability coefficient computed from each run. These data show that the permeability coefficient for the seawater supply is adheres to the formulations suggested by (DOW, 2006). For this case, the maximum deviation from average is shown to be approximately 13%. However, data presented in Table 17 indicate that equation (94) does not completely describe the salt passage rates. For the artificial brackish water trials, the computed membrane salt permeability coefficient is observed to decrease with decreasing supply pressure and deviates by more than 35% from the average (see Table 17).

Table 15: Results—Calculated Concentrations and Osmotic Pressures

run #	x_s	P_s	ΔP_s	RR	x_c	x_{avg}	Π_s	Π_c	Π_p	NDP
	(ppt)	(psig)	(in wc)		(ppt)	(ppt)	(atm)	(atm)	(atm)	(psi)
1	36	560	10	6.17%	38.3	37.1	25.6	27.2	1.02	187
2	36	560	10	5.67%	38.1	37.0	25.6	27.1	1.02	188
3	36	570	15	4.91%	37.8	36.9	25.6	26.9	0.95	199
4	36	560	15	4.74%	37.7	36.9	25.6	26.8	0.95	189
5	36	560	5	7.04%	38.6	37.3	25.6	27.5	1.15	187
6	36	560	20	4.06%	37.5	36.7	25.6	26.6	0.94	190
7	36	530	25	3.05%	37.1	36.5	25.6	26.3	1.03	164
8	36	580	15	5.19%	37.9	37.0	25.6	26.9	0.99	209
9	36	580	25	3.36%	37.2	36.6	25.6	26.4	0.96	212
10	36	580	10	6.10%	38.2	37.1	25.6	27.2	1.11	209
11	36	560	25	3.83%	37.4	36.7	25.6	26.6	0.98	191
12	36	500	10	3.90%	37.4	36.7	25.6	26.6	1.42	138
13	36	500	15	3.37%	37.2	36.6	25.6	26.4	1.35	138
14	36	500	25	2.85%	37.0	36.5	25.6	26.3	1.20	137
15	36	500	10	16.77%	12.0	11.0	7.05	8.5	0.12	388
16	10	500	20	12.31%	11.4	10.7	7.05	8.1	0.11	391
17	10	400	10	13.40%	11.5	10.8	7.05	8.1	0.13	290
18	10	400	20	9.48%	11.0	10.5	7.05	7.8	0.11	293
19	10	300	10	9.29%	11.0	10.5	7.05	7.8	0.15	193
20	10	300	20	6.58%	10.7	10.3	7.05	7.5	0.14	195
21	10	200	10	4.95%	10.5	10.3	7.05	7.4	0.23	97
22	10	200	20	3.43%	10.3	10.2	7.05	7.3	0.22	98

Table 16: Membrane Salt Permeability—36 ppt Supply

run #	x_p	x_{avg}	P_s	ΔP_s	Salt Leak Rate	B	B-Deviation
	(ppm)	(ppm)	(psig)	(in wc)	(lbm/hr)	lbm/(hr m^2)	
1	1300	37141	560	10	2.95E-02	1.37	-6.1%
2	1300	37042	560	10	2.78E-02	1.29	-0.2%
3	1220	36899	570	15	2.82E-02	1.32	-2.0%
4	1220	36865	560	15	2.75E-02	1.28	0.6%
5	1475	37307	560	5	2.74E-02	1.27	1.4%
6	1200	36737	560	20	2.69E-02	1.26	2.2%
7	1310	36545	530	25	2.42E-02	1.15	11.3%
8	1260	36951	580	15	2.94E-02	1.37	-6.1%
9	1230	36604	580	25	2.53E-02	1.19	7.8%
10	1420	37124	580	10	3.12E-02	1.46	-12.8%
11	1250	36692	560	25	2.94E-02	1.38	-7.2%
12	1820	36693	500	10	2.55E-02	1.22	5.6%
13	1720	36597	500	15	2.64E-02	1.26	2.3%
14	1540	36506	500	25	2.62E-02	1.25	3.2%
						B_{avg}=1.29	

Table 17: Membrane Salt Permeability—10 ppt Supply

run #	x_p	x_{avg}	P_s	ΔP_s	Salt Leak Rate	B	B-Deviation
	(ppm)	(ppm)	(psig)	(in wc)	(lbm/hr)	lbm/(hr m^2)	
15	159	10992	500	10	1.05E-02	1.62	-35.3%
16	136	10693	500	20	9.32E-03	1.47	-23.2%
17	166	10761	400	10	8.52E-03	1.34	-12.3%
18	145	10516	400	20	7.52E-03	1.21	-1.1%
19	197	10502	300	10	6.79E-03	1.10	8.1%
20	180	10346	300	20	6.35E-03	1.04	12.9%
21	298	10253	200	10	5.45E-03	0.91	23.5%
22	282	10172	200	20	5.15E-03	0.87	27.4%
						B_{avg}=1.19	

In order to better describe the experimental results, a pressure term is added to equation (94) and expressed as equation (95) with B_D the salt diffusion coefficient, B_P the salt pressure coefficient, $\overline{P}_c$ the average concentrate side pressure, and P_p the permeate pressure.

$$\dot{m}_{salt} = B_D \cdot A \cdot \left(\overline{x}_c - x_p \right) + B_P \cdot \left(\overline{P}_c - P_p \right) \tag{95}$$

In order to estimate B_D and B_P, Microsoft Excel is used to perform multiple regression. The first independent variable in the regression is $A \cdot \left(\overline{x}_c - x_p \right)$ and is reported in Table 18 for seawater and Table 19 for brackish water. The second independent variable is $\left(\overline{P}_c - P_p \right)$. Since the permeate pressure is maintained at local atmospheric pressure, and the concentrate side pressure drop is very low (less than 1 psid) the value of $\left(\overline{P}_c - P_p \right)$ simplifies to P_s .

The regression results are given in Table 18 and Table 19. The regressions yielded R-squared values above 0.99 for both the seawater and brackish water samples. Using the computed coefficients, equation (95) is applied using the measured concentration and pressure data to produce the "Leak Estimated" columns in Table 18 and Table 19. Comparing the estimated salt rates to the estimated salt rates show that the model deviation is less than 13% for all cases.

Table 18: Salt Permeability Multiple Regression—36 ppt Supply

run #	x_p	x_{avg}	ΔP_s	P_s	$A\cdot\left(\overline{x}_c - x_p\right)$	Leak Rate*	Leak Estimated**	error
	(ppm)	(ppm)	(in wc)	(psig)	(m^2)	(lbm/hr)	(lbm/hr)	
1	1300	37141	10	560	0.0215	2.95E-02	2.79E-02	-5.3%
2	1300	37042	10	560	0.0214	2.78E-02	2.79E-02	0.5%
3	1220	36899	15	570	0.0214	2.82E-02	2.82E-02	0.0%
4	1220	36865	15	560	0.0214	2.75E-02	2.79E-02	1.5%
5	1475	37307	5	560	0.0215	2.74E-02	2.79E-02	2.0%
6	1200	36737	20	560	0.0213	2.69E-02	2.78E-02	3.4%
7	1310	36545	25	530	0.0211	2.42E-02	2.68E-02	10.5%
8	1260	36951	15	580	0.0214	2.94E-02	2.85E-02	-2.8%
9	1230	36604	25	580	0.0212	2.53E-02	2.84E-02	12.6%
10	1420	37124	10	580	0.0214	3.12E-02	2.85E-02	-8.5%
11	1250	36692	25	560	0.0213	2.94E-02	2.78E-02	-5.5%
12	1820	36693	10	500	0.0209	2.55E-02	2.57E-02	0.7%
13	1720	36597	15	500	0.0209	2.64E-02	2.57E-02	-2.7%
14	1540	36506	25	500	0.0210	2.62E-02	2.57E-02	-1.9%

*Calculated directly from experimental results.

**Calculated with results from multiple regression: $B_{diffusion}$=0.443 & $B_{pressure}$=3.28E-05

Table 19: Salt Permeability Multiple Regression—10 ppt Supply

run #	x_p	x_{avg}	ΔP_s	P_s	$A\cdot\left(\overline{x}_c - x_p\right)$	Leak Rate*	Leak Estimated**	error
	(ppm)	ppm	(in wc)	(psig)		lbm/hr		
15	159	10992	10	500	0.0065	1.05E-02	9.75E-03	-7.1%
16	136	10693	20	500	0.006334	9.32E-03	9.69E-03	4.0%
17	166	10761	10	400	0.006357	8.52E-03	8.24E-03	-3.3%
18	145	10516	20	400	0.006223	7.52E-03	8.19E-03	9.0%
19	197	10502	10	300	0.006183	6.79E-03	6.72E-03	-1.1%
20	180	10346	20	300	0.0061	6.35E-03	6.68E-03	5.3%
21	298	10253	10	200	0.005973	5.45E-03	5.18E-03	-5.1%
22	282	10172	20	200	0.005934	5.15E-03	5.16E-03	0.3%

*Calculated directly from experimental results.

**Calculated with results from multiple regression: $B_{diffusion}$=0.378 $B_{pressure}$=1.46E-05

9.6.2. Permeate Production Rates

The permeate mass flow rate through the membrane is proportional to the active area of the membrane and the net driving pressure. This formulation is given in equation (96) with F, the membrane water permeability and NDP the net driving pressure (DOW, 2006).

$$\dot{m}_p = F \cdot A \cdot (NDP) \tag{96}$$

The net driving pressure is "extra" driving pressure above the minimum to halt osmosis. As given in equation (97) the net driving force is compute by taking the difference of the transmembrane pressure $(P_s - P_p)$ and the net osmotic pressure $\left(\overline{\Pi}_c - \Pi_p\right)$.

$$NDP = (P_s - P_p) - \left(\overline{\Pi}_c - \Pi_p\right) \tag{97}$$

For the osmotic pressure on the concentrate side, the arithmetic average of the inlet feedwater osmotic pressure and outlet concentrate pressure is used.

$$\overline{\Pi}_c = \frac{\Pi_s + \Pi_c}{2} \tag{98}$$

For each experimental run, the membrane water permeability is computed. The results are given in Table 20 for artificial seawater (36 ppt) and Table 21 for artificial brackish (10 ppt) seawater. The average permeability coefficient is

computed to be $0.187 \frac{\text{lbm/hr}}{\text{psi}} \left(3.42 \text{ x } 10^{-9} \frac{\text{kg/s}}{\text{Pa} \cdot \text{m}^2} \right)$ for seawater and $0.299 \frac{\text{lbm/hr}}{\text{psi}}$ $\left(5.46 \text{ x } 10^{-9} \frac{\text{kg/s}}{\text{Pa} \cdot \text{m}^2} \right)$ for brackish water. Comparing the average values to the coefficients computed for each run shows the maximum deviation from average for the seawater coefficients is less than 14%, and the maximum deviation for the brackish water is approximately 5%.

Table 20: Water Permeability—36 ppt Supply

run #	P_s	ΔP_s	$\dot{m}_p$	RR	Π_s	Π_c	Π_p	NDP	F	$F_{deviation}$
	(psig)	(in wc)	(lbm/hr)		(atm)	(atm)	(atm)	(psi)	$\left(\frac{\text{lbm/hr}}{\text{psi}\cdot\text{m}^2}\right)$	
1	560	10	22.7	6.2%	25.6	27.2	1.02	187.1	0.202	7.72%
2	560	10	21.4	5.7%	25.6	27.1	1.02	188.1	0.189	0.91%
3	570	15	23.1	4.9%	25.6	26.9	0.955	198.7	0.194	3.39%
4	560	15	22.5	4.7%	25.6	26.8	0.955	189.1	0.198	5.79%
5	560	5	18.5	7.0%	25.6	27.5	1.15	187.3	0.165	-12.0%
6	560	20	22.4	4.1%	25.6	26.6	0.939	190.2	0.197	4.85%
7	530	25	18.5	3.1%	25.6	26.3	1.03	163.5	0.188	0.51%
8	580	15	23.3	5.2%	25.6	26.9	0.986	208.6	0.186	-0.74%
9	580	25	20.5	3.4%	25.6	26.4	0.962	212.0	0.162	-13.8%
10	580	10	22.0	6.1%	25.6	27.2	1.11	208.6	0.176	-6.37%
11	560	25	23.5	3.8%	25.6	26.6	0.978	191.3	0.205	9.41%
12	500	10	14.0	3.9%	25.6	26.6	1.42	137.8	0.169	-9.60%
13	500	15	15.3	3.4%	25.6	26.4	1.35	137.7	0.186	-0.92%
14	500	25	17.0	2.9%	25.6	26.3	1.20	136.6	0.208	10.8%
									F_{avg} =0.187	

Table 21: Water Permeability—10 ppt Supply

run #	P_s	ΔP_s	$\dot{m}_p$	RR	Π_s	Π_c	Π_p	NDP	F	$F_{deviation}$
	(psig)	(psid)	(lbm/hr)		(atm)	(atm)	(atm)	(psi)	$\left(\frac{\text{lbm/hr}}{\text{psi}\cdot\text{m}^2}\right)$	
15	500	10	66.1	16.77%	7.05	8.45	0.124	388.0	0.284	-4.96%
16	500	20	68.5	12.31%	7.05	8.03	0.106	390.8	0.292	-2.16%
17	400	10	51.3	13.40%	7.05	8.13	0.130	290.4	0.295	-1.33%
18	400	20	51.8	9.48%	7.05	7.78	0.114	292.7	0.295	-1.17%
19	300	10	34.5	9.29%	7.05	7.76	0.154	193.5	0.297	-0.57%
20	300	20	35.3	6.58%	7.05	7.54	0.141	194.9	0.302	0.98%
21	200	10	18.3	4.95%	7.05	7.41	0.233	97.2	0.314	5.07%
22	200	20	18.3	3.43%	7.05	7.30	0.221	97.9	0.311	4.13%
									F_{avg} =0.299	

10. Design Alternatives for Future Study

Three major design alternatives are presented utilizing the concept of deep submerged reverse osmosis.

10.1. Submerged RO with Surface Pretreatment

Figure 23 illustrates a system that is similar to the primary system proposed in this work (see Figure 1). The modification to system in Figure 1includes moving the low pressure pump and pretreatment to a platform at the surface. The RO membrane and high pressure pump would still be located at a depth sufficient to drive the reverse osmosis process. This depth would be approximately 1100 ft to 1500 ft depending on membrane characteristics and water salinity. The low pressure pump at the surface would simply deliver the pressure required to overcome frictional losses of the water flowing through pretreatment filters, piping, and the concentrate side pressure loss for the RO unit. The energy savings for this system are almost equivalent to those calculated for the system shown in Figure 1.

The primary benefit is operational and maintenance access to the low pressure pump and pretreatment equipment. A potential secondary benefit is increased production rates due to higher temperature (and lower viscosity) feedwater.

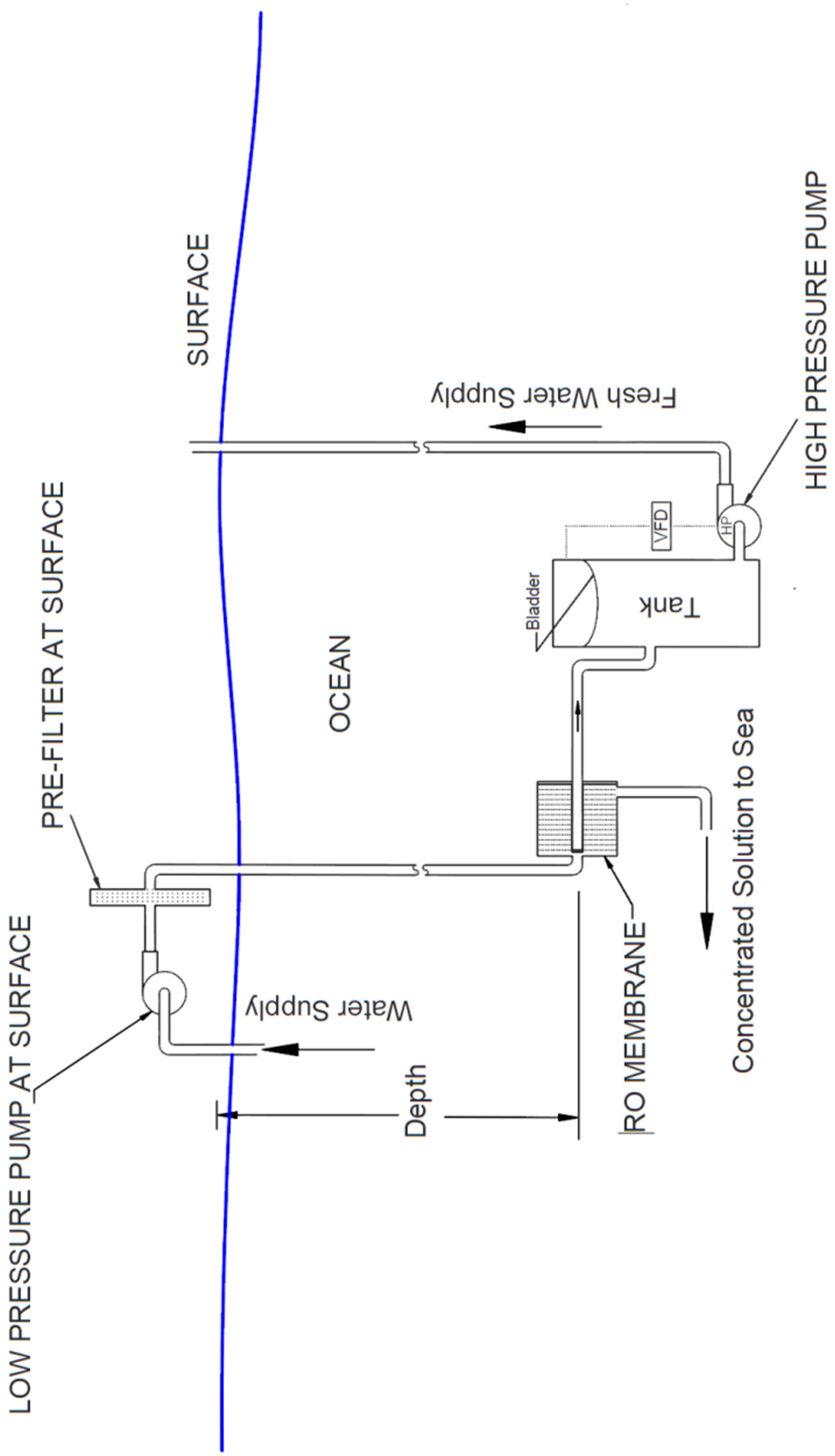

Figure 23: Design Option-Surface Pretreatment

10.2. Submerged RO with No Low Pressure Pump

Figure 24 illustrates another system that is similar to the primary system proposed in Figure 1. This modification requires ocean currents with enough kinetic energy to overcome the frictional losses caused by pretreatment and concentrate side pressure loss in the reverse osmosis unit. Again, this unit would be located at a depth with sufficient static pressure to drive the reverse osmosis, and only fresh water flows through the pump.

Pressure drops observed during experimental work are less than 1 psi. In some oceanic waters, stream with velocities that exceed 2 m/s near the surface and 0.7 m/s at a depth of 1000 m have been reported (Johns, 1995). Utilizing Bernoulli's equation the stagnation pressure, $P_{stagnation}$, is computed to be 512 Pa (0.07 psi) for a 1 m/s water flow and 2050 Pa (0.28 psi) for a 2m/s water flow. The simplified form for Bernoulli's equation is given as equation (99) with v the velocity and ρ the density of water.

$$P_{stagnation} = \frac{v^2}{2}\rho \tag{99}$$

In niche locations with swift ocean currents, it is possible to design systems with very low pressure drop and eliminate the low pressure pump. The resulting system would be most energy efficient with recovery rates that approach zero. In order to position the intake in the high water velocity region, it can be moved to a depth closer to the surface (as compared to the RO unit) with a vertical stand pipe.

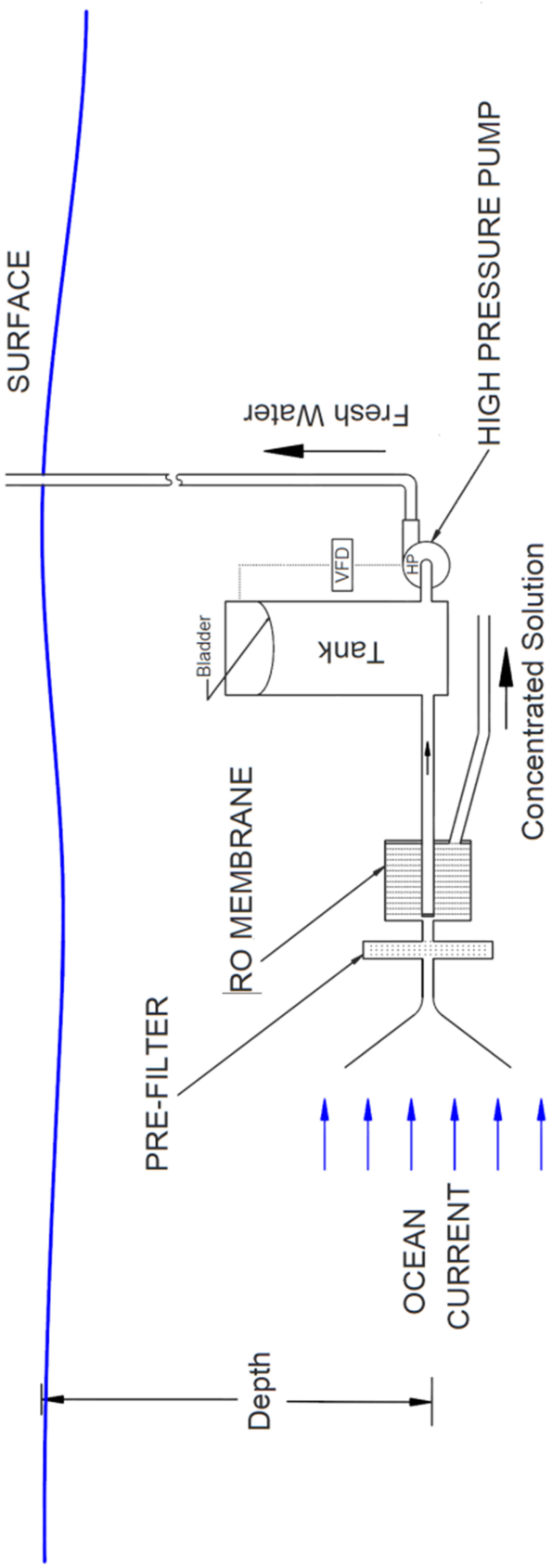

Figure 24: Design Option-Use Ocean Current

10.3. Submerged RO in a Brackish or Seawater Well

The third major design option is land based and requires a well deep enough to provide the static pressure to drive the reverse osmosis. This plan also requires a concentrate discharge line at the bottom of the well that extends horizontally to the ocean.

Of course, the depth of the well is determined by the salinity of the water in the well. The upper limit of brackish water is 10 ppt. To desalinate this water, the required well depth is around 460 feet. The required well depth decreases with decreasing salinity.

Note that the low pressure pump and pretreatment are located at the surface. In cases where brackish water is available, but the water table is not near the surface, the depth from the water surface in the well to the RO unit must provide the static pressure. However, the pretreatment equipment is still maintained and operated at the surface.

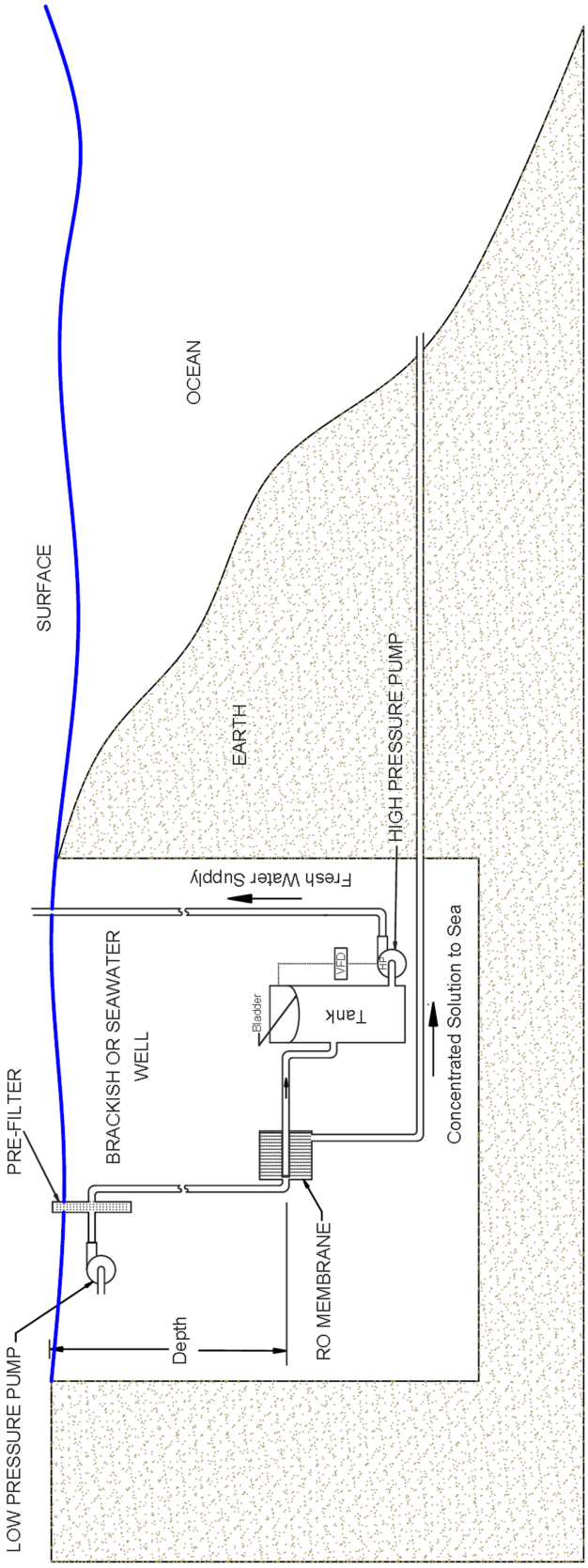

Figure 25: Design Option-Land Based Well

11. Conclusions and Recommendations

From an energy consumption optimization this work shows that the proposed system has promising potential. When compared to a conventional two stage reverse osmosis system with pump and turbine efficiency of 90%, analysis shows the submerged system could cut power consumption by over 30% (assuming a net driving pressure of 10 atm). Of course, energy consumption alone does not characterize large scale desalination. Other factors such as capital costs and maintenance costs must be analyzed to determine the economic viability of proposed design. Capital costs will likely be significantly different when comparing the proposed system to traditional systems. Since the proposed system operates with a single stage and no recovery turbine, costs will be reduced. However, installing and maintaining submerged equipment presents challenges not faced with traditional land based plants. These factors along with fresh water delivery costs will likely impact the economics of the proposed system negatively.

The 30% energy savings noted above, do not include energy costs to transport the fresh water over horizontal distances. The horizontal distance from production to user will likely be different when comparing offshore production to land based production. Calculations are performed with varying pipe diameters to give for a typical plant size of 50,000 km^3/day. For example, it is shown that for a pipe with a

diameter of 1 m results in a flow velocity of 0.74 m/s, a head loss rate of 3.78 kPa/km, and a work rate of 1.21 x 10^{-3} kWh/m^3/kg. These data, along with capital cost data not presented herein, may be used cost comparison and optimization studies.

The minimum work of separation computed by (Mistry, 2013) is verified using the Gibb's function approach. An osmotic pressure calculator is presented and compared to data generated by (Bromley, Singh, Ray, Sridhar, & Read, 1974). The calculator is shown to have good accuracy. Using this calculator, a separate approach is used for computing the minimum work of separation by assuming the supply pressure is equivalent to the osmotic pressure. The results from the "osmotic pressure" approach are consistent with the result from the "Gibb's" function approach.

A model is developed for traditional multi-stage reverse osmosis with non-ideal pumping and non-ideal energy recovery. The results of this model show a two stage traditional RO system has the potential of cutting energy consumption by around 17%. However a 10 stage system reduces energy consumption by less than 5% when compared to the 2 stage model. There is likely no economic payback in adding stages beyond the second stage.

A batch process system is designed and built to process approximately 50 gallons of artificial seawater or brackish water per run for supply pressures limited to less than 600 psig. It is shown that the membrane used in this work is incapable of producing high quality drinking water. However, it is noted that (Vince, Marechal,

Aoustin, & Breant, 2008) reported a salt passage permeability coefficient of 2.5E-5 $kg/m^2/s$ for the SW30-HR380 membrane. The average salt passage coefficient found in this work is around 16×10^{-5} $kg/m^2/s$ or the SW-30-2514 membrane. Based on these data, one should expect the membrane used by Vince to reduce salt passage by around 85% when compared to the results of the current work.

Also, for the current work, the water permeability coefficient is calculated to be around $\left(3.42 \times 10^{-9} \frac{kg/s}{Pa \cdot m^2}\right)$ for seawater. Vince reports a water permeability coefficient of $\left(2.5 \times 10^{-9} \frac{kg/s}{Pa \cdot m^2}\right)$ for the SW-30-2514. So it is expected that the membrane used by Vince would reduce permeate production by around 25%.

Therefore, it is reasonable to conclude that by choosing the correct membrane, it is possible to produce acceptable drinking water from seawater (36 ppt) with supply pressures in the range of 500 psig to 600 psig. Also, during this experimental work good water is produced from brackish water (10 ppt) at pressures under 200 psig. The ocean depth required for seawater desalination is then 1100 ft to 1400 ft, and the depth required for brackish water desalination is less than 460 ft.

Design alternatives to the primary design proposal are described. All alternatives include submerged reverse osmosis. The alternatives included submerged RO with surface pretreatment, ocean current kinetic energy utilization, and land based seawater or brackish water deep well desalination.

The work proves the possibility of operating the proposed system at low net driving pressures with high recovery rates. This study also quantifies potential energy savings (when compared to traditional RO systems). However, to determine the total economic viability of the proposed system, more research is required. In particular, capital and operating costs of a submerged desalination plant should be estimated. Coupled with the work described herein, this would provide information needed for total cost comparison with traditional desalination systems.

References

Bonta, D. (2011, March 25). Factors That Impact RO Filter Performance. *Water Quality Magizine*.

Borsani, R. (2005, May). Fundamentals and costing of MSF desalination plants and comparison with other technologies. *Desalination*, 29-37.

Bromley, L., Singh, D., Ray, P., Sridhar, S., & Read, S. (1974, March). Thermodynamic Properies of Seawater. *AlChE*, 326-335.

Burch, D. (1992). Masters Thesis: Modeling and optimization of the Reverse osmosis Process for Desalination of Seawater. *Auburn University*.

Buros, O. (2000). *ABCs of Desalinatoin, Second Edition.* International Desalination Association.

Cole. (1969). *Patent No. 3,456,802.* United States.

DOW. (2006). *Design a Reverse Osmosis System: Design Equations and Parameters.*

Greenlee, L. (2009, May). Reverse osmosis desalination: Water sources, technology, and today's challenges. *Water Research*, 2317–2348.

Johns, W., Shay, T., Bane, J. M., & Watts, D. (1995). Gulf Steream Structure, Transport, and Recirculation. *Journal of Geophysical Research*, 817-838.

Kim, S. (2009, January). Energy saving methodology for the SWRO desalination process: control of operating temperature and pressure. *Desalination*, 260-270.

Krock, H. (2010). *Patent No. US 7,658,843 B2.* United States.

Maghrabi, A. (2005). *Effect of High Temperature Feed on Nano Filtration and RO Performance.* Al-Jubail, Saudi Arabia: Saline Water Conversion Corporation.

Mistry, K. (2013, May). Generalized Least Energy of Separation for Desalination and Other Chemical Separation Process. *Entropy*, 2046-2080.

NOAA . (2014, June). Retrieved from National Geophysical Data Center: http://maps.ngdc.noaa.gov/viewers/bathymetry/

Puyate, Y. (2008, March). Variability with depth of some physico-chemical and biological parameters of Atlantic. *Journal of Applied Science and Evironmental Management*, 87-91.

Sagle, A. (n.d.). *Fundamentals of Membranes for Water Treatment.* Austin: University of Texas at Austin.

Sharqawya, M., Lienhard, J., & Zubair, S. (2010, April). Thermophysical properties of seawater: a review of existing. *Desalination and Water Treatment*, 354-380.

Sonntag, R. (2003). *Fundamentals of Thermodynamics 6h Ed.* John Wiley and Sons Inc.

Vince, F., Marechal, F., Aoustin, E., & Breant, P. (2008, February). Multi-objectiv optimizationof RO desalination plants. *Desalination*, 96-118.

Wade, N. (2001, May). Distillation plant development and cost update. *Desalination*, 3-12.

Wade, N. M. (1993, August). Technical and economic evaluation of distillation and reverse osmosis desalination processes. *Desalination*, 343–363.

White, F. (1991). *Viscous Fluid Flow Second Edition.* New York: McGraw Hill.

Whyte, G. (2013). *Patent No. 61/552,319.* United States.

Appendix A MATLAB Code

Program 1: Conventional System Pump Work

```
%MATLAB Script
%Compute conventional system pump work  line
clear;clc
rho_p=1000;     %density of fresh water kg/m^3
rho_s=1025;     %density of fresh water kg/m^3
RR=.5;          %recovery rate
CF=(rho_p/(rho_p-rho_s*RR))   %concentration factor
dPS=5;  % pressure drop on the supply side of the RO
system (psi)
dPS=dPS/14.67;  % convert to atm
pi_s=26;  % osmotic pressure of ocean water(atm)
NDP=7;  % net driving pressure(atm)
nth_pump=.86; %pump efficiency
nth_erd=0.97;  %efficiency of energy recovery device

P_ts=CF*pi_s+NDP+dPS;  %RO supply pressure (atm)
w_ts_v=(1/RR)*P_ts/nth_pump-nth_erd*(1/RR-1)*(P_ts-dPS);
%work per unit volume(atm)
w_ts_v=w_ts_v*101;  %convert to kPa
w_ts_v=w_ts_v/3600 %convert to kWh/m^3
```

Program 2: Determine Darcy Friction Factor

```
function out=darcy( e,D,reynolds)
%darcy( e,D,reynolds) computes the Darcy friction factor
%e is the roughness (m)
%D is the pipe diameter (m)
%Re is the Reynolds number

colebrook=inline('1/(((-
2.*log10(e./D./3.7+2.51./Re./(f.^.5))))^2)');
p(1)=.1;
n=1;er=1;
while n==1 || er>10^-10
    p(n+1)=colebrook(D,reynolds,e,p(n));
    er=abs(p(n+1)-p(n));
    n=n+1;
    if n>1000
        error('exceeds max iterations')
    end
    out=p(n-1);
end
```

Program 3: Determine Reynolds Number

```
function [ out ] = Re( rho,v,D,mu )
%Re( rho,v,D,mu ) returns the reynolds number
%rho is density in kg/m^3
%v is velocity in m/s
%D is diameter in m
% mu is dynamic viscosity in N*s/m^2

out=rho*v*D/mu;

end
```

Program 4: Head Loss and Pumping Power to Overcome Friction

```
%MATLAB Script
%Head Loss Due to Friction
clear;clc;clf
Vdot=50000;  %volume m^3/day
Vdot=Vdot/24/3600; %volumetric rate m^3/s
g=9.81; %gravity (m/s^2)
e=.046;  %Roughness (mm)
e=e/1000;  %m
rho=1000;  %kg/m^3
Dmin=.4; Dinc=.005;Dmax=1; %diameter (m)
D=Dmin;  %pipe diameter(m)
nth_hp=0.86;  %high pressure pump efficiency
n=1
while D(n)<=Dmax
    A=pi*(D(n)^2)/4;  %flow area (m^2)

    v(n)=Vdot/A ; %m/s
    mu=1.3*10^-3;  %Ns/m^2
    reynolds=Re(rho,v(n),D(n),mu);
    rv(n)=reynolds;
    f=darcy(e,D(n),reynolds);
    fv2(n)=f;
    HL(n)=f*(v(n)^2)/(D(n)*2*g);   %meters h2o/meter
length
    HL(n)=HL(n)*rho*g ;    %kPa/km length
    n=n+1;
    D(n)=D(n-1)+Dinc;
end
work=HL/3600/nth_hp;  %kWh/m^3/ km
clf;
plot(D(1:length(D)-1),HL/101.3,'b+','MarkerSize',4)
hold on
plot(D(1:length(D)-1),v,'r.','MarkerSize',4)
xlabel('Pipe Diameter (m)')
legend('Head Loss (atm/km)','Velocity (m/s)')
title('Friction Losses')

figure(2);clf;a=30;
plot(D(a:length(D)-
1),work(a:length(work)),'r.','MarkerSize',4)
xlabel('Pipe Diameter (m)')
ylabel('Work (kWh/m^3/km)')
title(' Work to Overcome Friction Losses')
```

Program 5: Submerged System Total Pump Work (Excluding Line Loss)

```
%MATLAB Script
%Compute pump work neglecting friction loss in shore line

clear;clc;clf;
O_s=25;          %typical osmotic pressure in atm
dPt=10;          %transmembrane pressure (atm)
dPs=[1,5,10];    %differential pressure a from supply to
concentrate (psi)
rho_s=1025;      %density of supply sea water (kg/m^3)
rho_p=1000;      %density of permeate (kg/m^3)
CF=1.01:.01:2;   %vector of different values for
concentration factor
nth_LP=.86;      %low pressure pump efficiency
nth_HP=0.86;     %high pressure pump efficiency
for n=1:length(dPs)
    w_v_total(n,:)=w_LP_v( rho_p,rho_s,CF,dPs(n),nth_LP
)+w_hp1_v( rho_p,rho_s,CF,O_s,dPt,nth_HP );
end

%plot the results
hold on
plot(CF,w_v_total(1,:),'r.','MarkerSize',4)
plot(CF,w_v_total(2,:),'b+','MarkerSize',4)
plot(CF,w_v_total(3,:),'k-','MarkerSize',4)

axis([1,1.7,1,1.7])
legend('\DeltaP_s=1 psi','\DeltaP_s=5 psi','\DeltaP_s=10
psi')
xlabel('CF')
ylabel('Power_t_o_t_a_l (kWh/m^3)')
grid on
set(gca,'xtick',[1:.1:1.7])
set(gca,'ytick',[1:.1:2.5])
title('Total Pump Power Neglecting Line Losses')

%determine the optimum values for CF
[A,B]=min(w_v_total');
CF_best=CF(B)';
m(1:3,:)=CF_best;
m(1,2)=w_v_total(1,B(1));
m(2,2)=w_v_total(2,B(2));
m(3,2)=w_v_total(3,B(3));
fprintf('\nCF_best\tW (kWh/m^3)\n')
```

```
fprintf('%7.2f\t%10.2f\n',m')
```

Program 6: Submerged System Low Pressure Pump Work

```
function [ out ] = w_LP_v( rho_p,rho_s,CF,dPs,n_th )
%w_LP_v( rho_p,rho_s,CF,O_s,dPt ) computes the lift LP
pump work per unit
%volume of permeate in kWh/m^3
%rho_p is the density of the permeate
%rho_s is the density of the supply (seawater)
%CF is the concentration factor
%dPs is the differential pressure from supply to
concentrate (psi)
%n_th is the pump efficiency
dPs=dPs*101.3/14.69; %kPa
out=(rho_p/rho_s).*(CF./(CF-1))*dPs/n_th; %kJ/m^3
out=out/3600; %kWh/m^3
```

Program 7: Submerged System High Pressure Pump Work

```
function [ out ] = w_hp1_v( rho_p,rho_s,CF,O_s,dPt,n_th )
%w_hp1_v( rho_p,rho_s,CF,O_s,dPt ) computes the lift work
per unit volume
%of permeate in kWh/m^3
%rho_p is the density of the permeate
%rho_s is the density of the supply (seawater)
%CF is the concentration factor
%O_s is the osmotic pressure of the supply (atm)
%dPt is the transmembrane pressure (atm)
%n_th is the pump efficiency
O_s=O_s*101.3; %kPa
dPt=dPt*101.3; %kPa
out=(rho_p/rho_s).*(CF*O_s+dPt)/n_th; %kJ/m^3
out=out/3600; %kWh/m^3
end
```

Program 8: Minimum Work of Separation—Gibb's Function

```
%MATLAB Script
%Compute minimum work of separation using Gibb's function

clear;clc;clf;
```

```
T=25;  % temperature in celcius
RR_min=.0001;RR_inc=.001;RR_max=.7;  % recovery rate
range

%----------------run 1 supply concentration 35 ppt-------
---------
c1=35000;  %inlet concentration (ppm)
c2=0;      %out concentration of pure water (don't
change)
n=1;RR=RR_min;
while RR<RR_max
    c3=(1/(1-RR))*c1;  % outlet concentrationof waste
stream
    R_v(n)=RR;

g1=SW_Gibbs(T,'C',c1,'ppm');g2=SW_Gibbs(T,'C',c2,'ppm');g
3=SW_Gibbs(T,'C',c3,'ppm');
    w_min=(-g1/RR)+g2+((1/RR)-1)*g3;
    w_min=w_min/1000;  % min work in kJ/kg
    w_v(n)=w_min;
    n=n+1;RR=RR+RR_inc;
end
plot(R_v,w_v,'.')
wmin_35ppt=w_v(1)
hold on

%----------------run 2 supply concentration 20 ppt-------
---------
c1=20000;  %inlet concentration (ppm)
c2=0;      %out concentration of pure water (don't
change)
n=1;RR=RR_min;
while RR<RR_max
    c3=(1/(1-RR))*c1;  % outlet concentrationof waste
stream
    R_v(n)=RR;

g1=SW_Gibbs(T,'C',c1,'ppm');g2=SW_Gibbs(T,'C',c2,'ppm');g
3=SW_Gibbs(T,'C',c3,'ppm');
    w_min=(-g1/RR)+g2+((1/RR)-1)*g3;
    w_min=w_min/1000;  % min work in kJ/kg
    w_v(n)=w_min;
    n=n+1;RR=RR+RR_inc;
end
plot(R_v,w_v,'b-')
wmin_20ppt=w_v(1)
```

```
%----------------run 3 supply concentration 5 ppt--------
--------
c1=5000;  %inlet concentration (ppm)
c2=0;      %out concentration of pure water (don't
change)
n=1;RR=RR_min;
while RR<RR_max
    c3=(1/(1-RR))*c1;  % outlet concentrationof waste
stream
    R_v(n)=RR;

g1=SW_Gibbs(T,'C',c1,'ppm');g2=SW_Gibbs(T,'C',c2,'ppm');g
3=SW_Gibbs(T,'C',c3,'ppm');
    w_min=(-g1/RR)+g2+((1/RR)-1)*g3;
    w_min=w_min/1000;  % min work in kJ/kg
    w_v(n)=w_min;
    n=n+1;RR=RR+RR_inc;
end

%----------------Plot the results--------

plot(R_v,w_v,'--')
legend('35 ppt','20 ppt','5 ppt')

xlabel('Recovery Rate', 'FontSize', 12)
ylabel('w_{min} (kJ/kg)', 'FontSize', 15)
title('Work per kg of Permeate', 'FontSize', 12)
```

Program 9: Function to Compute Osmotic Pressure

```
function [ out] = osmotic_P( T,ppm )
%osmotic_P( T,ppm ) estimates the osmotic pressure of
seawater
%T is temperature in C
%ppm is concentration in ppm
%pressure reported in atm

I=2;  %mols ions/mol NaCl
R=.08205;  %L atm/ mol K
M=58.43; %mols NaCl/gram NaCl
ppt=ppm/1000;
%compute the osmotic coeficient using the calculator
avaiable at http://web.mit.edu/seawater/
phi=SW_Osmotic(T,'C',ppt,'ppt');
out=phi*I*R*(T+273)*ppt/M;
%estimate the ionic concentration by scaling the standard
concentration of
%seawater
MC_ion=1.12*ppm/35000;
out=phi*R*(T+273)*MC_ion;
end
```

Program 10: Compare Minimum Work Calculations

```
clear;clc;clf;
c1=35000;  %inlet concentration (ppm)
c2=0;      %out concentration of pure water (don't
change)
T=25;  % temperature in celcius
Gibbs_error=0.005;  % error of calculator plus minus .5%
RR_min=.01;RR_inc=.001;RR_max=.5; % recovery rate range
n=1;RR=RR_min;
while RR<RR_max
    c3=(1/(1-RR))*c1;  % outlet concentrationof waste
stream
    R_v(n)=RR;

g1=SW_Gibbs(T,'C',c1,'ppm');g2=SW_Gibbs(T,'C',c2,'ppm');g
3=SW_Gibbs(T,'C',c3,'ppm');
    %use maximum error reported with calculator to find
maximum and minimum
    %work values
    g1_max=g1*(1+Gibbs_error);g1_min=g1*(1-Gibbs_error);
    g2_max=g2*(1+Gibbs_error);g2_min=g2*(1-Gibbs_error);
    g3_max=g3*(1+Gibbs_error);g3_min=g3*(1-Gibbs_error);
    w_min_low=((-g1_min/RR)+g2_max+((1/RR)-
1)*g3_max)/1000; %low band of work accounting for Gibb's
function error
    w_min_hi=((-g1_max/RR)+g2_min+((1/RR)-
1)*g3_min)/1000; %high band of work accounting for Gibb's
function error
    w_min=(-g1/RR)+g2+((1/RR)-1)*g3;  %actual minimum
work if no error in Gibb's data
    w_min=w_min/1000;  % min work in kJ/kg
    w_v(n)=w_min;
    w_v_low(n)=w_min_low;
    w_v_hi(n)=w_min_hi;
    n=n+1;RR=RR+RR_inc;
end
plot(R_v,w_v,'.')
wmin_35ppt=w_v(1)
hold on
plot(R_v,w_v_hi,'r--')
plot(R_v,w_v_low,'g--')
```

```
%--------------------now compute work with osmotic
pressure
%n_stages is the number of RO stages
clear w_v
n_stages_max=1000;  %set the number of stages high to
give the optimum result
c0=c1;  % stage 1 inlet concentration  in ppm
rcount=1;p_0=101; %reference pressure in kPa
for RR=.01:.01:.5
    RR
    f=1;n_stages=n_stages_max;
    %determine waste stream concentration for the nth
stage
    c(n_stages)=(1/(1-RR))*c0;
    %distribute the stages equally according to
concentration increase
    c(n_stages)=(1/(1-RR))*c0;
    c=linspace(c0,c(n_stages),n_stages+1);
    %compute the step size of the concentration between
stages
    if n_stages>1
            dc=c(2)-c(1);
    end
     %loop to compute the net work of each stage

     n=1;
     while n<=n_stages
        p(n)=osmotic_P(T,c(n))*101+p_0;  %kpa
        p(n+1)=osmotic_P(T,c(n+1))*101+p_0;  %kpa
        p_B(n)=osmotic_P_Bromley(c(n))*101+p_0;  %kpa
        p_B(n+1)=osmotic_P_Bromley(c(n+1))*101+p_0;  %kpa
        v(n)=SW_Volume(T,'C',c(n),'ppm');
        v(n+1)=SW_Volume(T,'C',c(n+1),'ppm');
        if n==1
            w(n)=(1/RR)*v(n)*(p(n+1)-p_0);
            w_B(n)=(1/RR)*v(n)*(p_B(n+1)-p_0);
        else
            %  reduce mass flow rate for each pump
            f=(1/RR)*(c(1)/c(n));
            w(n)=f*v(n)*(p(n+1)-p(n));
            w_B(n)=f*v(n)*(p_B(n+1)-p_B(n));
        end
        n=n+1;
     end
        stage_v(n_stages)=n_stages;
        wplot(n_stages)=sum(w);
```

```
        wplot_B(n_stages)=sum(w_B);


     w_t=((1/RR)-1)*v(n)*(p(n)-p_0);
     w_t_B=((1/RR)-1)*v(n)*(p_B(n)-p_0);
    rr_v(rcount)=RR;
    w_v(rcount)=sum(w)-w_t;
    w_v_B(rcount)=sum(w_B)-w_t_B;
    rcount=rcount+1;
end
%clf
plot(rr_v,w_v,'r.')

%hold on
plot(rr_v,w_v_B,'r+')
legend('W_{gibbs}','W_{gibbs,max}','W_{gibbs,min}','W_{p\
cdotdv}','W_{pdv,Bromley}')
xlabel('Recovery Rate', 'FontSize', 12)
ylabel('w_{min} (kJ/kg)', 'FontSize', 15)
title('Work per kg of Permeate', 'FontSize', 12)
```

Program 11: Minimum Work—Non-Ideal Pumping and Recovery

```
%MATLAB SCRIPT
%This script compares the work requirement of a submerged
%and traditional
%RO
%Pump and turbine efficiencies may be set between 1 (for
ideal) and 0
%The net driving pressure may be entered.  Set the net
%driving pressure to 0 to establish the absolute minimum
%work

clear;clc;clf;hold on
ppt0=35;  %supply concentration (in parts per thousand)
T=25; %temperature in Celcius
nth_pump=1; % pump efficiciency
nth_turbine=1; % recovery turbine efficiency
c0=ppt0*1000;% stage 1 inlet concentration  in ppm
p_0=101; % reference pressure kPa
NDP=0;  %net driving pressure in atm
NDP=NDP*101;  %kPa
for n_stages=[1,2,10,100]; %several examples of total
number of stages
rcount=1;
for RR=.01:.01:.7
    f=1;
        %determine waste stream concentration for the nth
stage
        %distribute the stages equally according to
concentration increase
        c(n_stages)=(1/(1-RR))*c0;
        c=linspace(c0,c(n_stages),n_stages+1);
        if n_stages>1
            dc=c(2)-c(1);
        end

     %loop to compute the net work of each stage
     n=1;f=(1/RR)*(c(1)/c(n));
     while n<=n_stages
        p(n)=osmotic_P(T,c(n))*101+p_0+NDP;  %kpa
        p(n+1)=osmotic_P(T,c(n+1))*101+p_0+NDP;  %kpa
        p_B(n)=osmotic_P_Bromley(c(n))*101+p_0+NDP;  %kpa
        p_B(n+1)=osmotic_P_Bromley(c(n+1))*101+p_0+NDP;
%kpa
```

```
            v(n)=SW_Volume(T,'C',c(n),'ppm');
            v(n+1)=SW_Volume(T,'C',c(n+1),'ppm');
            if n==1
                w(n)=(1/RR)*v(n)*(p(n+1)-p_0);
                w_B(n)=(1/RR)*v(n)*(p_B(n+1)-p_0);
            else

                f=(1/RR)*(c(1)/c(n+1));
                w(n)=f*v(n)*(p(n+1)-p(n));
                w_B(n)=f*v(n)*(p_B(n+1)-p_B(n));
            end
            n=n+1;
        end
            stage_v(n_stages)=n_stages;
            wplot(n_stages)=sum(w);
            wplot_B(n_stages)=sum(w_B);

        w_t=((1/RR)-1)*v(n)*(p(n)-p_0);
        w_t=w_t*nth_turbine;
        w_t_B=((1/RR)-1)*v(n)*(p_B(n)-p_0);
        w_t_B=w_t_B*nth_turbine;
        rr_v(rcount)=RR;
        w=w./nth_pump;
        w_v(rcount)=sum(w)-w_t;
        w_B=w_B./nth_pump;
        w_v_B(rcount)=sum(w_B)-w_t_B;
        v_permeate=SW_Volume(T,'C',0,'ppm');
        w_v_submerged(rcount)=v_permeate*(p(length(p))-p_0);
        w_v_submerged(rcount)=w_v_submerged(rcount)/nth_pump;
        rcount=rcount+1;

    end
    w_v_submerged=w_v_submerged/nth_pump;
    plot(rr_v,w_v,'b.')
    end


    v_permeate=SW_Volume(T,'C',0,'ppm');
    w_submerged=v_permeate*(p(1)-p_0)
    plot(rr_v,w_v_submerged,'rs')
    xlabel('Recovery Rate', 'FontSize', 12)
    ylabel('w (kJ/kg)', 'FontSize', 15)
    title('Work per kg of Permeate', 'FontSize', 12)
    legend('1 Stage','2 Stages','10 Stages','100
    Stages','Ideal Submerged')
    ylim([0,10])
```

Appendix B Manufacturer Figures

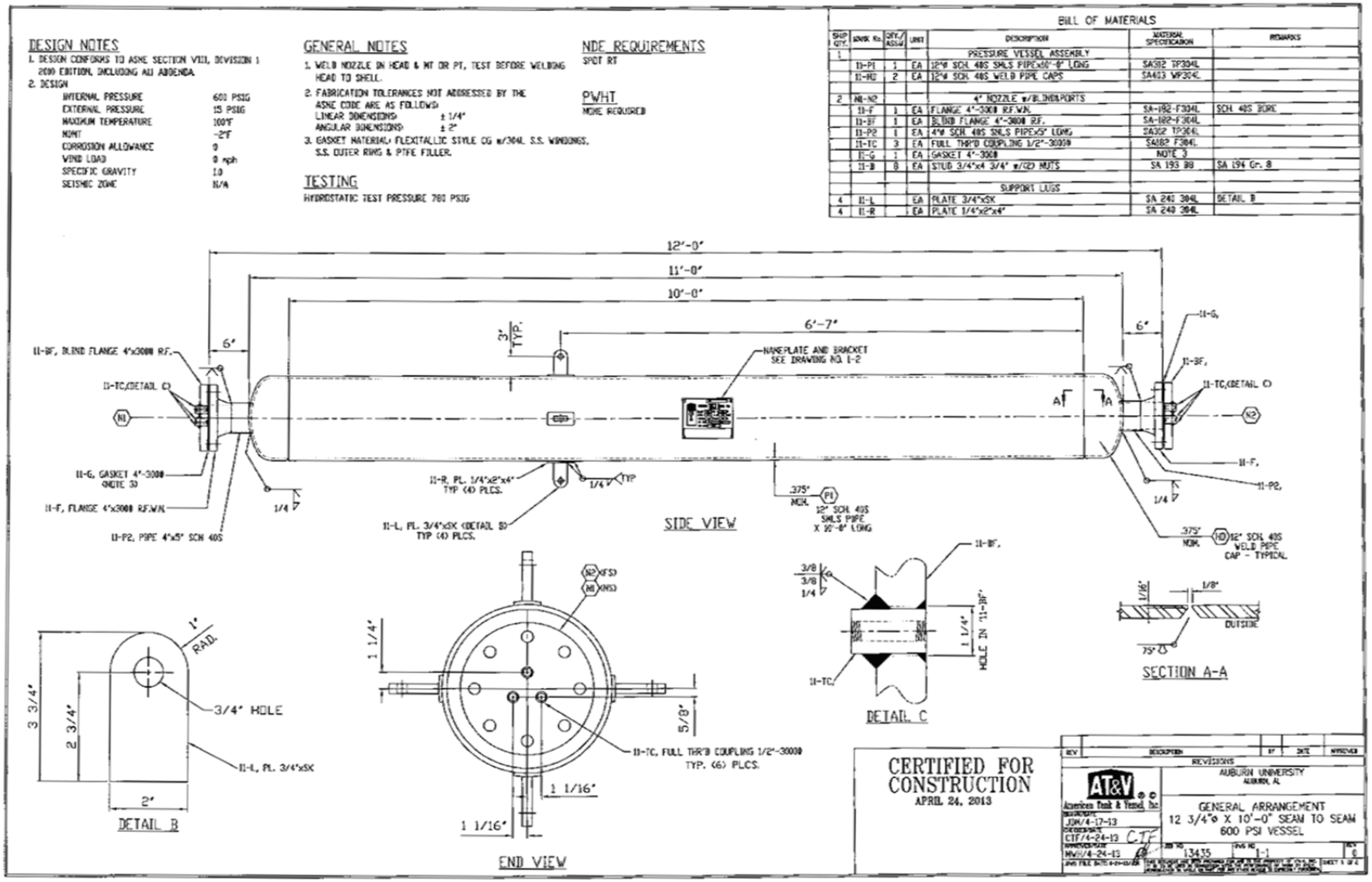

Figure B- 1: Process Tank Construction Drawing

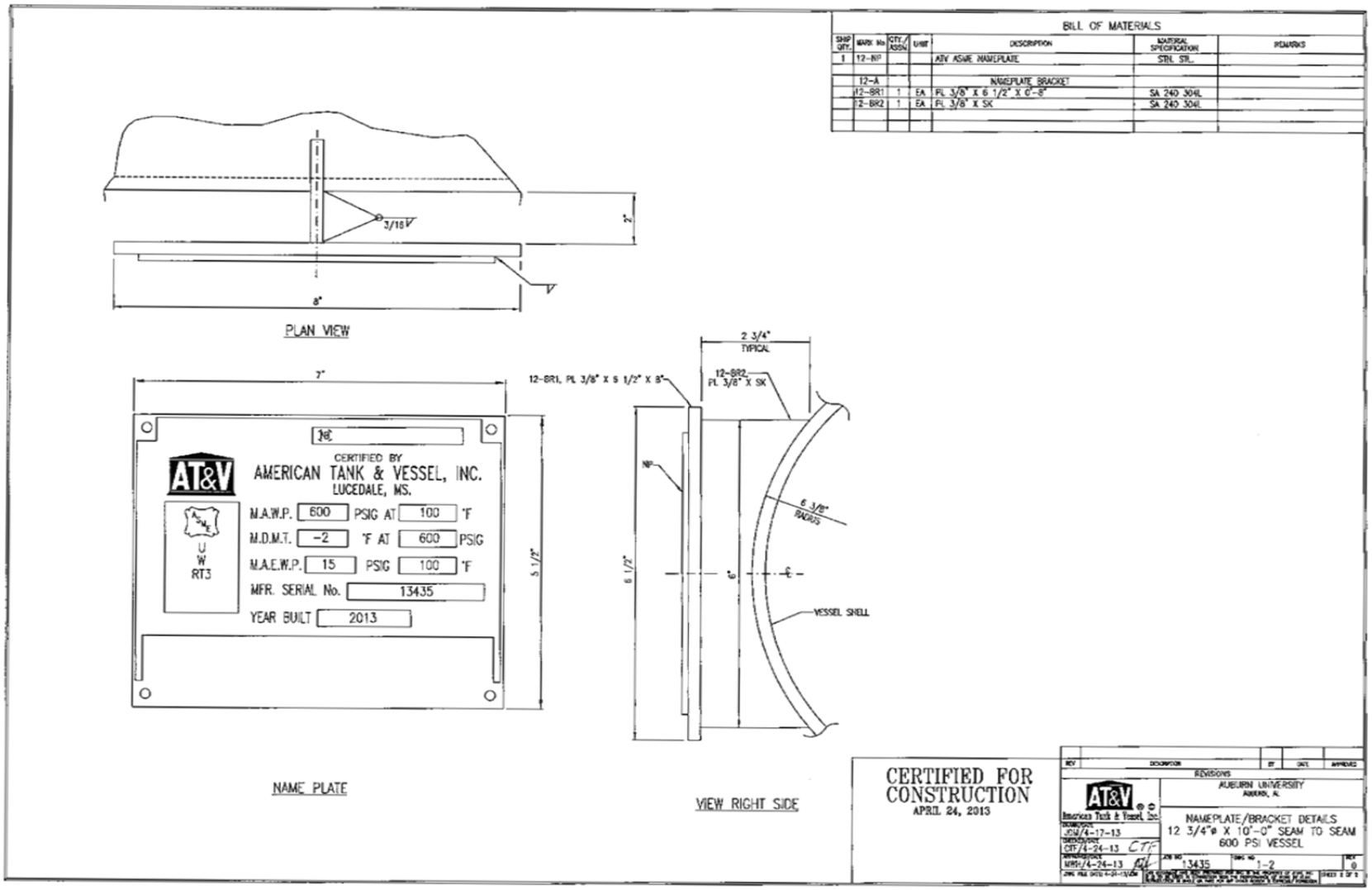

Figure B- 2: Process Tank Construction Drawing (Details)

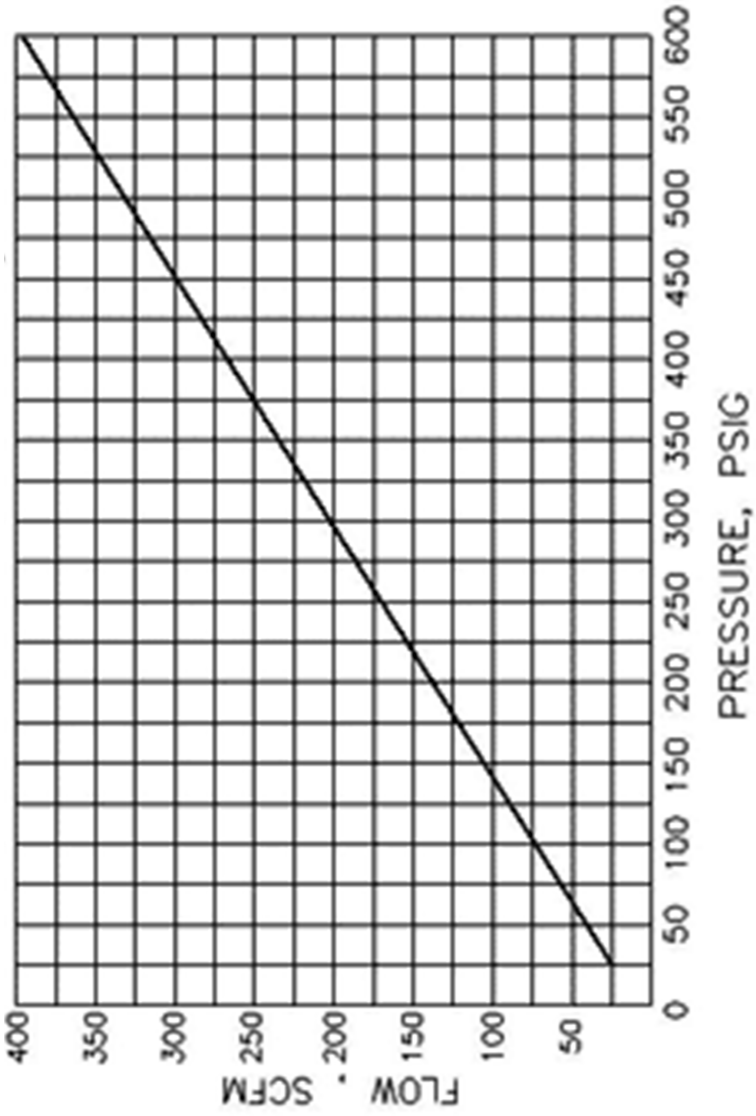

Figure B- 3: Pressure Relief Valve Capacity

Lake Products Company LLC

PO Box 2658 Florissant, MO 63032 USA
Tel: 314-770-2299 Email: Mark.Youngberg@lakeproductscompany.com

TECHNICAL BULLETIN

"SEA-SALT" ASTM D 1141-98 (Re-approved 2008) Formula A, Table X1.1
Original Standard: ASTM D 1141-52, Formula A, Table 1, Section 4

DESCRIPTION: Sea-Salt is a simulated sea salt mix containing elements found in natural sea water in quantities greater than 0.0004%. Sea Salt is granular and colorless. Mixture contains U.S.P., N.F. and High Grade Commercial Salts.

DIRECTIONS: Dissolve 41.953 grams Sea-Salt in water with enough water added to make one liter total solution, or dissolve 5 ½ ounces (156 grams) Sea-Salt in water, then add enough water to make 1 gallon total solution of synthetic seawater. After mixing, adjust pH to 8.2 using 0.1 N solution of sodium hydroxide or hydrochloric acid.

SPECIFICATIONS: Meets American Standard for Testing and Materials Standard D 1141-52, Formula a, Table 1, Section 4 and the updated Standard ASTM D 1141-98 (2008) Formula a, Table X1.1, Section 6 for duplicating ocean water.

COMPOSITION:

of Sea Salt mix		of Substitute Ocean Water solution	
NaCl	58.490%	NaCl	24.53 g/L
$MgCl_2 \bullet 6H_2O$	26.460%	$MgCl_2$	5.20 g/L
Na_2SO_4	9.750%	Na_2SO_4	4.09 g/L
$CaCl_2$	2.765%	$CaCl_2$	1.16 g/L
KCl	1.645%	KCl	0.695 g/L
$NaHCO_3$	0.477%	$NaHCO_3$	0.201 g/L
KBr	0.238%	KBr	0.101 g/L
H_3BO_3	0.071%	H_3BO_3	0.027 g/L
$SrCl_2 \bullet 6H_2O$	0.095%	$SrCl_2$	0.025 g/L
NaF	0.007%	NaF	0.003 g/L
Density of Sea Water equals 1.025 at 15°C		Total	36.032 g/L

APPLICATIONS

(Not intended for human consumption)

CORROSION STUDIES: Accelerated corrosion studies where effects of sea water on the following: Ferrous and non-ferrous metals, plastics, protective coatings, paint, electrochemical processes, surface active agents and ceramics.

BIOLOGICAL: Supports marine biological life; also as a tissue and muscle preservative.

CHEMICAL PROCESSING: Activity effects of minor trace elements may be compared in chemical processing units.

OCEAN INSTRUMENT TESTING: Standardizes sea water environment for consistent test comparisons.

2013-1

Figure B- 4: Artificial Seawater Mix Specification Sheet

Product Information

FILMTEC™ Membranes

FILMTEC Seawater RO Elements for Marine Systems

Features

Improved FILMTEC™ seawater reverse osmosis elements offer the highest productivity while maintaining excellent salt rejection.

- FILMTEC SW30 membrane elements have the highest flow rates available to meet the water demands of both sea-based and land-based desalinators.
- FILMTEC SW30 elements may also be operated at lower pressure to reduce pump size, cost and operating expenses.
- Improved FILMTEC seawater membrane combined with automated, precision element fabrication result in the most consistent product performance available.

Product Specifications

Product	Part Number	Active Area ft^2 (m^2)	Applied Pressure psig (bar)	Permeate Flow Rate gpd (m^3/d)	Stabilized Salt Rejection (%)
SW30-2514	80733	6.5 (0.6)	800 (55)	150 (0.6)	99.4
SW30-2521	80734	13 (1.2)	800 (55)	300 (1.1)	99.4
SW30-2540	80737	29 (2.8)	800 (55)	700 (2.6)	99.4
SW30-4021	80740	33 (3.1)	800 (55)	800 (3.0)	99.4
SW30-4040	80741	80 (7.4)	800 (55)	1,950 (7.4)	99.4

1. Permeate flow and salt rejection based on the following test conditions: 32,000 ppm NaCl, pressure specified above, 77°F (25°C) and the following recovery rates; SW30-2514 – 2%, SW30-2521 & SW30-4021 – 4%, SW30-2540 & SW30-4040 – 8%.
2. Permeate flows for individual elements may vary +/-20%.
3. For the purpose of improvement, specifications may be updated periodically.

Figure 1

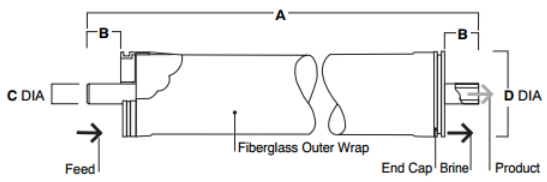

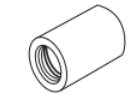

FilmTec sells coupler part number 89055 for use in multiple element housings. Each coupler includes two 2-210 EPR o-rings, FilmTec part number 89255.

Product	Maximum Feed Flow Rate gpm (m^3/h)	Dimensions – Inches (mm) A	B	C	D
SW30-2514	6 (1.4)	14.0 (356)	1.19 (30.2)	0.75 (19)	2.4 (61)
SW30-2521	6 (1.4)	21.0 (533)	1.19 (30.2)	0.75 (19)	2.4 (61)
SW30-2540	6 (1.4)	40.0 (1,016)	1.19 (30.2)	0.75 (19)	2.4 (61)
SW30-4021	16 (3.6)	21.0 (533)	1.05 (26.7)	0.75 (19)	3.9 (99)
SW30-4040	16 (3.6)	40.0 (1,016)	1.05 (26.7)	0.75 (19)	3.9 (99)

1. Refer to FilmTec Design Guidelines for multiple-element systems.
2. SW30-2514, SW30-2521 and SW30-2540 elements fit nominal 2.5-inch I.D. pressure vessels. SW30-4021 and SW30-4040 elements fit nominal 4-inch I.D. pressure vessel.

1 inch = 25.4 mm

Figure B- 5: Membrane Data Sheet Page 1 of 2

Operating Limits

Membrane Type	Polyamide Thin-Film Composite
Maximum Operating Temperature	113°F (45°C)
Maximum Operating Pressure	1,000 psi (69 bar)
Maximum Pressure Drop	15 psig (1.0 bar)
pH Range, Continuous Operation[a]	2 - 11
pH Range, Short-Term Cleaning[b]	1 - 13
Maximum Feed Silt Density Index	SDI 5
Free Chlorine Tolerance[c]	<0.1 ppm

[a] Maximum temperature for continuous operation above pH 10 is 95°F (35°C).
[b] Refer to Cleaning Guidelines in specification sheet 609-23010.
[c] Under certain conditions, the presence of free chlorine and other oxidizing agents will cause premature membrane failure. Since oxidation damage is not covered under warranty, FilmTec recommends removing residual free chlorine by pretreatment prior to membrane exposure. Please refer to technical bulletin 609-22010 for more information.

Important Information

Proper start-up of reverse osmosis water treatment systems is essential to prepare the membranes for operating service and to prevent membrane damage due to overfeeding or hydraulic shock. Following the proper start-up sequence also helps ensure that system operating parameters conform to design specifications so that system water quality and productivity goals can be achieved.

Before initiating system start-up procedures, membrane pretreatment, loading of the membrane elements, instrument calibration and other system checks should be completed.

Please refer to the application information literature entitled "Start-Up Sequence" (Form No. 609-02077) for more information.

Operation Guidelines

Avoid any abrupt pressure or cross-flow variations on the spiral elements during start-up, shutdown, cleaning or other sequences to prevent possible membrane damage. During start-up, a gradual change from a standstill to operating state is recommended as follows:

- Feed pressure should be increased gradually over a 30-60 second time frame.
- Cross-flow velocity at set operating point should be achieved gradually over 15-20 seconds.
- Permeate obtained from first hour of operation should be discarded.

General Information

- Keep elements moist at all times after initial wetting.
- If operating limits and guidelines given in this bulletin are not strictly followed, the limited warranty will be null and void.
- To prevent biological growth during prolonged system shutdowns, it is recommended that membrane elements be immersed in a preservative solution.
- The customer is fully responsible for the effects of incompatible chemicals and lubricants on elements.
- Maximum pressure drop across an entire pressure vessel (housing) is 50 psi (3.4 bar).
- Avoid static permeate-side backpressure at all times.

FILMTEC™ Membranes
For more information about FILMTEC membranes, call the Dow Liquid Separations business:

North America:	1-800-447-4369
Latin America:	(+55) 11-5188-9222
Europe:	(+32) 3-450-2240
Pacific:	+60 3 7958 3392
Japan:	+813 5460 2100
China:	+86 21 2301 9000

http://www.filmtec.com

Form No. 609-00377-0406

Figure B- 6: Membrane Data Sheet Page 2 of 2